HDL-CR-85-052-1
February 1985

A Theory of Electromagnetic Shielding with Applications to MIL-STD-285, IEEE-299, and EMP Simulation

by Richard L. Monroe

Prepared by
Richard L. Monroe Associates
1911 R Street, NW
Suite 203
Washington, DC 20009

Under contract
DAAK21-83-C-0052

U.S. Army Electronics Research
and Development Command
Harry Diamond Laboratories
Adelphi, MD 20783-1197

Approved for public release; distribution unlimited.

The findings in this report are not to be construed as an official Department of the Army position unless so designated by other authorized documents.

Citation of manufacturers' or trade names does not constitute an official indorsement or approval of the use thereof.

Destroy this report when it is no longer needed. Do not return it to the originator.

UNCLASSIFIED

SECURITY CLASSIFICATION OF THIS PAGE (When Data Entered)

REPORT DOCUMENTATION PAGE

READ INSTRUCTIONS BEFORE COMPLETING FORM

1. REPORT NUMBER HDL-CR-85-052-1	2. GOVT ACCESSION NO. A154 913 / 3. RECIPIENT'S CATALOG NUMBER
4. TITLE (and Subtitle) A Theory of Electromagnetic Shielding with Applications to MIL-STD-285, IEEE-299 and EMP Simulation	5. TYPE OF REPORT & PERIOD COVERED Contractor Report 6. PERFORMING ORG. REPORT NUMBER
7. AUTHOR(s) Richard L. Monroe HDL Contract Monitor: Ronald J. Chase	8. CONTRACT OR GRANT NUMBER(s) DAAK21-83-C-0052
9. PERFORMING ORGANIZATION NAME AND ADDRESS Richard L. Monroe Associates 1911 R Street, NW, Suite 203 Washington, DC 20009	10. PROGRAM ELEMENT, PROJECT, TASK AREA & WORK UNIT NUMBERS 6.21.20A 1L162120AH25
11. CONTROLLING OFFICE NAME AND ADDRESS Harry Diamond Laboratories 2800 Powder Mill Road Adelphi, MD 20783-1197	12. REPORT DATE February 1985 13. NUMBER OF PAGES 198
14. MONITORING AGENCY NAME & ADDRESS(if different from Controlling Office)	15. SECURITY CLASS. (of this report) UNCLASSIFIED 15a. DECLASSIFICATION/DOWNGRADING SCHEDULE

16. DISTRIBUTION STATEMENT (of this Report)

Approved for public release; distribution unlimited.

17. DISTRIBUTION STATEMENT (of the abstract entered in Block 20, if different from Report)

18. SUPPLEMENTARY NOTES

HDL Project: X852XR, X853EC

19. KEY WORDS (Continue on reverse side if necessary and identify by block number)

Electromagnetic shielding, Impedance boundary conditions, Shielding standards, Shielding effectiveness, Hertzian dipoles, Loop antennas, Schelkunoff's formula, Correction factors, Electromagnetic pulse (EMP), Transient analysis, Transient shielding effectiveness, EMP simulation

20. ABSTRACT (Continue on reverse side if necessary and identify by block number)

A shielding theory based on Impedance Boundary Conditions is developed and used to obtain formal expressions for the fields transmitted to the interior of a generalized metallic structure from an arbitrary, external, time harmonic, electromagnetic source. The structure is an assemblage of planar sheets that may be penetrated by a finite number of narrow rectangular slots. It includes both a single sheet (continuous or slotted) and a rectangular enclosure (continuous or slotted) as special cases.

DD FORM 1 JAN 73 1473 EDITION OF 1 NOV 65 IS OBSOLETE

UNCLASSIFIED

SECURITY CLASSIFICATION OF THIS PAGE (When Data Entered)

20. Abstract (Cont'd)

Explicit expressions are then derived for the transmitted electric and magnetic fields at points on the inside surfaces of plane sheets (continuous and slotted) and rectangular enclosures (continuous and slotted) when these structures are exposed to fields from elementary electric and magnetic dipoles and small rectangular loop antennas. These expressions are then used to obtain the shielding effectiveness of sheets and enclosures.

The shielding theory is extended from time harmonic sources to transient sources for several cases of interest. These include transient fields in the form of decaying exponentials incident on continuous and slotted enclosures. In each case, the field transmitted to the inside surface of the enclosure is evaluated explicitly using analytic approximations to the inverse Laplace transforms. The results show that transient fields inside slotted enclosures differ markedly from those inside continuous enclosures even when both are exposed to the same field. The field inside a slotted enclosure is usually much larger and much more likely to contain a high frequency component in the form of internal pulses reflected between the front (closest to the source) and back walls. Besides being smaller, the field in a continuous enclosure is likely to be greatly delayed and stretched in time compared to the field in a slotted enclosure.

On the basis of these results, it is argued that a single internal field measurement at a given frequency as called for by MIL-STD-285 and IEEE 299 is insufficient to determine the shielding effectiveness of an enclosure against both electric and magnetic fields from a specified electromagnetic source. It is also argued that a small loop antenna carrying a properly designed transient current can be used to simulate an EMP field for purposes of measuring the time domain shielding effectiveness of small electronics shelters against EMP fields.

FOREWORD

This report is the outgrowth of electromagnetic shielding studies by the author that go back to 1972. During this time, he has received encouragement, advice, and assistance from many individuals, and to all of these, he would like to express his sincere appreciation. Special thanks are due to Dr. John Bombardt and Mr. John Sweton who introduced the author to the subject of electromagnetic shielding and first suggested the idea that there must be an analytical relationship between EMP shielding effectiveness and MIL-STD-285 and to Mr. Joseph Miletta and Mr. Ronald Chase who provided outstanding technical and administrative support for this effort.

CONTENTS

CONTENTS (cont'd)

CONTENTS (cont'd)

FIGURES

FIGURES (con't)

FIGURES (cont'd)

BACKGROUND

In the Fall of 1972, a project was begun at Harry Diamond Laboratories to develop an analytical relationship between the shielding effectiveness of a metallic enclosure as measured by small loop and monopole antennas in accordance with MIL-STD-285[1] and the shielding effectiveness of the same enclosure when exposed to a plane wave Electromagnetic Pulse (EMP). The basic objective of the project was to obtain some relatively simple, closed form approximations that could be useful in interpreting data from measurements that were being planned as part of field tests to determined the vulnerability of the Safeguard System to damage from EMP fields. A longer range objective was to provide an analytical basis for the development of small, low cost, mobile simulators that could be used to measure the shielding effectiveness of various types of enclosures against EMP fields generated by a wide range of natural and man-made sources including lightning and high altitude nuclear explosions.

Using a heuristic approach that made liberal use of engineering approximations, the principal investigator obtained a single expression relating the shielding effectiveness of an enclosure against plane wave electromagnetic fields to the shielding effectiveness of the same enclosure against near fields generated by small loop and monopole antennas. This expression was described in Monroe[2] where it was cast in the form of a correction factor that can be used to adjust shielding effectiveness measurements made with loop and monopole antennas located 12 inches from an enclosure to give the shielding effectiveness

---

1 Anonymous, MIL-STD-285 Method of Attenuation Measurements for Enclosures, Electromagnetic Shielding, for Electronic Test Purposes, Dept. of Defense, (25 June 1956).

2 R. L. Monroe, EMP Shielding Effectiveness and MIL-STD-285, Harry Diamond Laboratories, HDL-TR-1636, (July 1973).

by these investigators combined elements from problems 1 and 3. Moser[5], Schulz[16], and Cowdell[17] used small loop antennas located close to large, flat metal sheets;while Axford et al[9] used loop and monopole antennas to illuminate a shielded enclosure that has been penetrated by a narrow rectangular slot. On the theoretical side, Bannister[6] gave an independent derivation of Schelkunoff's equation for the case of a loop antenna oriented with its plane parallel to the plane of the sheet. His derivation is based directly on Maxwell's equations and makes no use of transmission theory. These results will be referred to as the extended transmission theory of shielding.

In spite of its successes, Schelkunoff's equation has not attained unanimous acceptance as a universal shielding formula. For example, Bridges and Miller[18] point out several apparent discrepancies between measurements and calculations based on equation (2.16) and between (2.16) and comparable expressions obtained by ostensibly more rigorous theories. These discrepancies range from 50 to 100 dB in the frequency range from 100 Hz to 10^4 Hz when (2.16) is applied to shielded enclosures in the manner suggested by Cowdell[14] and Babcock[15]. Moreover, the predictions based on (2.16) fall on the optimistic side so that

---

5 J. R. Moser, IEEE Trans. EMC, EMC-9 (1967), 6.

6 P. R. Bannister, IEEE Trans. EMC. EMC-10 (1968), 2.

9 R. Axford, R. McCormack, and R. Mittra, Evaluation of the Applicability of Standard CW EMI-RFI Shielding Effectiveness Test Techniques of Assessment of EMP Hardness of Tactical Shelters, Construction Engineering Research Laboratories, CERL-TM-M-307, (March 1982).

14 R. B. Cowdell, Electronics, 40 (April 1967), 92.

15 L. F. Babcock, IEEE Trans. EMC, EMC-9 (Sept. 1967), 45.

16 R. B. Schulz, IEEE Trans. EMC, EMC-10 (March 1968), 95.

17 R. B. Cowdell, IEEE Trans. EMC, EMC-10 (March 1968), 158.

18 J. E. Bridges and D. A. Miller, IEEE Trans. EMC, EMC-10 (1968), 175.

this conviction when he used (2.16) to predict the shielding effectiveness of various electronics cabinets against low and high impedance fields. For the low impedance field he approximated Z_w with the wave impedance of an elementary magnetic dipole and for the high impedance field he used the wave impedance of an elementary electric dipole[12]. This approach was then used extensively by Schulz et al[13], Cowdell[14], and Babcock[15]. And, as noted previously, Monroe[2] applied it to an important class of discontinuous shields by replacing Z_i with the impedance of the discontinuity which was approximated by the impedance of rectangular slot. Experimental support for some - but by no means all - of these applications was obtained by Moser[5], Schulz[16], Cowdell[17], and Axford et al[9]. The arrangements of source and shield studied

---

2 R. L. Monroe, EMP Shielding Effectiveness and MIL-STD-285, Harry Diamond Laboratories, HDL-TR-1636 (July 1973).

5 J. R. Moser, IEEE Trans. EMC, EMC-9 (1967), 6.

9 R. Axford, R. McCormack, and R. Mittra, Evaluation of the Applicability of Standard CW EMI-RFI Shielding Effectiveness Test Techniques to Assessment of EMP Hardness of Tactical Shelters, Construction Engineering Research Laboratories, CERL-TM-M-307, (March 1982).

12 E.C. Jordan, Electromagnetic Waves and Radiating Systems, Prentice-Hall, Englewood Cliffs, N.J., (1950).

13 R. B. Schulz, V. C. Plantz, and D. R. Brush, Shielding Theory and Practice, Proc. 9th Tri-Service Conf.on Electromagnetic Compatibility, Chicago, Ill., (Oct. 1963).

14 R. B. Cowdell, Electronics, 40 (April 1967), 92.

15 L. F. Babcock, IEEE Trans. EMC, EMC-9 (Sept. 1967), 45.

16 R. B. Schulz, IEEE Trans. EMC, EMC-10 (March 1968), 95.

17 R. B. Cowdell, IEEE Trans. EMC, EMC-10 (March 1968), 158.

cylindrical wave evaluated at the inner surface of the shield. When the wavelength of the field is much larger than the inner radius of the cylinder, Schelkunoff showed that Z_w reduces to

$$Z_w = j2\pi f\mu_o a \ , \tag{2.15}$$

where a is the inner radius of the cylinder. And for problem 3, Z_w is the wave impedance of an elementary magnetic dipole evaluated at the inner surface of the sphere. When the wavelength of the field is much larger than the inner radius of the sphere, Z_w becomes formally identical to (2.15) with "a" replaced by the inner radius of the sphere.

Thus, we can summarize the principal results of Schelkunoff's theory very concisely as follows: The shielding effectiveness of plane, cylindrical, and spherical metal sheets against electric and magnetic fields is given by

$$\left.\begin{aligned} &SE = A + 20\log(|Z_w|/c|Z_i|) \quad = \quad SE(E) \quad = \quad SE(H), \\ &\text{where} \\ &A = 8.686(\pi\mu\sigma f)^{\frac{1}{2}}\, d, \\ &Z_i = (j2\pi f\mu/\sigma)^{\frac{1}{2}}, \\ &c = \begin{cases} 4 \text{ for planes and cylinders} \\ 3 \text{ for spheres,} \end{cases} \end{aligned}\right\} \tag{2.16}$$

and Z_w is the wave impedance of the source field evaluated at the surface of the shield.

In the years since Schelkunoff developed his theory, a conviction has grown among many investigators that (2.16) is in some sense a universal shielding formula applicable to virtually any combination of source and shield provided c and Z_w are chosen correctly. Vasaka[11] was apparently the first to act on

11 C. S. Vasaka, Rept. NADC-EL-N5507, U.S. Naval Air Development Center, (1955).

to

$$R = 20\log(1/4|k|) \tag{2.9}$$

and

$$R = 20\log(1/3|k|), \tag{2.10}$$

respectively. Thus the reflection term for all three problems can be written in the form

$$R = 20\log(|Z_w|/c|Z_i|), \tag{2.11}$$

where c is equal to 4 for problems 1 and 2 and 3 for problem 3. To evaluate Z_i, Schelkunoff again used his assumption that the shield is a good conductor and that the field within the shield is a plane wave. He obtained

$$Z_i = (j2\pi f\mu/\sigma)^{\frac{1}{2}}. \tag{2.12}$$

Thus Z_i like A is independent of shield and source geometry; it is given by (2.12) for all three problems. In contrast to Z_i, Z_w is not the same for all three problems, and it is this factor that largely accounts for the difference in SE shown by the three shields. Here Z_w is equal to the ratio of orthogonal components of the incident electric and magnetic fields tangent to the surface of the shield. That is,

$$Z_w = E_q^i/H_p^i . \tag{2.13}$$

Therefore, Z_w must be separately evaluated for each source. This is a relatively straightforward process for all three problems since the source fields all propagate in a direction perpendicular to the surfaces of the shields. That is, E_q^i and H_p^i are equal to the transverse components of the source fields. For problem 1, Z_w is the characteristic impedance of a plane wave

$$Z_w = (\mu_o/\varepsilon_o)^{\frac{1}{2}}, \tag{2.14}$$

where μ_o and ε_o are the permeabiltiy and permittivity of free space. For problem 2, Z_w is the characteristic impedance of a

the wall, and B accounts for the second and all succeeding reflections within the wall. In most cases of interest, $A + R >> B$ so that (2.4) reduces to

$$SE = A + R \ . \tag{2.5}$$

The absorption term depends only on the conductivity σ, permeability μ, and thickness d of the metal in the wall of the shield and on the frequency f of the source. For all three problems A is given by

$$A = 8.686(\pi\mu\sigma f)^{\frac{1}{2}} \ d \ . \tag{2.6}$$

Schelkunoff obtains equation (2.6) by assuming that the shield is a good conductor in the usual sense (displacement currents negligible compared to conduction currents) and that fields within the wall can be approximated by plane waves regardless of the shape of the shield or the character of the field outside the wall. Thus, A is independent of the type of shield and of the structure of the source field. The reflection term does depend on both the shape of the shield and the source field, but it does so in a very simple way. For problems 1 and 2, he obtained:

$$R = 20\log(|k + 1|^2 /4|k|) \tag{2.7}$$

and for problem 3

$$R = 20\log[|(k + 1)\ (k/2 +1)|/3|k|], \tag{2.8}$$

where k is the ratio of the intrinsic impedance of the shield Z_i to the wave impedance of the incident field Z_w. The magnitude $|k| = |Z_i/Z_w|$ is a measure of the change in structure undergone by the field as it enters or leaves the shield. Large ($>>1$) or small ($<<1$) values of $|k|$ correspond to large impedance mismatches at the surface of the shield which yield large values of R. For practical shields, $|k| << 1$ so that (2.7) and (2.8) reduce

of the incident field on one side of the shield and the transmitted field on the other side.

The expressions derived by Schelkunoff for the shield efficiency - now called shielding effectiveness - are remarkable in several respects. In the first place, the shielding properties of each combination of source and shield are characterized by a single expression for SE regardless of whether SE is defined in terms of electric or magnetic fields. That is, if

$$SE(H) \equiv 20\log(|H_p^i|/|H_p^t|) \tag{2.1}$$

and

$$SE(E) \equiv 20\log(|E_q^i|/|E_q^t|), \tag{2.2}$$

then

$$SE = SE(H) = SE(E), \tag{2.3}$$

where E_q^i and H_p^i are components of the incident electric and magnetic fields tangent to the surface of the shield, E_q^t and H_p^t are corresponding components of the transmitted fields, and p and q refer to an orthogonal coordinate system. Thus, each of these structures shields the electric field precisely as well,or poorly, as it shields the magnetic field when both fields are generated by the specified source.

Even more striking is the fact that for each problem SE can be written in the form

$$SE = A + R + B, \tag{2.4}$$

where A represents an absorption loss sustained by the field on a one way transit through the wall of the shield, R represents a loss due to initial reflections of the field at both surfaces of

2. INTRODUCTION

During the late 1930's and early 1940's, S. A. Schelkunoff developed a theory that attempted to encompass most of what was known about how an electromagnetic field generated by a time harmonic source can be effectively excluded from a specified region through the use of shields constructed from planar, cylindrical, and spherical sections of sheet metal.[3,10] He considered continuous shields with single walls of uniform composition and thickness,and he based his theory on a model of the source and shield as a discontinuous transmission line driven at one end by a generator and terminated at the other by a lumped impedance. Using the mathematical analogy between voltage and current waves on a transmission line and transverse electromagnetic fields propagating in a medium, he transformed solutions to the model transmission line equations into solutions of Maxwell's equations for the electric and magnetic fields on both surfaces of the shield. He called this the transmission theory of shielding, and he applied it to three classical shielding problems:

1. A plane sheet exposed to plane wave fields propagating in a direction perpendicular to the plane of the sheet.
2. A cylindrical shell exposed to fields from current filaments on the central axis of the cylinder.
3. A spherical shell exposed to fields from a small loop antenna at its center.

For each of these problems, Schelkunoff obtained a closed form expression representing the shield efficiency (SE) which he defined as the difference in dB between the amplitude levels

---

3 S. A. Schelkunoff, Electromagnetic Waves, Van Nostrand, Princeton, N.J. (1943).

10 S. A. Schelkunoff, Bell System Technical Journal,17 (1938), 17.

derived quantity and a theoretically derived expression would ordinarily be considered excellent. Evidently Axford et al[9] did not consider the fact that the correction factor is defined in terms of the difference between shielding effectiveness as seen by two different sources. This means that systematic errors in either measured or computed values of shielding effectiveness will not affect the correction factor provided the errors are the same for both sources. Since the largest errors observed by Axford et al are exactly of this type, these errors cancel, and $\delta^e = \delta - 3$ dB.

It is clear from the preceding that the assumptions used in Monroe[2] have raised important questions that remain unanswered: Under what circumstances can small loop and monopole antennas be approximated by magnetic and electric dipoles for near field calculations? And, when can Schelkunoff's formula be used to investigate practical enclosures? The first of these is a technical question that can be answered by the straightforward (but tedious) method of computing near fields of the antennas and comparing these with the near fields of the dipoles. The second, however, involves fundamental problems in electromagnetic shielding theory that have no easy solutions. These questions, among others will be discussed in the following sections.

---

2 R. L. Monroe, EMP Shielding Effectiveness and MIL-STD-285, Harry Diamond Laboratories, HDL-TR-1636, (July 1973).

9 R. Axford, R. McCormack, and R. Mittra, Evaluation of the Applicability of Standard CW EMI/RFI Shielding Effectiveness Test Techniques to Assessment of EMP Hardness of Tactical Shelters, Construction Engineering Research Laboratories, CERL-TM-M-307, (March 1982).

noted "reasonable" agreement for monopole antennas; but found that "agreement for loop antennas was not acceptable." They concluded that "extension of the transmission line theory approach to slotted shields yielded inaccurate results especially for loop antennas."

In reaching this conclusion, Axford et al [9] apparently overlooked or discounted the fact that their shielding effectiveness measurements are quite consistent with the correction factor obtained in Monroe[2] . This can be seen by taking the difference $SE_M^m - SE_L^m$, where SE_M^m and SE_L^m are the measured values of shielding effectiveness at a specified frequency for the monopole and loop, and comparing this difference with $SE_{ED} - SE_{MD} = 2\delta$ from equation (5.12) of Monroe[2] where SE_{ED} and SE_{MD} are the corresponding computed values of shielding effectiveness for electric and magnetic dipoles and δ is the correction factor (eq. 5.9). For the case of an enclosure with a ½ meter slot in one side, the reader can easily verify that the difference between $SE_M^m - SE_L^m$ and $SE_{ED} - SE_{MD}$ is approximately 6 dB over the entire range of frequencies at which measurements were made. Since the accuracy of these measurements is probably no better than 6 dB, this must be considered satisfactory agreement. Similar agreement is found in the case of an enclosure with a 1 meter slot. Furthermore, if one defines an experimental correction factor $\delta^e \equiv (SE_M^m - SE_L^m)/2$ and compares this with δ, the two quantities will be found to differ by only 3dB over the entire frequency range. Agreement like this between an experimentally

---

2 R. L. Monroe, EMP Shielding Effectiveness and MIL-STD-285, Harry Diamond Laboratories, HDL-TR-1636, (July 1973).

9 R. Axford, R. McCormack, and R. Mittra, Evaluation of the Applicability of Standard CW EMI/RFI Shielding Effectiveness Test Techniques to Assessment of EMP Hardness of Tactical Shelters, Construction Engineering Research Laboratories, CERL-TM-M-307, (March 1982).

than Schelkunoff's transmission line theory. However, they accepted those results in Monroe[2] that pertained to continuous shields as a "reasonable approximation" without attempting an independent verification, and they limited themselves to the case of a discontinuous plane shield with a narrow rectangular slot. Somewhat surprisingly in view of their stated preference, they did not use a plane wave expansion to analyze this problem. Rather, they applied a variation on the classical dipole approximation technique. With this approach,they computed the magnetic field transmitted through the shield from a magnetic dipole located 12 inches away, and with the aid of a reference field they constructed plots of the shielding effectiveness. Like the previous group, Axford et al [9] obtained no closed form expressions relying instead on purely numerical results. However, unlike their predecessors, they did no shielding effectiveness calculations for plane waves or electric dipole fields. Therefore, they were unable to compute a correction factor for comparison with those obtained in the earlier studies. Their experimental work, although very useful, was also incomplete. It did not include a direct test of the principal result of Monroe[2], namely, the correction factor, but was limited to shielding effectiveness measurements on a steel enclosure prepared with narrow slots on one wall. These measurements were made with small loop and monopole antennas following MIL-STD-285 procedures. When Axford et al compared their measurements with corresponding values computed with Schelkunoff's formula as modified in Monroe[2], they

---

2 R. L. Monroe, EMP Shielding Effectiveness and MIL-STD-285, Harry Diamond Laboratories, HDL-TR-1636, (July 1973).

9 R. Axford, R. McCormack, and R. Mittra, Evaluation of the Applicability of Standard CW EMI/RFI Shielding Effectiveness Test Techniques to Assessment of EMP Hardness of Tactical Shelters, Construction Engineering Research Laboratories, CERL-TM-M-307, (March 1982).

wave expansion technique to solve for the fields transmitted through a flat sheet of metal from electric and magnetic dipole sources located 12 inches away. Then they calculated a correction factor that differs from the one in Monroe[2] by approximately 6 dB over a frequency range of 8 decades. They interpreted this difference as an improvement in accuracy which they cited in support of their claim that plane wave expansions represent the most promising approach to shielding problems of this type. However, they presented no evidence to support their interpretation of the 6 dB difference, and they could not obtain a closed form expression for their correction factor. Their method yielded only numerical results whose accuracy cannot be assessed on the basis of the information provided in the report. Furthermore, they treated only the case of a continuous plane shield. They were unable to apply their technique to the more difficult case of a discontinuous shield. Thus, despite their claim, Davis et al[8] did not make a case for plane wave expansions as a preferred method for attacking shielding problems.

The problem was then studied by Axford et al[9] who used both a theoretical and an experimental approach. These investigators also expressed a preference for plane wave expansions as a "more rigorous and versatile" method for solving shielding problems

---

2 R. L. Monroe, EMP Shielding Effectiveness and MIL-STD-285, Harry Diamond Laboratories, HDL-TR-1636, (July 1973).

8 C.R. Davis, E. Villaseca, W. Blackwood, and W. Getson, An Investigation of the Validity of Applying MIL-STD-285 to EMP Shielding Effectiveness, Harris Electronic Systems Division, (15 April 1977).

9 R. Axford, R. McCormack, and R. Mittra, Evaluation of the Applicability of Standard CW EMI/RFI Shielding Effectiveness Test Techniques to Assessment of EMP Hardness of Tactical Shelters, Construction Engineering Research Laboratories, CERL-TM-M-307, (March 1982).

imated by Hertzian dipoles in the very near field and that Schelkunoff's formula can be adapted to general types of shielded enclosures. For example, it was pointed out that although Schelkunoff originally obtained his formula by applying transmission line theory to the case of an infinitely long metal cylinder enclosing axial current filaments[3] other investigators[5,6] studying different shielding problems without the aid of the transmission line theory have obtained formally identical expressions. And, with the aid of the Leontovich or impedance boundary condition[7], it was shown in Monroe[2] that Schelkunoff's transmission line theory of shielding could be applied to uniform, continuous, metallic structures of quite general shape. However a complete theoretical justification for the assumptions employed in Monroe[2] was outside the scope of the original project since time was limited and the study was undertaken in the belief that it would receive experimental verification. Unfortunately, support for the project was cut off before any measurements could be made.

Several years after the appearance of Monroe[2], the same problem was taken up by two groups of investigators who attempted to avoid some of the assumptions of the original study by taking more rigorous approaches. In 1977, Davis et al[8] used a plane

---

2 R.L. Monroe, EMP Shielding Effectiveness and MIL-STD-285. Harry Diamond Laboratories, HDL-TR-1636, (July 1973).

3 S. A. Schelkunoff, Electromagnetic Waves, Van Nostrand, Princeton, N.J., (1943).

5 J. R. Moser, IEEE Trans. EMC, EMC-9 (1967), 6.

6 P. R. Bannister, IEEE Trans. EMC, EMC-10 (1968), 2.

7 M. B. Kraichman, Handbook of Electromagnetic Propagation in Conducting Media, U.S. Gov't Printing Office, D.C., (1970).

8 C. R. Davis, E. Villaseca, W. Blackwood, and W. Getson, An Investigation of the Validity of Applying MIL-STD-285 to EMP Shielding Effectiveness, Harris Electronic Systems Division, (15 April 1977).

ficant degree of shielding (>10 dB) against dipole fields. In fact, it must be valid for all such enclosures since it is precisely the impedance mismatch between field and the wall that largely accounts for the shielding properties of the latter. In the case of an ideal continuous enclosure with no significant apertures or seams, Z_c is equal to the intrinsic impedance of the metal Z_i, and it can easily be verified that Z_i for metals most commonly used in enclosures (copper, steel , and aluminum) does satisfy the preceding inequality for all dipole fields at frequencies greater than 10 Hz. Figure 4 in Monroe[2] provides such a verification. Nonideal enclosures with surface discontinuities allow external fields to reach the interior without passing directly through any metal, and in this case the shielding properties of the enclosure may be determined primarily by a discontinuity rather than by Z_i. If a discontinuity is large enough, the characteristic impedance of the wall will be equal to the impedance of the discontinuity Z_d which is likely to be very much larger in magnitude than Z_i. That is, $|Z_c| = |Z_d| >> |Z_i|$. Since Z_d can vary over a wide range depending on the dimensions of the discontinuity, the inequality $|Z_c| = |Z_d| << |Z_w|$ will not be satisfied by all discontinuous enclosures. However, it was shown in Monroe[2] that enclosures with discontinuities in the form of a narrow rectangular slot do indeed have impedances satisfying this relationship.Moreover, such enclosures comprise a very important class since the rectangular slot is a working approximation to the type of seams and joints used most frequently in real structures[4].

Plausible arguments were given in Monroe[2] to support the the position that small loop and monopole antennas can be approx-

---

2 R. L. Monroe, EMP Shielding Effectiveness and MIL-STD-285, Harry Diamond Laboratories, HDL-TR-1636, (July 1973).

4 W. Jarva, IEEE Trans. EMC, EMC-12 (1970), 12.

that would have been measured if the enclosure had been exposed to a plane wave source at the same frequency. The correction factor allows one to estimate the protection afforded by a particular enclosure against plane wave EMP fields while avoiding the difficulty and expense of a conventional EMP simulator.

The analysis carried out in Monroe[2] is based on three fundamental assumptions. The first holds that, for purposes of computing source fields, loop and monopole antennas can be replaced by elementary magnetic and electric dipoles (Hertzian dipoles) when the distance between the antenna and the point where the field is computed is approximately equal to the loop diameter and the monopole length. The second claims that Schelkunoff's shielding formula[3] with some modifications is applicable to a general class of sources and enclosures. And the third maintains that the wave impedance of dipole fields incident on the surface of a typical metallic enclosure are much larger in magnitude than the characteristic impedance of the enclosure wall when the dipole is located 12 inches away. That is, $|Z_c| << |Z_w|$ where Z_c is the characteristic impedance of the enclosure wall, Z_w is the wave impedance of the dipole field, and Z_c and Z_w are evaluated at any point on the surface of the enclosure. The correction factor is obtained by substituting appropriate expressions for Z_c and Z_w into Schelkunoff's formula and applying the preceding inequality.

Of the three assumptions employed, only the last can be readily justified for the class of metallic enclosures considered in Monroe[2], namely, those enclosures that provide a signi-

---

2 R. L. Monroe, EMP Shielding Effectiveness and MIL-STD-285, Harry Diamond Laboratories, HDL-TR-1636, (July 1973).

3 S. A. Schelkunoff, Electromagnetic Waves, Van Nostrand, Princeton, N.J., (1943).

there would be a distinct possibility of under shielding if these predictions were used in the design of shielded enclosures according to Bridges and Miller[18]. Therefore, they recommend that Schelkunoff's equation not be used to predict the performance of shielded enclosures against low frequency fields. In defending Schelkunoff's equation, Schulz[19] claims that Cowdell[14] and Babcock[15] misused the theory; however he does not state specifically how they misused it.

Axford et al[9] also observed discrepancies between their measurements on a slotted enclosure and predictions based on Schelkunoff's equation as modified for discontinuous shields by Monroe[2]. However, these were much smaller than the discrepancies noted by Bridges and Miller[18]. They ranged from 10 to 20 dB over frequencies from 100 KHz to 20 MHz. Moreover, the predictions were all less than the measurements so that in this case a pessimistic or conservative estimate of shielding effectiveness is obtained.

---

2 R. L. Monroe, EMP Shielding Effectiveness and MIL-STD-285, Harry Diamond Laboratories, HDL-TR-1636 (July 1973).

9 R. Axford, R. McCormack, and R. Mittra, Evaluation of the Applicability of Standard CW EMI/RFI Shielding Effectiveness Test Techniques to Assessment of EMP Hardness of Tactical Shelters, Construction Engineering Research Laboratories, CERL-TM-M-307, (March 1982).

14 R. B. Cowdell, Electronics, 40 (April 1967), 92.

15 L. F. Babcock, IEEE Trans. EMC, EMC-9 (Sept. 1967), 45.

18 J. E. Bridges and D. A. Miller, IEEE Trans. EMC, EMC-10 (1968), 175.

19 R. B. Schulz, IEEE Trans. EMC, EMC-10 (March 1968), 176.

Critics of the extended transmission theory of shielding usually point to its somewhat restricted and apparently artificial basis to explain these discrepancies. They emphasize the fact that each source and shield in problems 1, 2, and 3 is carefully chosen so that the surface of the shield coincides with equiphase surfaces of the incident field exactly as required in a 1, 2, or 3 dimensional transmission line. Since this condition is not satisfied in most arrangements of source and shield, they argue that the theory cannot logically be extended to the general case. This argument is correct, but beside the point. The experimental work by Moser, Schulz, and Cowdell cited previously and the theoretical work of Moser and Bannister demonstrate conclusively that in at least one case the theory is in fact valid even though the shield is not an equiphase surface of the source. Evidently this is not a necessary condition for Schelkunoff's equation.

One must then ask: What condictions are necessary if Schelkunoff's equation is to be valid? One such condition is almost obvious, but is rarely, if ever, mentioned in the shielding literature. In all three of his shielding problems, Schelkunoff assumes that the wave impedance of the field that emerges from one surface of the shield is equal to the wave impedance of the field that was incident on the other surface. That is,

$$Z_w = E_q^i/H_p^i = E_q^t/H_p^t. \tag{2.17}$$

It is this assumption that accounts for the fact that the transmission theory predicts equal shielding for electric and magnetic fields. If (2.17) is not satisfied, then

$$E_q^i/E_q^t \neq H_p^i/H_p^t \qquad \text{and} \qquad SE(E) \neq SE(H). \tag{2.18}$$

In this case, equation (2.16) cannot be valid since it cannot equal both SE(E) and SE(H). Therefore, (2.17) is a necessary condition for Schelkunoff's equation, and one should expect to encounter difficulties when applying Schelkunoff's equation in

situations where (2.17) is not satisfied.

Schulz[19] was apparently aware of such difficulties when he pointed out that (2.17) will not be satisfied in the case of a practical shielded enclosure subject to an external field. He suggested that this fact contributed to the discrepancies between predicted and measured shielding effectiveness for enclosures. He described this simply as an erroneous assumption, but it can be described more accurately as a basic limitation of the transmission theory of shielding.

In this report, we will present a theory of shielding that does not use the transmission line model and does not assume the validity of (2.17). We will limit our development to the case of an arbitrary electromagnetic source located outside of a region that is either wholly or partly enclosed by a thin metallic shell; however it will be clear that our approach is equally valid when the source is located inside the shell. Like Schelkunoff, we will develop this theory by solving a series of canonical shielding problems; but, instead of obtaining exact solutions to a restricted class of problems, we will obtain approximate solutions to a somewhat larger class of problems. From these solutions we will recover some of the results of the extended transmission theory and pinpoint some of the errors that occur when transmission theory is applied in situations where its basic assumptions are violated.

Impedance boundary conditions are the tools we will use to construct approximate solutions to our shielding problems. A general discussion of impedance boundary conditions is given in the following section, and a technique by which they can be applied to shielding problems is described in Section 4. In

---

19 R. B. Schulz, IEEE Trans. EMC, EMC-10 (March 1968), 176.

Section 5, source fields of general interest are cast in a form that is suitable for use with impedance boundary conditions. These fields and the impedance boundary conditions are then used in Sections 6 and 7 to construct approximate solutions to a series of shielding problems of increasing complexity. In Sections 8 and 9 ,we consider transient electromagnetic sources and extend some of our results to time domain shielding problems. In later sections, we apply these to shielded enclosures exposed to EMP fields.

3. IMPEDANCE BOUNDARY CONDITIONS

3.1 General Theory

An impedance boundary condition (IBC) is a relationship between an impedance function and an electromagnetic field at the interface separating two electrically distinct media where the impedance function characterizes one medium and the electromagnetic field is defined in the other. These conditions stand in contrast to the standard boundary conditions employed in electromagnetic theory which establish relationships between comparable fields in both media. In its most frequently applied form, the IBC relates tangential field components at the interface to the impedance looking into one medium. With the two media labeled M1 and M2 as shown in figure 1, this condition can be written in vector form as follows:[20]

$$\bar{n} \times (\bar{n} \times \overline{E1}) = -\eta 2 \ (\bar{n} \times \overline{H1}), \qquad (3.1)$$

where $\overline{E1}$ and $\overline{H1}$ are electric and magnetic fields in M1, $\bar{n}$ is the unit vector normal to the interface pointing outward from M2, $\eta 2$ is the impedance looking into M2, and it is understood that (3.1) applies only at the interface. Equation (3.1) is an approximation, and only under special circumstances can it accurately represent the structure of the electromagnetic field at the interface between two media. It cannot be used to replace standard boundary conditions in the general case. However, in many cases of interest, it has been shown that (3.1) is a valid approximation, and, in these cases, the IBC can be used to simplify the problem of determining the fields in M1 and M2.

This simplification derives from the fact that (3.1) decouples the fields in M1 from the fields in M2 in a way that does not

---

20 T. B. A. Senior, IEEE Trans. on Antennas Propagt., AP-29 No. 2 (1981), 826.

IMPEDANCE BOUNDARY CONDITION
$\bar{n} \times (\bar{n} \times \overline{E1}) = -\eta 2\ (\bar{n} \times \overline{H1})$

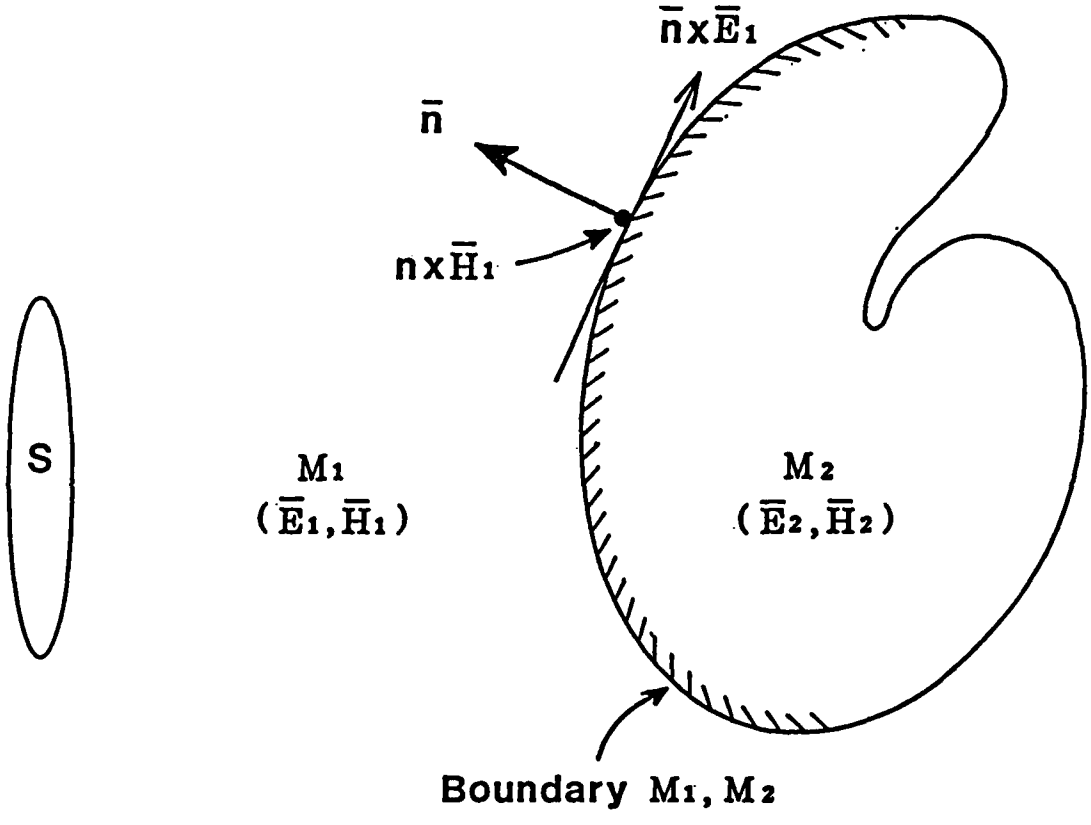

Figure 1. A medium M1 containing a source S and an electromagnetic field $\bar{E}1$, $\bar{H}1$ whose tangential components $\bar{n} \times \bar{E}1$ and $\bar{n} \times \bar{H}1$ at the boundary between M1 and a second medium M2 act as a primary source for the field $\bar{E}2$, $\bar{H}2$ in M2.

introduce spatial derivatives of the fields at the interface. This means that $\overline{E1}$ and $\overline{H1}$ can be computed independently of the fields $(\overline{E2},\overline{H2})$ in M2 and that both sets of fields can be obtained by applying standard techniques to Maxwell's equations. One first solves Maxwell's equations for $\overline{E1}$ and $\overline{H1}$ using (3.1) to replace M2 and then solves for $\overline{E2}$ and $\overline{H2}$ in M2 using $\overline{E1}$ and $\overline{H1}$ at the interface to replace M1. Since this two step process will usually be much easier than solving Maxwell's equations directly for $\overline{E1}$, $\overline{H1}$, $\overline{E2}$, and $\overline{H2}$, the utility of (3.1) is obvious. Moreover, if one is interested only in the fields in M1, then $\overline{E2}$ and $\overline{H2}$ need not be computed at all. Conversely if one is interested in $\overline{E2}$ and $\overline{H2}$, then it is only necessary to solve for $\overline{E1}$ and $\overline{H1}$ at the interface in order to determine the fields throughout M2. The latter describes the usual situation in shielding problems where M2 can be identified with the shielded volume, M1 is the region (usually free space) containing one or more electromagnetic sources, and only the fields transmitted into the shielded volume are of interest. In following sections it will be seen that the decoupling provided by (3.1) is a powerful technique for obtaining approximate solutions to a variety of shielding problems.

To take advantage of the IBC, it is necessary to establish the validity of (3.1) at the interface that defines the problem of interest. In general terms, this requires one to show that $\overline{E2}$ and $\overline{H2}$ propagate into M2 along $\bar{n}$ in the manner of a uniform plane wave. One way to do this is to show that the variation of $\overline{E2}$ and $\overline{H2}$ along $\bar{n}$ is much larger than the variation of $\overline{E1}$ and $\overline{H1}$ at the interface in directions transverse to $\bar{n}$. Specifically, one can show that the normal derivatives of $\overline{E2}$ and $\overline{H2}$ are much larger in magnitude than the transverse derivatives of $\overline{E1}$ and $\overline{H1}$ at the interface. When this condition is satisfied, $\overline{E1}$ and $\overline{H1}$ are approximately equal phase source fields at the interface, and $\overline{E2}$ and $\overline{H2}$ propagate into M2 along $\bar{n}$ as plane waves.

The impedance function is then well defined, and (3.1) accurately represents the boundary condition at the interface.

3.2 IBC for a Uniform, Planar Surface

The validity of (3.1) has been demonstrated under relatively weak restrictions in the case of a planar interface separating two homogeneous half-spaces as shown in figure 2 where M1 is free space and M2 consists of a material with complex permittivity $\varepsilon 2$ and permeability $\mu 2$. Equation (3.1) can be written in scalar form as follows

$$E1_x = -\eta 2 H1_y \quad , \quad E1_y = \eta 2 H1_x \quad \text{at} \quad z=0, \tag{3.2}$$

where the fields are referred to a rectangular coordinate system with its origin at the interface and its z axis directed out of M2 ($\bar{n} = \hat{i}_z$). It has been shown[21] that a condition sufficient to insure the accuracy of (3.2) is

$$|\mu 2 \varepsilon 2| >> \mu 1 \varepsilon 1 = \mu_o \varepsilon_o, \tag{3.3}$$

where $\varepsilon 2$ is given by

$$\varepsilon 2 = \varepsilon' - j\sigma/\omega \quad , \quad \varepsilon' > 0, \tag{3.4}$$

and ε_o and μ_o are the permittivity and permeability of free space. In (3.4), σ is the conductivity, and a time variation of $\exp(j\omega t)$ has been assumed. When (3.3) is satisfied, the fields in M2 are determined by one-dimensional, homogeneous wave equations:

$$\frac{\partial^2 \overline{E2}}{\partial z^2} + \omega^2 \mu 2 \varepsilon 2 \overline{E2} = 0 , \tag{3.5}$$

$$\frac{\partial^2 \overline{H2}}{\partial z^2} + \omega^2 \mu 2 \varepsilon 2 \overline{H2} = 0 , \tag{3.6}$$

---

21 T. B. A. Senior, Appl. Sci. Res., 8 (B) (1960), 418.

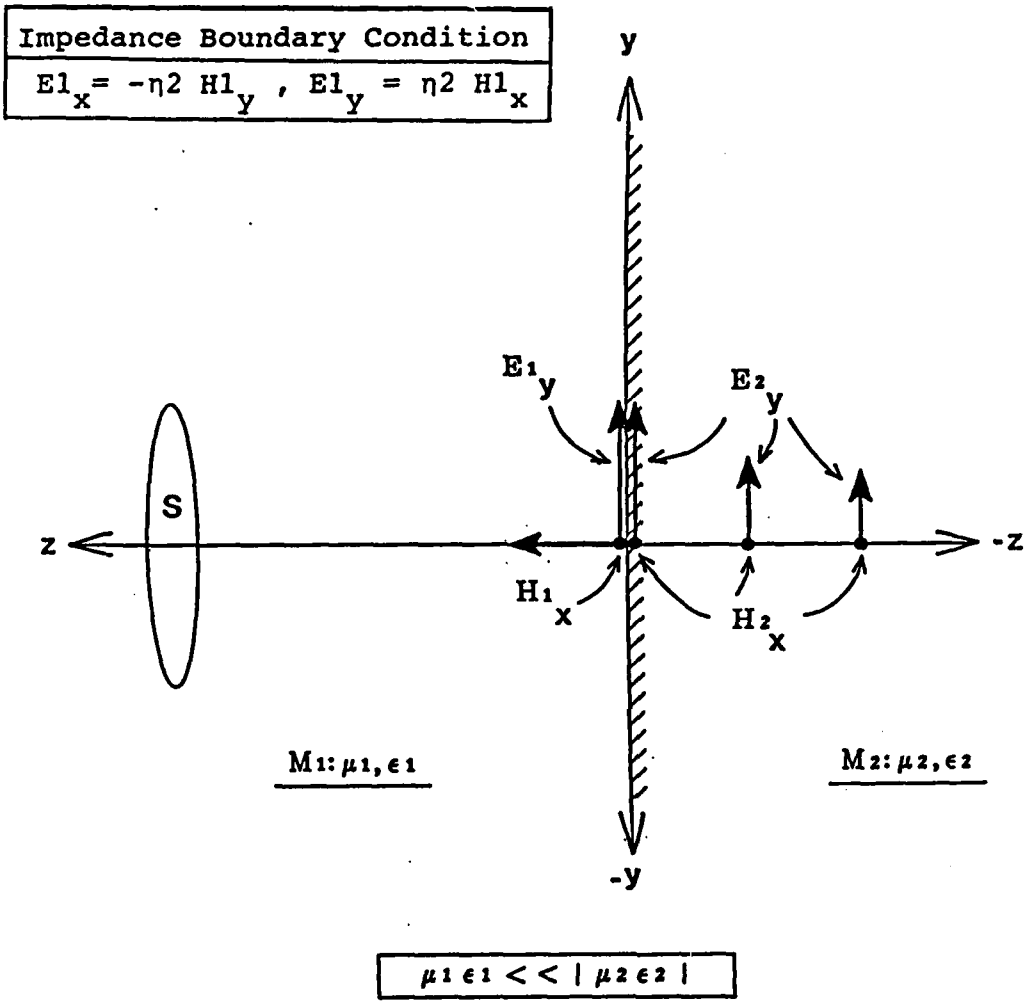

Figure 2. Two half-spaces M1 and M2 with a planar interface where an impedance boundary condition is satisfied by virtue of the relation $\mu 1\ \varepsilon 1 << |\mu 2\ \varepsilon 2|$.

and the impedance looking into M2 is equal to the intrinsic impedance of M2

$$\eta 2 = Z_i = \sqrt{\mu 2/\varepsilon 2} \ . \tag{3.7}$$

Since $\mu 2 \cong \mu_o$ in most cases of interest, (3.3) implies

$$|\eta 2| << Z_o = \sqrt{\mu_o/\varepsilon_o} = 120\pi \text{ (ohms)}, \tag{3.8}$$

where Z_o is the impedance of free space. That is, the magnitude of the impedance looking into M2 is very much smaller than the impedance of free space.

Since the real part of $\mu 2\varepsilon 2$ is defined to be positive, solutions to (3.5) and (3.6) travelling in the -z direction can be written in the form

$$\overline{E2}, \overline{H2} \propto \exp(j\omega z\sqrt{\mu 2\varepsilon 2}) = \exp[\omega z(-\text{Im}(\ ) + j\text{Re}(\ ))], \tag{3.9}$$

where Re( ) and Im( ) are the real and imaginary parts of $\sqrt{\mu 2\varepsilon 2}$ respectively. In (3.9), the decrease in amplitude with distance in M2 is controlled by the factor $\omega z\text{Im}(\ )$ which defines the skin depth δ_s according to the relation

$$\delta_s = 1/\omega|\text{Im}(\sqrt{\mu 2\varepsilon 2}\ )|. \tag{3.10}$$

When δ_s is small, the fields decay rapidly in the -z direction.

When (3.3) is satisfied, $\overline{E2}$ and $\overline{H2}$ are constrained to propagate into M2 like plane waves along the z axis, and the validity of (3.2) is assured. The latter is frequently referred to as the Leontovich Boundary Condition[22] although it was used prior to Leontovich by Rytov[23], Alpert[24], and Feinberg[25] during World War II in their work on ground wave propagation. Since

---

22 M. A. Leontovich, Investigations on Radiowave Propagation, Part II, Moscow: Academy of Sciences, (1948).

23 S. M. Rytov, J. Exp. Theor. Phys. USSR, 10 (1940), 180.

24 I. L. Alpert, J. Tech. Phys. USSR, 10 (1940), 1358.

25 E. L. Feinberg, J. Phys. USSR, 8 (1944), 317.

then, these and other investigators have shown that (3.1) is not limited in application to half-spaces but can be applied directly to more complicated structures such as the following.

3.3 Uniform, Planar Sheets

When the half-space M2 is replaced by a sheet of the same material with a uniform thickness d as shown in figure 3, the fields inside the sheet still satisfy (3.5) and (3.6) provided (3.3) remains valid. The impedance boundary condition (3.2) is then applicable at z=0 if the skin depth δ_s satisfies the additional condition

$$\delta_s < d \ . \qquad (3.11)$$

Since fields decrease in amplitude by a factor of $e^{-1} = .37 =$ 8.5 dB while travelling a distance equal to one skin depth in the sheet, (3.11) means that fields making a round trip from z=0 to z = -d and back to z=0 will be reduced by at least a factor of $e^{-2} = .14 = 17$ dB. This condition is necessary to prevent fields that are reflected at z = -d from reaching z=0 in sufficient strength to interfere with $\overline{E1}$ and $\overline{H1}$ at z=0 and render (3.1) inaccurate.

3.4 Inhomogeneous, Planar Sheet

If the electrical and magnetic properties of the sheet in figure 3 are functions of the lateral coordinates x and y, that is $\mu 2 = f(x,y)$ and $\varepsilon 2 = g(x,y)$, then the derivatives of $\mu 2$ and $\varepsilon 2$ with respect to x and y do not appear in the IBC[21], and (3.2) remains valid at all points on the boundary z=0 where (3.3), (3.8), and (3.11) are satisfied. In this case, (3.2) with $\eta 2(x,y) = \sqrt{\mu 2(x,y) / \varepsilon 2(x,y)}$ can be considered a local boundary condition.

---

21 T. B. A. Senior, Appl. Sci. Res., 8(B) (1960), 418.

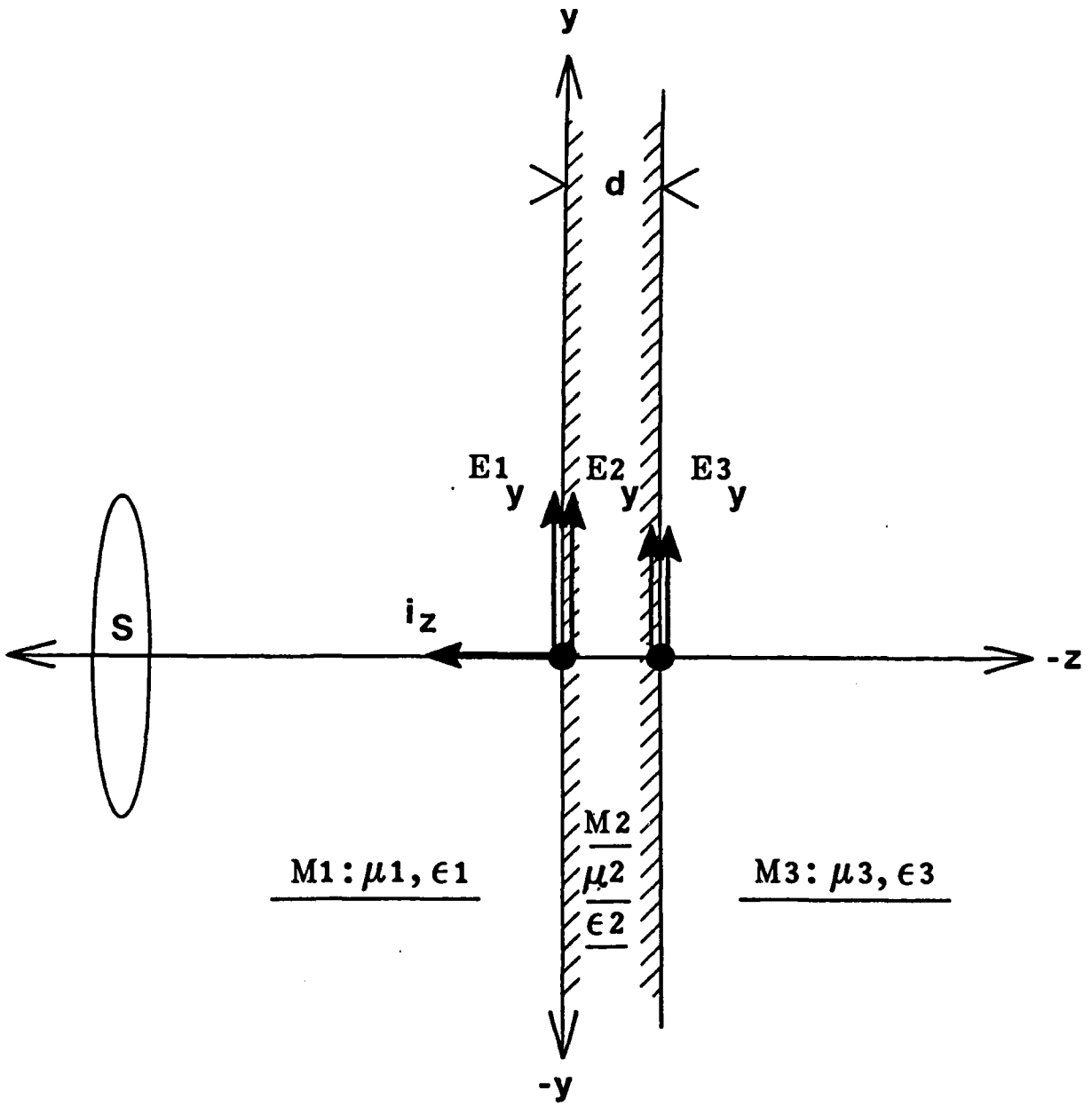

$$\mu 1 \epsilon 1 << |\mu 2 \epsilon 2|$$

$$\delta_s = 1/\omega \, \mathrm{Im}(\sqrt{\mu 2 \epsilon 2}) < d$$

Figure 3. A planar sheet of uniform thickness d separating media where an impedance boundary condition is satisfied at z = 0 by virtue of the relations $\mu 1\ \epsilon 1 << |\mu 2\ \epsilon 2|$ and $\delta_s < d$.

3.5 Uniform, Homogeneous Sheet with a Narrow, Rectangular Slot

When a narrow rectangular slot is cut through an otherwise uniform, homogeneous sheet, the sheet is rendered locally inhomogeneous and anisotropic - inhomogeneous because the effective permeability, permittivity, and impedance of the slot differ from those of the solid sheet and anisotropic because these quantities depend on the orientation of the slot. If the slot is oriented as shown in figure 4(a), then $E1_x$ and $H1_y$ will see a different impedance looking into the slot than will $E1_y$ and $H1_x$. With these two impedances denoted $\eta_x^2(x,y)$ and $\eta_y^2(x,y)$, a generalized IBC can be written

$$E1_x = -\eta_x^2(x,y)H1_y \quad ; \quad E1_y = \eta_y^2(x,y)H1_x, \tag{3.12}$$

where, in general, η_x^2 and η_y^2 are functions of the slot dimensions (l and w), the permeability and permittivity of the sheet ($\mu 2$ and $\varepsilon 2$), the permeability and permittivity of the material in the slot (if any), and ω - in addition to x and y for $-1/2 < x < 1/2$ and $-w/2 < y < w/2$. A similar IBC can be written for the vertical slot shown in figure 4(b)

$$E1_x = -\eta_x'^2(x,y)H1_y \quad ; \quad E1_y = \eta_y'^2(x,y)H1_x \ . \tag{3.13}$$

If the vertical slot is identical to the horizontal slot, then

$$\eta_x^2(0,0) = \eta_y'^2(0,0) \quad \text{and} \quad \eta_y^2(0,0) = \eta_x'^2(0,0) \ . \tag{3.14}$$

A condition sufficient to insure that $E2_x$, $H2_y$, $E2_y$, and $H2_x$ propagate in the manner of plane waves can be written

$$\left.\begin{matrix}|\eta_x^2| \\ |\eta_y^2|\end{matrix}\right\} << Z_o = \sqrt{\mu_o/\varepsilon_o} \ . \tag{3.15}$$

Horizontal Slot

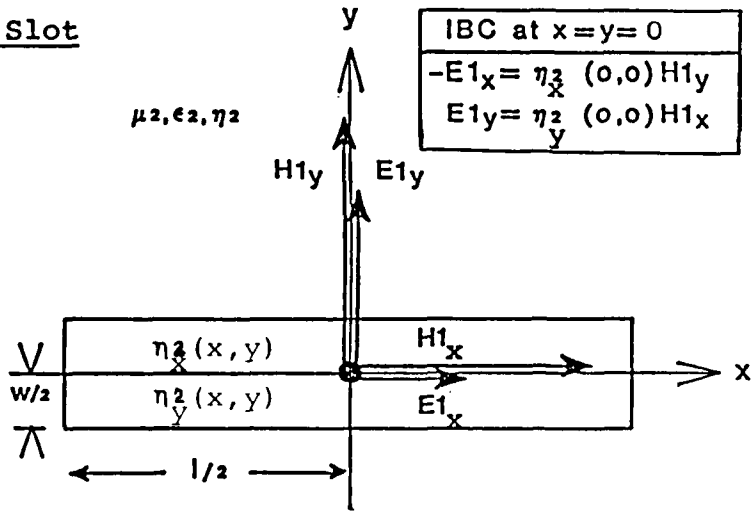

Vertical Slot

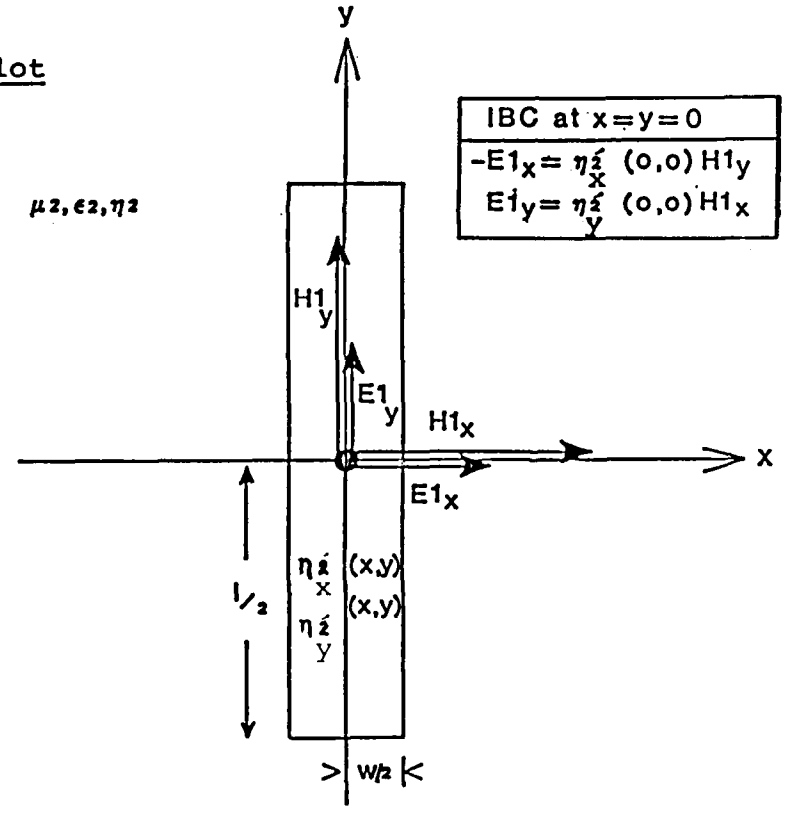

Figure 4. Impedance boundary conditions at the center of horizontal (a) and vertical (b) slots. For identical slots: $\eta_x^2 = \eta_y^{2'}$; $\eta_y^2 = \eta_x^{2'}$ at x = 0, y = 0.

!:M3 interface at P´(x,y,-d), formal expressions for $E3_x(x,y,-d)$, $_y(x,y,-d)$, $H3_x(x,y,-d)$, and $H3_y(x,y,-d)$ in terms of correspond-g components of the internal fields can be written as follows:

$$E3_x(x,y,-d) = TE\ E2_x(x,y,-d) ,$$

$$E3_y(x,y,-d) = TE\ E2_y(x,y,-d) ,$$

$$H3_x(x,y,-d) = TH\ H2_x(x,y,-d) , \tag{4.21}$$

$$H3_y(x,y,-d) = TH\ H2_y(x,y,-d) ,$$

here TE is the transmission coefficient for electric fields and H is the transmission coefficient for magnetic fields.For plane ave fields incident normally on a planar surface separating two issimilar media, TE and TH are given by[3]

$$TE = 2\ \eta 3\ /\ (\eta 2 + \eta 3) ,$$

$$TH = 2\ \eta 2\ /\ (\eta 2 + \eta 3) , \tag{4.22}$$

here η2 is the wave impedance of fields in M2 and η3 is the wave mpedance of the fields at z = -d looking into M3.

Finally, by substituting (4.19) into (4.21), we obtain the ollowing expressions for the fields inside the shield at ´(x,y,-d) in terms of the source fields incident on the outside f the shield at a point P(x,y,0) not located in a slot:

$$E3_x(x,y,-d) = -\ 2\ \eta 2\ H1_y^s(x,y,0)\ TE\ \exp(-j\omega d\sqrt{\mu 2\ \varepsilon 2}) ,$$

$$E3_y(x,y,-d) = \quad 2\ \eta 2\ H1_x^s(x,y,0)\ TE\ \exp(-j\omega d\sqrt{\mu 2\ \varepsilon 2}) , \tag{4.23}$$

$$H3_x(x,y,-d) = \quad 2\ H1_x^s(x,y,0)\ TH\ \exp(-j\omega d\sqrt{\mu 2\ \varepsilon 2}) ,$$

$$H3_y(x,y,-d) = \quad 2\ H1_y^s(x,y,0)\ TH\ \exp(-j\omega d\sqrt{\mu 2\ \varepsilon 2}) .$$

. S.A. Schelkunoff, Electromagnetic Waves, Van Nostrand, Princeton, N.Y., (1943).

$$H2_x(x,y,z) = 2\, H1_x^s(x,y,0)\, \exp(j\omega z\sqrt{\mu 2\ \varepsilon 2}) ,$$

$$H2_y(x,y,z) = 2\, H1_y^s(x,y,0)\, \exp(j\omega z\sqrt{\mu 2\ \varepsilon 2}) ,$$

And by a similar process using (4.7), we obtain the following expressions for the fields launched into M2 when P(x,y,0) lies in the i-th slot:

$$\begin{aligned}
E2_x(x,y,z) &= -2\, \eta 2_x^i\, H1_y^s(x,y,0)\, \exp(j\omega z\ \mu 2_x^i / \eta 2_x^i) , \\
H2_y(x,y,z) &= 2\, H1_y^s(x,y,0)\, \exp(j\omega z\ \mu 2_x^i / \eta 2_x^i) , \\
E2_y(x,y,z) &= 2\, \eta 2_y^i\, H1_x^s(x,y,0)\, \exp(j\omega z\ \mu 2_y^i / \eta 2_y^i) , \\
H2_x(x,y,z) &= 2\, H1_x^s(x,y,0)\, \exp(j\omega z\ \mu 2_y^i / \eta 2_y^i) .
\end{aligned} \qquad (4.20)$$

With (4.19) and (4.20), the solution to the internal problem is completely determined. This solution will also include field components in the z direction ($E2_z$ and $H2_z$); however, these are small compared to the transverse components, and we will not display them here. They can be computed by substituting (4.19) and (4.20) into Maxwell's Equations.

Having solved the internal problem for $\overline{E2}$ and $\overline{H2}$, we can now address the shielding problem. The latter requires us to compute the fields from S that penetrate M2 and reach the shielded volume M3 as shown in figure 5. Therefore, our objective is to compute the tangential components of $\overline{E3}$ and $\overline{H3}$ at a point P´(x,y,-d) on the interface between M2 and M3. Since these fields are generated by partial reflection and transmission of the internal field (4.19) and (4.20) incident normally on the

the validity of this approximation is due to the fact that the tangential magnetic field at the boundary is equal to the sum of two large, nearly equal quantities

$$\hat{i}_z \times \overline{H1}(x,y,0) = \hat{i}_z \times [\overline{H1}^s(x,y,0) + \overline{H1}^r(x,y,0)] ,$$

which is insensitive to a small error $\overline{H1}'$ in $\overline{H1}^r$. Hence,

$$\hat{i}_z \times \overline{H1}(x,y,0) = 2\ \hat{i}_z \times \overline{H1}^s(x,y,0) , \qquad (4.17)$$

which implies (4.11). This is in contrast to the tangential electric field at the boundary which is equal to the difference between two large, nearly equal quantities. Here a small error $\overline{E1}'$ in $\overline{E1}^r$ cannot be neglected because it would produce a large error in the tangential electric field. It is precisely the IBC that allows us to compute $\overline{E1}'$ so that the boundary condition can be satisfied.

With (4.11), we can eliminate $H1_x^r(x,y,0)$ and $H1_y^r(x,y,0)$ from (4.10) and obtain

$$\begin{aligned} E2_x(x,y,0) &= -\ 2\ \eta 2\ H1_y^s(x,y,0) , \\ E2_y(x,y,0) &= \quad 2\ \eta 2\ H1_x^s(x,y,0) , \\ H2_x(x,y,0) &= 2\ H1_x^s(x,y,0) , \\ H2_y(x,y,0) &= 2\ H1_y^s(x,y,0) . \end{aligned} \qquad (4.18)$$

Substituting (4.18) into (4.6), we obtain the following expressions for the fields launched into M2 at P(x,y,0)

$$\begin{aligned} E2_x(x,y,z) &= -\ 2\ \ \eta 2\ H1_y^s(x,y,0)\ \exp(\ j\omega z\sqrt{\mu 2\ \varepsilon 2}\ ) , \\ E2_y(x,y,z) &= \quad 2\ \ \eta 2\ H1_x^s(x,y,0)\ \exp(\ j\omega z\sqrt{\mu 2\ \varepsilon 2}\ ) , \end{aligned} \qquad (4.19)$$

component of the reflected magnetic field is approximately equal to the tangential component of the incident field:

$$\hat{i}_z \times \overline{H1}^r(x,y,0) = \hat{i}_z \times \overline{H1}^s(x,y,0) \ . \qquad (4.11)$$

Now it must be clearly understood that in using (4.11), we are <u>not</u> attempting to substitute a perfect conductor for a good conductor. The difference between a perfect conductor and a good conductor can be described as follows: At the surface of a perfect conductor the tangential electric field is zero

$$\hat{i}_z \times \overline{E1}(x,y,0) = \hat{i}_z \times [\overline{E1}^s(x,y,0) + \overline{E1}^r(x,y,0)] = 0 \ . \qquad (4.12)$$

This implies

$$\hat{i}_z \times \overline{E1}^r(x,y,0) = - \hat{i}_z \times \overline{E1}^s(x,y,0) \ , \qquad (4.13)$$

and

$$\hat{i}_z \times \overline{H1}^r(x,y,0) = \hat{i}_z \times \overline{H1}^s(x,y,0) \ . \qquad (4.14)$$

On the other hand, at the surface of a good (but not perfect) conductor, $\hat{i} \times \overline{E1}(x,y,0)$ is small but not zero. This implies

$$\hat{i}_z \times \overline{E1}^r(x,y,0) = - \hat{i}_z \times \overline{E1}^s(x,y,0) + \overline{E1}' \ , \qquad (4.15)$$

where $|\overline{E1}'| << |\overline{E1}^r|, |\overline{E1}^s|$ and

$$\hat{i}_z \times \overline{H1}^r(x,y,0) = \hat{i}_z \times \overline{H1}^s(x,y,0) + \overline{H1}' \ , \qquad (4.16)$$

where $|\overline{H1}'| << |\overline{H1}^s|, |\overline{H1}^r|$. Although it happens that the approximation represented by (4.11) is identical to (4.14), this fact is irrelevant in the present application. Equation (4.11) is actually an approximation to (4.16). As Adler et al[26] point out,

---

26 R. B. Adler, L. J. Chen, and R. M. Fano, <u>Electromagnetic Energy Transmission and Radiation</u>, John Wiley and Sons,Inc., N.Y., p. 432 (1960).

If the external problem has been solved for $\overline{E1}$ and $\overline{H1}$, then $E2_x(x,y,0)$, $E2_y(x,y,0)$, $H2_x(x,y,0)$, and $H2_y(x,y,0)$ can be computed directly from (4.9) to obtain a solution to the internal problem. However, a complete solution to the external problem is not necessary in order to solve the internal problem. Suppose the external problem has been solved for $\overline{H1}$ but not $\overline{E1}$. Equation (4.9) can still be used to compute $H2_x(x,y,0)$ and $H2_y(x,y,0)$, but it cannot be used to compute $E2_x(x,y,0)$ and $E2_y(x,y,0)$ because $E1_x(x,y,0)$ and $E1_y(x,y,0)$ have not been determined. Here the IBC (Equations (4.4) and (4.5)) can be used to replace $E1_x(x,y,0)$ and $E1_y(x,y,0)$ in (4.9). With (4.4) this gives

$$
\begin{aligned}
E2_x(x,y,0) &= -\eta 2\,[H1_y^s(x,y,0) + H1_y^r(x,y,0)]\ , \\
E2_y(x,y,0) &= \eta 2\,[H1_x^s(x,y,0) + H1_x^r(x,y,0)]\ , \\
H2_x(x,y,0) &= H1_x^s(x,y,0) + H1_x^r(x,y,0)\ , \\
H2_y(x,y,0) &= H1_y^s(x,y,0) + H1_y^r(x,y,0)\ .
\end{aligned}
\tag{4.10}
$$

And with (4.5) similar expressions can be written when $P(x,y)$ lies in the i-th slot. When the right side of (4.10) is known, $E2_x(x,y,0)$, $E2_y(x,y,0)$ etc., can be determined as before. Thus, the IBC can be used to obtain the internal field even when the external problem has not been completely solved.

But how can $H1_x(x,y,0)$ and $H1_y(x,y,0)$ be computed without resorting to a complete solution to the external problem? Since our objective is to solve the internal problem in terms of the source fields ($H1_x^s(x,y,0)$ and $H1_y^s(x,y,0)$, this question reduces to: How can we compute the reflected fields $H1_x^r(x,y,0)$ and $H1_y^r(x,y,0)$ without solving the external problem? To answer this question, we make use of an approximation that is always valid at the surface of a good conductor. Namely, that the tangential

and

$$E2_x(x,y,z) = E2_x(x,y,0)\ \exp(\ j\omega z\ \ \mu_{x}^{i2}\ /\ \eta_{x}^{i2}\ )\ ,$$

$$H2_y(x,y,z) = H2_y(x,y,0)\ \exp(\ j\omega z\ \ \mu_{x}^{i2}\ /\ \eta_{x}^{i2}\ )\ ,$$

$$E2_y(x,y,z) = E2_y(x,y,0)\ \exp(\ j\omega z\ \ \mu_{y}^{i2}\ /\ \eta_{y}^{i2}\ )\ , \qquad (4.7)$$

$$H2_x(x,y,z) = H2_x(x,y,0)\ \exp(\ j\omega z\ \ \mu_{y}^{i2}\ /\ \eta_{y}^{i2}\ )\ ,$$

where (4.6) applies when P(x,y,0) is not in one of the slots and (4.7) applies when P(x,y,0) lies in the i-th slot.

Equations (4.6) and (4.7) show clearly how the IBC simplifies the solution to the internal problem: To determine the internal fields traveling away from the interface, we need only evaluate $E2_x(x,y,0)$, $H2_y(x,y,0)$, $E2_y(x,y,0)$, and $H2_x(x,y,0)$. This can be done by applying standard boundary conditions at z = 0 since these conditions are in no way superceded by IBC's. Continuity of tangential field components at z = 0 gives

$$\lim_{z\longrightarrow 0^+}\ [\ \hat{i}_z \times \overline{E1}(x,y,z)\ ] = \lim_{z\longrightarrow \bar{0}}\ [\ \hat{i}_z \times \overline{E2}(x,y,z)\ ]\ ,$$

and (4.8)

$$\lim_{z\longrightarrow 0^+}\ [\ \hat{i}_z \times \overline{H1}(x,y,z)\ ] = \lim_{z\longrightarrow \bar{0}}\ [\ \hat{i}_z \times \overline{H2}(x,y,z)\ ]\ .$$

Or, explicitly

$$E2_x(x,y,0) = E1_x(x,y,0) = E1_x^s(x,y,0) + E1_x^r(x,y,0)\ ,$$

$$E2_y(x,y,0) = E1_y(x,y,0) = E1_y^s(x,y,0) + E1_y^r(x,y,0)\ , \qquad (4.9)$$

$$H2_x(x,y,0) = H1_x(x,y,0) = H1_x^s(x,y,0) + H1_x^r(x,y,0)\ ,$$

$$H2_y(x,y,0) = H1_y(x,y,0) = H1_y^s(x,y,0) + H1_y^r(x,y,0)\ .$$

that l_i is much smaller than the wavelength of $\overline{E1}$ and $\overline{H1}$ and if d is sufficient to reduce the amplitude of any field passing through any slot by at least 10 dB, then it can be shown that conditions (3.15) and (3.26) are satisfied. Under these conditions, an IBC will be valid at all points on the surface of M2. At the point P(x,y,0) on ES1, the IBC can be written

$$E1_x^s(x,y,0) + E1_x^r(x,y,0) = -\eta 2\ [H1_y^s(x,y,0) + H1_y^r(x,y,0)],$$
$$E1_y^s(x,y,0) + E1_y^r(x,y,0) = \eta 2\ [H1_x^s(x,y,0) + H1_x^r(x,y,0)], \tag{4.4}$$

when P(x,y,0) is not a point in one of the slots, and

$$E1_x^s(x,y,0) + E1_x^r(x,y,0) = -\eta 2_x^i(x,y)\ [H1_y^s(x,y,0) + H1_y^r(x,y,0)],$$
$$E1_y^s(x,y,0) + E1_y^r(x,y,0) = \eta 2_y^i(x,y)\ [H1_x^s(x,y,0) + H1_x^r(x,y,0)], \tag{4.5}$$

when P(x,y,0) is in the i-th slot. These IBC's imply that $E2_x$, $H2_y$, $E2_y$, and $H2_x$ have the form of plane waves traveling away from the interface in the -z direction. We can therefore write these fields in the following form using (3.9), (3.20) and (3.21):

$$E2_x(x,y,z) = E2_x(x,y,0)\ \exp(\ j\omega z\sqrt{\mu 2\ \varepsilon 2}\ ),$$
$$H2_y(x,y,z) = H2_y(x,y,0)\ \exp(\ j\omega z\sqrt{\mu 2\ \varepsilon 2}\ ),$$
$$E2_y(x,y,z) = E2_y(x,y,0)\ \exp(\ j\omega z\sqrt{\mu 2\ \varepsilon 2}\ ), \tag{4.6}$$
$$H2_x(x,y,z) = H2_x(x,y,0)\ \exp(\ j\omega z\sqrt{\mu 2\ \varepsilon 2}\ ),$$

Since the z axis is constrained to pass through C, the location of O with respect to the edges of ES1 depends on S. But the position of S is arbitrary with respect to ES1; hence, the position of O on ES1 is also arbitrary. That is, the coordinate system is attached to the source, and must move when the source is moved parallel to ES1. Here, again, it is convenient to choose a special arrangement: namely, the one shown in figure 5(b) where the z axis passes through the geometric center of ES1. This in no way limits the application of IBC's since one is always free to move the location of O on ES1 when S is moved. With this understanding, the components of $\overline{E1}$ and $\overline{H1}$ tangent to ES1 at a point P(x,y,0) can be written from (4.1):

$$
\begin{aligned}
E1_x(x,y,0) &= E1_x^s(x,y,0) + E1_x^r(x,y,0) \ , \\
E1_y(x,y,0) &= E1_y^s(x,y,0) + E1_y^r(x,y,0) \ , \\
H1_x(x,y,0) &= H1_x^s(x,y,0) + H1_x^r(x,y,0) \ , \\
H1_y(x,y,0) &= H1_y^s(x,y,0) + H1_y^r(x,y,0) \ .
\end{aligned}
\tag{4.3}
$$

Our first objective is to compute $E2_x(x,y,z)$, $E2_y(x,y,z)$, $H2_x(x,y,z)$, and $H2_y(x,y,z)$ for $-d < z < 0$ in terms of the tangential components $H1_x^s(x,y,0)$ and $H1_y^s(x,y,0)$ of the source magnetic field.

If M2 like all electromagnetic shields is composed of material belonging to the class of "good conductors" and if the thickness d of this material is sufficient to reduce the amplitude of any field passing through the shield by at least 10 dB, then it can be shown[2] that conditions (3.3) and (3.11) are satisfied. Likewise, if all the slots penetrating M2 are such

---

2 R. L. Monroe, EMP Shielding Effectiveness and MIL-STD-285, Harry Diamond Laboratories, HDL-TR-1636, (July 1973).

and thickness except in certain areas where they are penetrated by narrow, rectangular slots S1, S2...Sn. The material comprising the uniform part of the shield is characterized by permeability $\mu 2$, permittivity $\varepsilon 2$, and intrinsic impedance $\eta 2$ as defined in section 3.2. The slots are characterized by pairs of functions representing their effective permeabilities, permittivities, and impedances as defined in section 3.5. For the i-th slot, these can be denoted by μ_{2x}^{i} and μ_{2y}^{i}, ε_{2x}^{i} and ε_{2y}^{i}, and η_{2x}^{i} and η_{2y}^{i} respectively. The lengths and widths (not shown in the figure) of the slots are l_i and w_i, and for convenience we have assumed that they are oriented with their lengths in either the x or y directions. Each slot is assumed to lie in a single sheet, but its location is otherwise unrestricted. The source with dimensions a,b,c, is located with its geometric center C at a distance D from the nearest sheet ES1. The dimensions of ES1 are H, W, and d.

M2 can easily be transformed into several structures of considerable theoretical and practical importance. By specifying 6 or more sheets ES6, ES7 ...., it can become an enclosure completely surrounding M3. By eliminating all sheets except ES1 and letting $H,W \longrightarrow \infty$, it becomes an infinite plane sheet separating two half-spaces. And, by letting $d \longrightarrow \infty$, it becomes a simple half-space. In following sections we will consider examples of each of these structures.

To facilitate the discussion, we adopt a rectangular/cylindrical coordinate system in which the origin O is located on the outside surface of ES1 and the z axis passes through C pointing away from ES1. With this arrangement, the x,y (ρ,ϕ) plane includes the surface of ES1. The orientation of the x,y axes is arbitrary; however, for convenience, we assume that the axes are parallel to the horizontal and vertical edges of ES1.

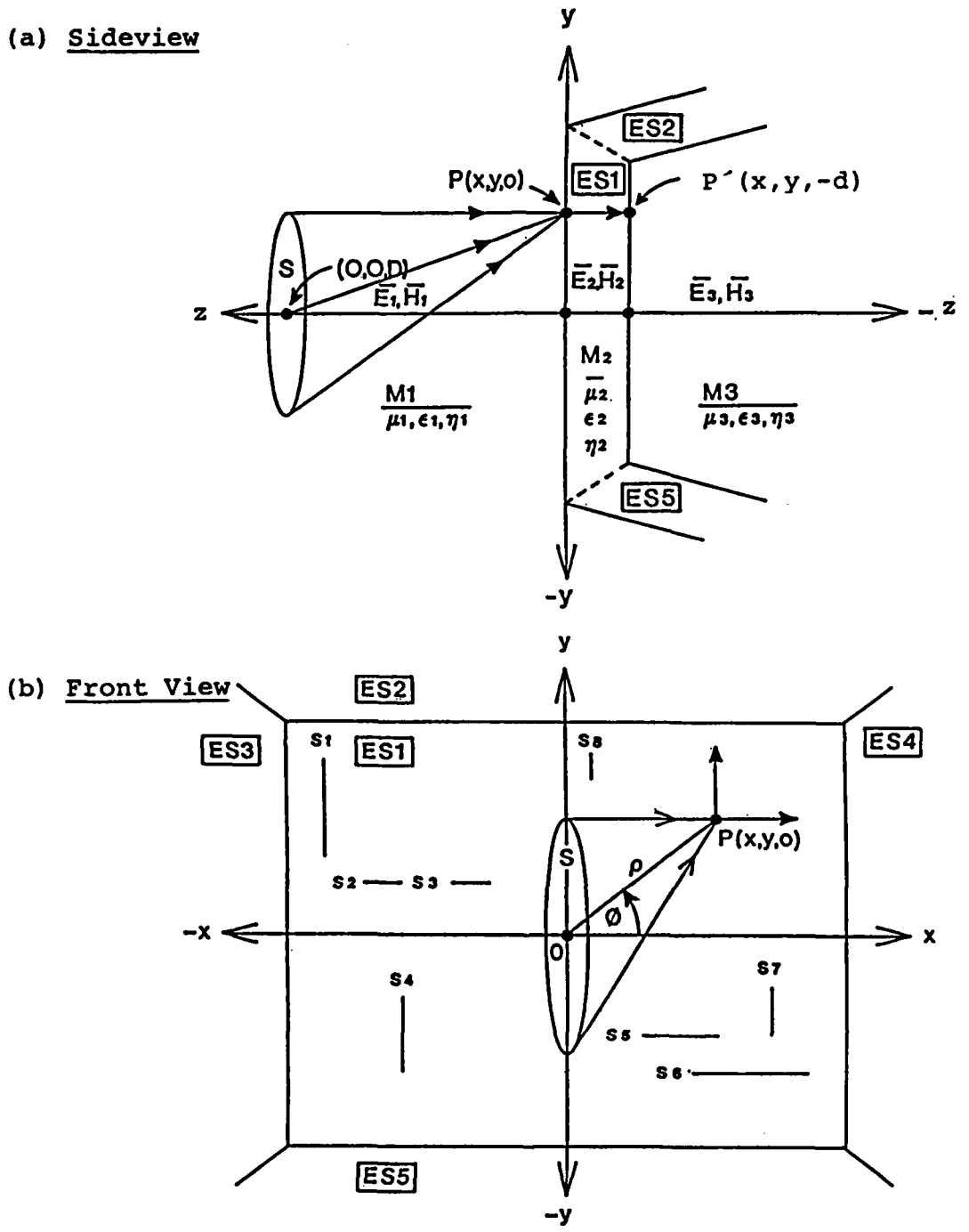

Figure 5. A generalized electromagnetic shield M2 with an arbitrary source S.

4. APPLICATION OF IMPEDANCE BOUNDARY CONDITIONS TO SHIELDING PROBLEMS

IBC's were developed originally to simplify certain scattering and propagation problems in which an electromagnetic source (S) illuminates a medium M2 that is immersed in a homogeneous medium M1 as shown in figure 1. These are called external problems because the sole objective is to compute the fields $\overline{E1}$ and $\overline{H1}$ in M1 ,

$$\overline{E1} = \overline{E1}^{s} + \overline{E1}^{r}$$
$$\overline{H1} = \overline{H1}^{s} + \overline{H1}^{r} \quad , \tag{4.1}$$

where $\overline{E1}^{s}$ and $\overline{H1}^{s}$ are the source fields and $\overline{E1}^{r}$ and $\overline{H1}^{r}$ are the reflected fields from M2. An IBC applied at the interface I between M1 and M2 ,

$$\bar{n} \times (\bar{n} \times (\overline{E1}^{s} + \overline{E1}^{r})) = -\eta 2 \, (\bar{n} \times (\overline{H1}^{s} + \overline{H1}^{r})) \quad , \tag{4.2}$$

simplifies such a problem by decoupling the fields in M1 from those in M2. This allows one to solve the external problem for $\overline{E1}$ and $\overline{H1}$ without the necessity of solving the "internal"problem for $\overline{E2}$ and $\overline{H2}$. However,in many applications such as underground communications and electromagnetic shielding, the internal problem is of equal or greater importance than the external problem, and it is natural to ask if (4.2) can be used to simplify the problem of computing $\overline{E2}$ and $\overline{H2}$. In this section we will show that the IBC can indeed be used to obtain approximate solutions to certain internal problems by relatively simple means and that the latter lead naturally to solutions to a general class of shielding problems.

We consider the problem of computing fields inside the generalized electromagnetic shield M2 shown in figure 5 when it is illuminated by an arbitrary source S. The shield consists of planar sheets ES1, ES2...ESm which are uniform in composition

As in the case of the homogeneous sheet, the fields in the slot must satisfy a condition involving the skin depth and the sheet thickness in addition to (3.15) in order for the IBC's to accurately represent the structure of the fields at the interface. Here, there are two skin depths δx and δy defined as follows

$$\delta x = L_x/\mu_x^2 \ , \qquad \delta y = L_y/\mu_y^2 \ , \tag{3.25}$$

and the condition (analogous to (3.11)) is

$$\left.\begin{matrix}\delta x \\ \delta y\end{matrix}\right\} < d \ . \tag{3.26}$$

This condition insures that the impedance at $z = 0$ is unaffected by the discontinuity at $z = -d$. When (3.15) and (3.20) are satisfied, IBC's (3.12) and (3.13) are local boundary conditions over the suface of the slot. If the sheet has more than one slot, these IBC's can be applied at each slot provided (3.15) and (3.23) are satisfied.

Results analogous to (3.15) - (3.26) can be easily obtained for vertical slots and for slots with other orientations provided the appropriate slot impedances can be determined.

corresponding to fields decreasing in the -z direction have the form

$$\left.\begin{matrix} E2_x \\ H2_y \end{matrix}\right\} \propto \exp\left(j\omega z\mu_x^2/\eta_x^2\right), \tag{3.20}$$

$$\left.\begin{matrix} E2_y \\ H2_x \end{matrix}\right\} \propto \exp\left(j\omega z\mu_y^2/\eta_y^2\right). \tag{3.21}$$

In this case, the real parts of η_x^2 and η_y^2 are negligible, and

$$\eta_x^2 \cong j\omega L_x(x,y,l,w), \qquad \eta_y^2 \cong j\omega L_y(x,y,l,w), \tag{3.22}$$

where L_x and L_y are the slot inductances. Relations (3.20) and (3.21) then reduce to

$$\left.\begin{matrix} E2_x \\ H2_y \end{matrix}\right\} \propto \exp\left(z\mu_x^2/L_x\right), \tag{3.23}$$

$$\left.\begin{matrix} E2_y \\ H2_x \end{matrix}\right\} \propto \exp\left(z\mu_y^2/L_y\right). \tag{3.24}$$

The latter show that the slot acts like a waveguide below cut-off resulting in an exponential decay of the internal fields for $z < 0$. The rates of decay depends primarily on the slot inductances which depend in turn on the length and width of the slot among other factors. As the length and width of the slot decrease, L_x and L_y also decrease and the rate of decay increases.

Since $\eta 2_x$ and $\eta 2_y$ can be defined in terms of effective permeabilities and permittivities

$$\eta 2_x = \sqrt{\mu 2_x / \varepsilon 2_x}$$
$$\eta 2_y = \sqrt{\mu 2_y / \varepsilon 2_y}\,, \tag{3.16}$$

where $\mu 2_x$, $\mu 2_y \geq \mu_o$, the relationship (3.15) implies

$$\left.\begin{vmatrix} \mu 2_x & \varepsilon 2_x \\ \mu 2_y & \varepsilon 2_y \end{vmatrix}\right\} >> \mu_o \varepsilon_o \tag{3.17}$$

which is completely analogous to (3.3).

In the slot, $E2_x$, $H2_y$, and $E2_y$, $H2_x$ satisfy separate sets of homogeneous wave equations corresponding to $\eta 2_x$

$$\frac{\partial^2 E2_x}{\partial z^2} + (\omega \mu 2_x / \eta 2_x)^2 E2_x = 0\,,$$
$$\frac{\partial^2 H2_y}{\partial z^2} + (\omega \mu 2_x / \eta 2_x)^2 H2_y = 0\,, \tag{3.18}$$

and to $\eta 2_y$

$$\frac{\partial^2 E2_y}{\partial z^2} + (\omega \mu 2_y / \eta 2_y)^2 E2_y = 0\,,$$
$$\frac{\partial^2 H2_x}{\partial z^2} + (\omega \mu 2_y / \eta 2_y)^2 H2_x = 0\,. \tag{3.19}$$

For airfilled slots with dimensions that are small compared to the wavelength of $\overline{E1}$, $\overline{H1}$ (the usual situation when (3.15) is satisfied), $\mu 2_x$ and $\mu 2_y$ are real and the imaginary parts of $\eta 2_x$ and $\eta 2_y$ are positive (inductive). Solutions to (3.18) and (3.19)

And by substituting (4.20) into (4.21), we obtain the following expressions for the fields inside the shield in terms of the source fields incident at a point P(x,y,0) located in the i-th slot:

$$
\begin{aligned}
E3_x(x,y,-d) &= -2\,\eta2^i_x\, H1^s_y(x,y,0)\, TE^i_x \exp(-j\omega d\mu2^i_x / \eta2^i_x)\ , \\
H3_y(x,y,-d) &= 2\, H1^s_y(x,y,0)\, TH^i_x \exp(-j\omega d\mu2^i_x / \eta2^i_x)\ , \\
E3_y(x,y,-d) &= 2\,\eta2^i_y\, H1^s_x(x,y,0)\, TE^i_y \exp(-j\omega d\mu2^i_y / \eta2^i_y)\ , \\
H3_x(x,y,-d) &= 2\, H1^s_x(x,y,0)\, TH^i_y \exp(-j\omega d\mu2^i_y / \eta2^i_y)\ ,
\end{aligned}
\tag{4.24}
$$

where

$$
\begin{aligned}
TE^i_x &= 2\,\eta3 / (\eta2^i_x + \eta3)\ , \\
TE^i_y &= 2\,\eta3 / (\eta2^i_y + \eta3)\ , \\
TH^i_x &= 2\,\eta2^i_x / (\eta2^i_x + \eta3)\ , \\
TH^i_y &= 2\,\eta2^i_y / (\eta2^i_y + \eta3)\ .
\end{aligned}
\tag{4.25}
$$

Equations (4.23) and (4.24) represent formal solutions to the shielding problem for the generalized structure shown in figure 5. To obtain explicit solutions to particular problems, it is necessary to specify the source S and the shielded volume M3 in sufficient detail so that $H1^s_x(x,y,0)$, $H1^s_y(x,y,0)$, and $\eta3$ can be determined. In the following sections, we will obtain such solutions for several combinations of sources and shields.

5. ELECTROMAGNETIC SOURCE FIELDS

In this section, we will compute the fields generated by several electromagnetic sources in a form suitable for use with equations (4.23) and (4.24). The sources we will consider are elementary (Hertzian) electric and magnetic dipoles and small rectangular loop antennas. Our principal objective for each of these sources is to obtain the magnetic fields tangent to the x, y plane of the rectangular/cylindrical coordinate system in figure 5. These are the source fields $H1_x^s(x,y,0)$ and $H1_y^s(x,y,0)$ that will be used in section 6 to obtain expressions for the fields inside typical electromagnetic shields.

5.1 Elementary Electric and Magnetic Dipoles

The electromagnetic fields generated by elementary electric and magnetic dipoles are, of course, well known, and in most applications they require little discussion. A basic characteristic of the dipole field is its family of equiphase surfaces in the form of concentric spheres centered on the dipole. These surfaces reflect the fact that the field is expressed in simplest form by reference to a spherical coordinate system with the origin located at the dipole. This is, quite naturally, the preferred means of representing these fields, and it is the only representation found in most reference works. Here, however, we must give up the simplicity of the dipole centered spherical system in favor of a rectangular/cylindrical system with the source located at an arbitrary point on the z axis as shown in figure 6. This system is identical to the one in figure 5 except that is has been rotated 90 degrees for purposes of clarity. The dipole (electric and magnetic) is positioned on the z axis at a distance D above the x,y plane with its moment parallel to the x axis and pointing in the positive direction. With this arrangement, the electric dipole can be used to approximate a short, linear current element with a uniform current distribu-

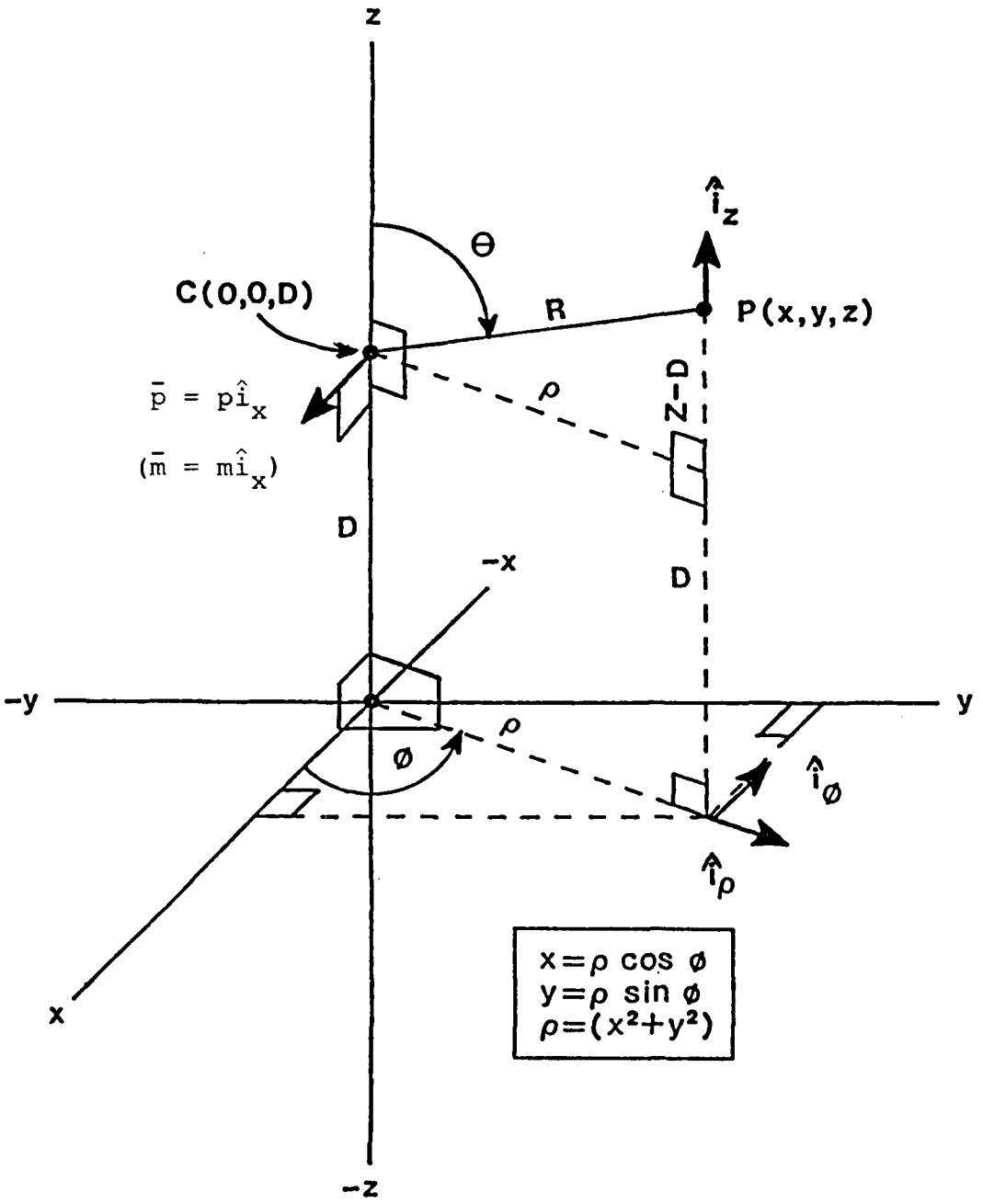

Figure 6. Rectangular/cylindrical coordinate system with an elementary electric (magnetic)dipole $\bar{p}$ ($\bar{m}$) at C (0,0,D) pointing in the x direction.

tion parallel to the x,y plane. Similarly, the magnetic dipole approximates a small, loop antenna with the plane of the loop in the y,z plane. In a situation where the x,y plane coincides with the surface of the earth, these would be described as horizontal dipoles.

We could obtain the dipole fields simply by transforming the classical expressions from spherical to rectangular or cylindrical coordinates; however, it will be useful to obtain our results directly from solutions to Maxwell's equations since we will need to use the same method in the following section to obtain the fields of a small, but finite, rectangular loop. Taking the electric dipole first, we write Maxwell's equations in the form[27]

$$\nabla \times \bar{E} = - j k_o Z_o \bar{H} ,$$
$$\nabla \times \bar{H} = j k_o \bar{E} / Z_o + \bar{J}_o , \tag{5.1}$$

where Z_o is the impedance of free space and k_o is defined as follows:

$$k_o = 2 \pi f \sqrt{\mu_o \epsilon_o} . \tag{5.2}$$

The source term $\bar{J}_o$ is given by

$$\bar{J}_o = \hat{i}_x \, p \, \delta(x) \, \delta(y) \, \delta(z-D) , \tag{5.3}$$

where $\hat{i}_x$ is a unit vector in the x direction, p is the current moment (ampere-meter), and $\delta( )$ is the Dirac delta function. Solutions to (5.1) can be written in terms of the Hertz vector potential $\bar{\pi}$ as follows:

$$\bar{H} = j k_o \nabla \times \bar{\pi} / Z_o , \tag{5.4}$$

$$\bar{E} = \nabla \nabla \cdot \bar{\pi} + k_o^2 \bar{\pi} , \tag{5.5}$$

where $\bar{\pi}$ satisfies the vector Helmholtz equation

$$(\nabla^2 + k_o^2) \, \bar{\pi} = j Z_o \bar{J}_o / k_o . \tag{5.6}$$

---

27 A. Banos, Jr., Dipole Radiation in the Presence of a Conduction Half-Space, Pergamon Press, Oxford, U.K., p.4, (1966).

Solutions to (5.6) can be written in terms of the vector Green's function $\overline{G}$ as follows

$$\overline{\pi} = - j\, p\, Z_o\, \overline{G} \,/\, k_o \quad . \tag{5.7}$$

In rectangular coordinates, $\overline{G}$ is given by

$$\overline{G}(x,y,z) = \hat{i}_x\, W(R) \quad , \tag{5.8}$$

where

$$W(R) = \exp(- j\, k_o\, R) \,/\, 4\pi R \quad , \tag{5.9}$$

and

$$R = \sqrt{x^2 + y^2 + (z-D)^2} \quad . \tag{5.10}$$

In cylindrical coordinates, (5.8) becomes

$$\overline{G}(\rho,\phi,z) = [\, \hat{i}_\rho \cos(\phi) - \hat{i}_\phi \sin(\phi)]\, W(R) \quad , \tag{5.11}$$

where W(R) is again given by (5.9) and

$$R = \sqrt{\rho^2 + (z-D)^2} \quad . \tag{5.12}$$

When (5.8) or (5.11) is inserted into (5.7) and the latter into (5.4) and (5.5), the electric dipole fields can be computed by straightforward (but lengthy) vector-differential operations. Using (5.11), we obtain the following expressions for the fields in the cylindrical coordinate system:

Electric Dipole Fields

$$E_\rho = p\, Z_o \cos\phi\, [\Omega(j\, k_o\, R + 1) + \cos^2\theta\, k_o^2\, R^2]\, W(R) \,/\, j\, k_o\, R^2 \quad ,$$

$$E_\phi = p\, Z_o \sin\phi\, (j\, k_o\, R + 1 - k_o^2\, R^2)\, W(R) \,/\, j\, k_o\, R^2 \quad , \tag{5.13}$$

$$E_z = p\, Z_o \cos\phi\, (3 + 3j\, k_o\, R - k_o^2\, R^2) \sin\theta \cos\theta\, W(R) \,/\, j\, k_o\, R^2 ,$$

$$H_\rho = - p \sin\phi \, (j k_o R + 1) \cos\theta \, W(R)/R \ ,$$

$$H_\phi = - p \cos\phi \, (j k_o R + 1) \cos\theta \, W(R)/R \ , \qquad (5.14)$$

$$H_z = p \sin\phi \, (j k_o R + 1) \sin\theta \, W(R)/R \ ,$$

where

$$\Omega = 2 \sin^2\theta - \cos^2\theta \ ,$$

$$\cos\theta = (z - D)/R \ , \qquad (5.15)$$

$$\sin\theta = \rho/R \ ,$$

and W(R) and R are as defined previously. Rectangular field components can be obtained from (5.13) and (5.14) using the relations

$$E_x = E_\rho \cos\phi - E_\phi \sin\phi \ ; \quad H_x = H_\rho \cos\phi - H_\phi \sin\phi \ ,$$

$$E_y = E_\rho \sin\phi + E_\phi \cos\phi \ ; \quad H_y = H_\rho \sin\phi + H_\phi \cos\phi \ . \qquad (5.16)$$

When the electric dipole is replaced by a magnetic dipole, Maxwell's equations can be written in the form

$$\nabla \times \bar{E} = - j k_o Z_o \, (\bar{H} + \bar{M}_o) \ ,$$

$$\nabla \times \bar{H} = j k_o \bar{E} / Z_o \ , \qquad (5.17)$$

where the source term $\bar{M}_o$ is given by

$$\bar{M}_o = \hat{i}_x \, m \, \delta(x)\delta(y)\delta(z - D) \ , \qquad (5.18)$$

and m is the loop magnetic moment (ampere-meter^2). Solutions to (5.17) can be constructed with the aid of the vector potential in the same way that solutions to (5.1) were obtained.The result in cylindrical coordinates is the following:

Magnetic Dipole Fields

$$E_\rho = m Z_o \sin\phi \cos\theta \, jk_o \, (jk_oR + 1) \, W(R) / R \ ,$$

$$E_\phi = m Z_o \cos\phi \cos\theta \, jk_o \, (jk_oR + 1) \, W(R) / R \ , \qquad (5.19)$$

$$E_z = - m Z_o \sin\phi \sin\theta \, jk_o (jk_o R + 1) W(R) / R ,$$

$$H_\rho = m \cos\phi [\Omega(jk_o R + 1) + \cos^2\theta \, k_o^2 R^2] W(R) / R^2 ,$$

$$H_\phi = m \sin\phi (jk_o R + 1 - k_o^2 R^2) W(R) / R^2 , \qquad (5.20)$$

$$H_z = m \cos\phi \sin\theta \cos\theta (3 + 3jk_o R - k_o^2 R^2) W(R) / R^2 ,$$

where all quantities are as defined previously and the rectangular field components can again be computed from (5.16).

Equations (5.13), (5.14), (5.19),and (5.20) are the fields of point dipole sources where the source strength has been expressed in terms of the current moment p in the case of the electric dipole and the loop magnetic moment m in the case of the magnetic dipole. The usefulness of these expressions is due to the fact that they can also be applied to finite dipole and loop antennas when the antenna dimensions are much smaller than the wavelength of the radiated field. To obtain the fields of a dipole antenna of length 1_o with current I, replace p in equations (5.13) and (5.14) with

$$p = I \, 1_o . \qquad (5.21)$$

And similarly, to obtain the fields of a loop antenna of cross sectional area A and current I, replace m in equations (5.19) and (5.20) with

$$m = I A . \qquad (5.22)$$

5.2 Rectangular Loop Antenna

Equations (5.13),(5.14), (5.19), and (5.20) - or their spherical equivalents - are known to represent good approximations to the fields of dipole and loop antennas when the dimensions of the antennas are small compared to the wavelength λ

of the radiated field

$$l_o \, , \sqrt{A} \ll \lambda = C_o / f \qquad (C_o = \text{vel. of light}) \, , \qquad (5.23)$$

and also small compared to the distance between the source location at C(0,0,D) and the observation point P(x,y,z)

$$l_o \, , \sqrt{A} \ll R = \sqrt{x^2 + y^2 + (z - D)^2} \, . \qquad (5.24)$$

On this basis, the fields presented in the preceding section can be used to investigate a variety of practical problems some of which will be discussed later in this report. However, in many cases of interest, one or the other of relations (5.23) and (5.24) will not be satisfied, and, when this occurs, the validity of this approximation is open to question. This is especially true in some shielding problems where (5.23) is easily satisfied but (5.24) is not.

In this section, we will consider one such case,namely, that of a rectangular loop antenna of width a and length b where a and b are arbitrary except for the restriction $a,b \ll \lambda$. As shown in figure 7, the loop lies in the y,z plane with its geometric center C(0,0,D) located at a distance D above the x,y plane. It consists of four filaments each of which carries a current I flowing in directions indicated by the arrows. Our objective is to compute the fields at an arbitrary observation point P(x,y,z).

In this case (5.1) is the appropriate form of Maxwell's equations. But now, the source term $\bar{J}_o$ consists of four terms corresponding to the four sections of the loop as labeled in the figure:

$$\bar{J}_o(0,y,z) = \hat{i}_y \, J_1(0,y,D-a/2) + \hat{i}_z \, J_2(0,b/2,z)$$

$$- \hat{i}_y \, J_3(0,y,D+a/2) - \hat{i}_z \, J_4(0,-b/2,z) \, . \qquad (5.25)$$

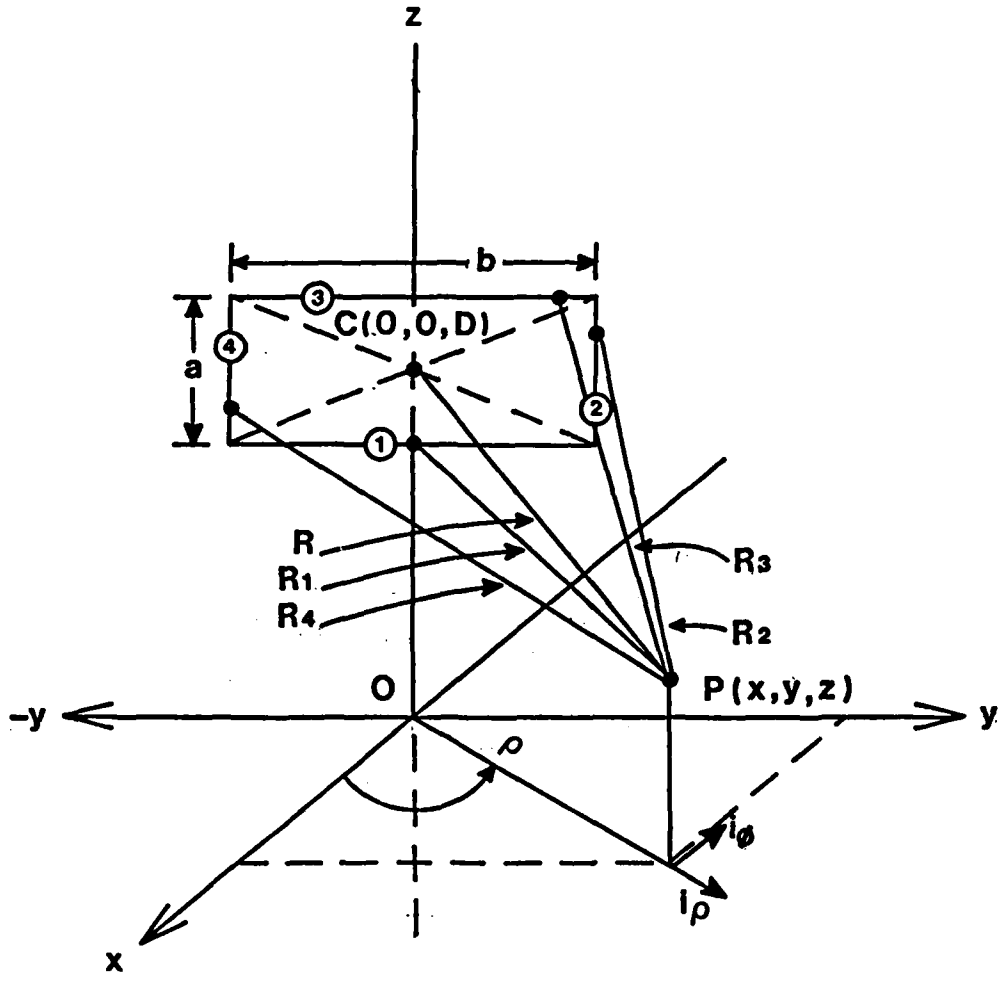

Figure 7. A rectangular loop lying in the y, z plane with its geometric center C at the point (0,0,D).

The solution to the vector Helmholtz equation (5.6) for a source $\bar{J}_o$ (0,y,z) with finite dimensions is

$$\bar{\pi} = \bar{A}/jk_o\sqrt{\mu_o\varepsilon_o} \quad , \tag{5.26}$$

where

$$\bar{A} = \int_V \frac{\bar{J}_o(0,y',z')\ \exp(-jk_oR')}{4\pi R'}\, dV' \quad . \tag{5.27}$$

In (5.27), R' is the distance between a point on the loop $P'(0,y',z')$ and the observation point $P(x,y,z)$

$$R' = \sqrt{x^2 + (y - y')^2 + (z - z')^2} \quad , \tag{5.28}$$

and the integration is taken over the volume containing the loop. Substituting (5.25) into (5.27), we can write A as the sum of four terms

$$\bar{A} = \bar{A}_1 + \bar{A}_2 + \bar{A}_3 + \bar{A}_4 \quad , \tag{5.29}$$

where

$$\begin{aligned}
\bar{A}_1 &= \hat{i}_y \int_{V_1} \frac{J_1(0,y',D-a/2)\ \exp(-jk_oR_1)}{4\pi R_1}\, dV_1 \quad , \\
\bar{A}_2 &= \hat{i}_z \int_{V_2} \frac{J_2(0,b/2,z')\ \exp(-jk_oR_2)}{4\pi R_2}\, dV_2 \quad , \\
\bar{A}_3 &= -\hat{i}_y \int_{V_3} \frac{J_3(0,y',D+a/2)\ \exp(-jk_oR_3)}{4\pi R_3}\, dV_3 \quad , \\
\bar{A}_4 &= -\hat{i}_z \int_{V_4} \frac{J_4(0,-b/2,z')\ \exp(-jk_oR_4)}{4\pi R_4}\, dV_4 \quad ,
\end{aligned} \tag{5.30}$$

$$R_1 = \sqrt{x^2 + (y - y')^2 + (z - D + a/2)^2} \quad ,$$

$$R_2 = \sqrt{x^2 + (y - b/2)^2 + (z - z')^2} \quad ,$$

$$R_3 = \sqrt{x^2 + (y - y')^2 + (z - D - a/2)^2} \quad , \tag{5.31}$$

$$R_4 = \sqrt{x^2 + (y + b/2)^2 + (z - z')^2} \quad ,$$

and V_1, V_2, V_3, and V_4 are the volumes occupied by the current filaments. When these integrals have been evaluated, the fields can be computed by substituting A into (5.26) and the latter into (5.4) and (5.5).

The volume integrals in (5.30) consist of an integration over the cross sectional area of the filament and an integration along its length. The integrals of J_1, J_2, J_3, and J_4 over the cross section are simply the currents I_1, I_2, I_3, and I_4 in each segment of the loop. However, (5.23) implies

$$I_1 = I_2 = I_3 = I_4 = I \quad , \tag{5.32}$$

where I is independent of the loop coordinates y' and z', and

$$\exp(-jk_oR_1) \cong \exp(-jk_oR_2) \cong \exp(-jk_oR_3) \cong \exp(-jk_oR_4) \cong \exp(-jk_oR) \quad , \tag{5.33}$$

where

$$R = \sqrt{x^2 + y^2 + (z - D)^2} \quad , \tag{5.34}$$

(the distance between the geometric center of the loop and P) is also independent of y' and z'. Therefore, (5.30) reduces to

$$\bar{A}_1 = \hat{i}_y \, I \exp(-jk_oR) \int_{-b/2}^{b/2} \frac{dy'}{4\pi R_1} \quad ,$$

$$\bar{A}_2 = \hat{i}_z \, I \exp(-jk_o R) \int_{D-a/2}^{D+a/2} \frac{dz'}{4\pi R_2} \quad ,$$

$$\bar{A}_3 = - \hat{i}_y \, I \exp(-jk_o R) \int_{-b/2}^{b/2} \frac{dy'}{4\pi R_3} \quad , \tag{5.35}$$

$$\bar{A}_4 = - \hat{i}_z \, I \exp(-jk_o R) \int_{D-a/2}^{D+a/2} \frac{dz'}{4\pi R_4} \quad ,$$

The integrals in (5.35) are elementary: hence,

$$\bar{A}_1 = \hat{i}_y \, Q \ln \left[\frac{b - 2y + 2(K1 - by + b^2/4)^{\frac{1}{2}}}{-b - 2y + 2(K1 + by + b^2/4)^{\frac{1}{2}}} \right] ,$$

$$\bar{A}_2 = \hat{i}_z \, Q \ln \left[\frac{2(D+a/2) - 2z + 2[K2 - 2z(D+a/2) + (D+a/2)^2]^{\frac{1}{2}}}{2(D-a/2) - 2z + 2[K2 - 2z(D-a/2) + (D-a/2)^2]^{\frac{1}{2}}} \right] ,$$

$$\bar{A}_3 = \hat{i}_y \, Q \ln \left[\frac{-b - 2y + 2(K3 + by + b^2/4)^{\frac{1}{2}}}{b - 2y + 2(K3 - by + b^2/4)^{\frac{1}{2}}} \right] , \tag{5.36}$$

$$\bar{A}_4 = \hat{i}_z \, Q \ln \left[\frac{2(D-a/2) - 2z + 2[K4 - 2z(D-a/2) + (D-a/2)^2]^{\frac{1}{2}}}{2(D+a/2) - 2z + 2[K4 - 2z(D+a/2) + (D+a/2)^2]^{\frac{1}{2}}} \right] ,$$

where

$$Q = I \exp(-jk_o R)/4\pi \quad , \tag{5.37}$$

and

$$K1 = x^2 + y^2 + (z - D + a/2)^2 \quad ,$$

$$K2 = x^2 + (y - b/2)^2 + z^2 \quad , \tag{5.38}$$

$$K3 = x^2 + y^2 + (z - D - a/2)^2 \quad ,$$

$$K4 = x^2 + (y + b/2)^2 + z^2 \quad .$$

When (5.26) is substituted into (5.4) and (5.5) using (5.36), (5.37), and (5.38), a lengthy calculation is required to determine the loop fields. This effort can be mitigated somewhat by using cylindrical coordinates as in the preceding section. However, even when expressed in cylindrical coordinates, the fields are such complicated functions that we cannot give the complete set of components here. Instead, we limit ourselves to the components of principal interest in this study, that is, H_ρ and H_ϕ . These are given by the following:

$$H_\rho = \frac{I \cos\phi \exp(-jk_o R)}{4\pi}\left[b\beta - \xi - jk_o(z - D)\psi/R\right] ,$$

$$H_\phi = \frac{I \exp(-jk_o R)}{4\pi}\left[\sin\phi\ [\xi - jk_o(z-D)\psi/R] - \zeta + jk_o\rho\nu/R\right] , \tag{5.39}$$

where

$$\beta = -\frac{1}{\beta 1[2(D+a/2) - 2z + 2\beta 1]} + \frac{1}{\beta 2[2(D-a/2) - 2z + 2\beta 2]}$$
$$- \frac{1}{\beta 3[2(D+a/2) - 2z + 2\beta 3]} + \frac{1}{\beta 4[2(D-a/2) - 2z + 2\beta 4]} \quad ,$$

$$\xi = \frac{2(z-D+a/2)}{\xi 1(b-2y+2\xi 1)} - \frac{2(z-D+a/2)}{\xi 2(-b-2y+2\xi 2)} - \frac{2(z-D-a/2)}{\xi 3(b-2y+2\xi 3)}$$
$$+ \frac{2(z-D-a/2)}{\xi 4(-b-2y+2\xi 4)} \quad ,$$

$$\zeta = \frac{2\rho - b\sin\phi}{\beta 1[2(D+a/2) - 2z + 2\beta 1]} - \frac{2\rho - b\sin\phi}{\beta 2[2(D-a/2) - 2z + 2\beta 2]}$$

$$- \frac{2\rho + b\sin\phi}{\beta 3[2(D+a/2) - 2z + 2\beta 3]} + \frac{2\rho + b\sin\phi}{\beta 4[2(D-a/2) - 2z + 2\beta 4]} ,$$

$$\psi = \ln\left(\frac{[b - 2y + 2\xi 1][-b - 2y + 2\xi 4]}{[-b - 2y + 2\xi 2][b - 2y + 2\xi 3]}\right) ,$$

$$\nu = \ln\left(\frac{[2(D+a/2) - 2z + 2\beta 1][2(D-a/2) - 2z + 2\beta 4]}{[2(D-a/2) - 2z + 2\beta 2][2(D+a/2) - 2z + 2\beta 3]}\right) ,$$

$$\beta 1 = \sqrt{K3 - 2z(D+a/2) + (D+a/2)^2} ,$$

$$\beta 2 = \sqrt{K3 - 2z(D-a/2) + (D-a/2)^2} ,$$

$$\beta 3 = \sqrt{K4 - 2z(D+a/2) + (D+a/2)^2} ,$$

$$\beta 4 = \sqrt{K4 - 2z(D-a/2) + (D-a/2)^2} ,$$

$$\xi 1 = \sqrt{K1 - by + b^2/4} ,$$

$$\xi 2 = \sqrt{K1 + by + b^2/4} ,$$

$$\xi 3 = \sqrt{K2 - by + b^2/4} ,$$

$$\xi 4 = \sqrt{K2 + by + b^2/4} ,$$

wever, in certain special cases, useful approximations can be tained. For example, in the case of an air filled slot, $\mu_x^2 = = \mu_o$, and η_y^2 can be approximated by the impedance of a center d slot antenna.[2] The resulting expression is quite complicated d will not be reproduced here. However, when (6.20) is satis-ed, this expression reduces to (3.22)

$$\eta_y^2 = j\omega L_y(0,0,l,w) = j\omega L_s \ , \tag{6.25}$$

ere L_s, the slot inductance, is a function of l and w. With ese approximations, the transmitted fields from the magnetic pole (6.23) become

$$E3_y(0,0,-d) = 2\ j\omega L_s\ H1_x^s(0,0,0)\ TE\ \exp(-d\mu_o/L_s) \ ,$$

$$H3_x(0,0,-d) = 2\ H1_x^s(0,0,0)\ TH\ \exp(-d\mu_o/L_s) \ , \tag{6.26}$$

ere

$$TE = 2\ \eta 3/(j\omega L_s + \eta 3) \ ,$$

$$TH = 2\ j\omega L_s/(j\omega L_s + \eta 3) \ . \tag{6.27}$$

For slots ranging in length from .01 to 1 meter, L_s can be mputed with the aid of figure 7 in Monroe[2] by dividing the ot impedance by $2\pi f$. This gives

$$L_s = 3.2\times10^{-8}\,H \text{ for } l = .5\,m \text{ and } w = .0016\,m \ , \tag{6.28}$$

d L_s can be obtained for slots of other dimensions by interpo-lating between the curves in the figure.

The reader can verify that expressions for the fields trans-tted by the vertical slot shown in figure 4(b) when it is ex-sed to the x directed electric dipole can be obtained from

---

R. L. Monroe, EMP Shielding Effectiveness and MIL-STD 285, Harry Diamond Laboratories, HDL-TR-1636 (July, 1973).

l (6.16) evaluated at P'(0,0,-d). Although a slot will in gen-
ıl transmit four tangential field components as indicated by
.24) for each source, there will only be two non-zero compo-
ıts at P'(0,0,-d) for each dipole source. In the case of the
ectric dipole, $H1_x^s(0,0,0) = 0$; hence, $E3_y(0,0,-d) = H3_x(0,0,-d)$
), and (4.24) reduces to the following:

$$E3_x(0,0,-d) = -2\eta_x^2 H1_y^s(0,0,0)\, T_x^E \exp(-j\omega d\mu_x^2/\eta_x^2) ,$$
$$H3_y(0,0,-d) = \quad 2 H1_y^s(0,0,0)\, T_x^H \exp(-j\omega d\mu_x^2/\eta_x^2) , \tag{6.21}$$

ere $H1_y^s(0,0,0)$ is obtained from (6.4), $\eta 3$ is given by (6.15),

$$T_x^E = 2\ \eta 3/(\eta_x^2 + \eta 3) ,$$
$$T_x^H = 2\ \eta_x^2/(\eta_x^2 + \eta 3) , \tag{6.22}$$

d we have dropped the index i since we are considering a
ngle slot.

Similarly, in the case of the magnetic dipole, $H1_y^s(0,0,0) =$
$(0,0,-d) = H3_y(0,0,-d) = 0$, and (4.24) reduces to

$$E3_y(0,0,-d) = 2\eta_y^2 H1_x^s(0,0,0)\, T_y^E \exp(-j\omega d\mu_y^2/\eta_y^2) ,$$
$$H3_x(0,0,-d) = 2 H1_x^s(0,0,0)\, T_y^H \exp(-j\omega d\mu_y^2/\eta_y^2) , \tag{6.23}$$

ere $H1_x^s(0,0,0)$ is obtained from (6.5), $\eta 3$ is given by (6.16), and

$$T_y^E = 2\ \eta 3/(\eta_y^2 + \eta 3) ,$$
$$T_y^H = 2\ \eta_y^2/(\eta_y^2 + \eta 3) . \tag{6.24}$$

To compute the fields transmitted by the slot using equa-
ons (6.21) and (6.23), the remaining parameters μ_x^2, μ_y^2, η_x^2, and
must be determined. In general this is a difficult task;

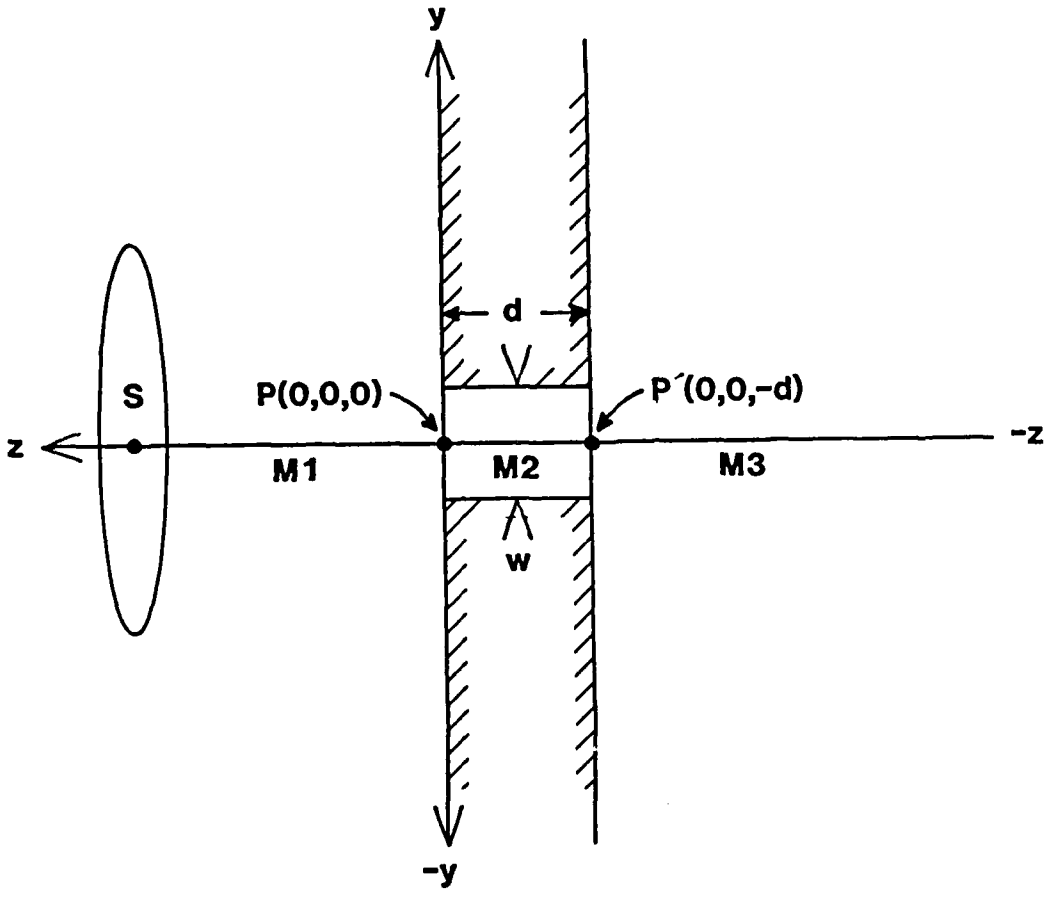

Figure 11. Side view of a horizontal slot of width w in an infinite plane sheet of thickness d. (Side view of figure 4(a).

And for magnetic dipoles (5.19) and (5.20) give

$$\eta 3 = Z_0 \left[\frac{jk_oR\ (jk_oR + 1)}{jk_oR + 1 - k_o^2R^2}\right] , \tag{6.16}$$

where

$$R = \sqrt{\rho^2 + (d + D)^2} . \tag{6.17}$$

If

$$d << D \tag{6.18}$$

then,

$$R = \sqrt{\rho^2 + D^2} ,$$

and

$$\eta 3 \cong E1_\rho^s(\rho,\phi,0)/H1_\phi^s(\rho,\phi,0) = - E1_\phi^s(\rho,\phi,0)/H1_\rho^s(\rho,\phi,0)$$
$$\cong \eta 1 . \tag{6.19}$$

That is, when the thickness of the sheet is much smaller than the distance between the source and the sheet, $\eta 3$ is approximately equal to the wave impedance of the source field in M1 at $z = 0$.

6.3 Infinite Plane Sheet With a Rectangular Slot

If the sheet described in the preceding section is penetrated by a narrow rectangular slot as shown in figures 4(a) and 11, where

$$w < d << 1 << \lambda , \tag{6.20}$$

then the field transmitted into M3 at P´(0,0,-d) is given by equations (4.24) and (4.25). For sources consisting of electric and magnetic dipoles oriented in the x direction, the incident source fields at P(0,0,0) are $H1_x^s(0,0,0) = H1_\rho^s(0,0,0)$ and $H1_y^s(0,0,0) = H1_\phi^s(0,0,0)$. These fields can be determined by evaluating (6.4) and (6.5) at P(0,0,0). Similarly, $\eta 3$ is again given by (6.15)

As in the preceding section, we consider dipole sources where $H1_\rho^s$ and $H1_\phi^s$ are given by (6.4) and (6.5). To completely specify the fields entering M3 at $P'(\rho,\phi,-d)$, $\eta 3$, the wave impedance of the field looking into M3 at $P'(\rho,\phi,-d)$ in the $-z$ direction must be determined. If M3 like M1 is free space, then the fields in M3 must satisfy the same radiation condition for $z \longrightarrow -\infty$ that the source field satisfies when the sheet is removed. Furthermore, the wave impedance of the fields in M3 must approach the same limit ($Z_0 = 120\pi$ ohms) as that of the source field when $z \longrightarrow -\infty$. It follows that the wave impedance at given point in M3 will be approximately equal to the wave impedance of the source field at that point and, in particular, that $\eta 3$ is approximately equal to the impedance of the source field at $z = -d$ when the sheet is removed. That is,

$$\eta 3 = E_\rho^s(\rho,\phi,-d)/H_\phi^s(\rho,\phi,-d) \ , \tag{6.11}$$

or

$$-\eta 3 = E_\phi^s(\rho,\phi,-d)/H_\rho^s(\rho,\phi,-d) \ . \tag{6.12}$$

For a given source, (6.11) and (6.12) do not give consistent expressions for $\eta 3$ at all points on the interface $z = -d$. However, at points in the vicinity of the z axis where

$$\sin\theta \cong 0 \quad \text{and} \quad \cos\theta \cong 1 \ , \tag{6.13}$$

the two expressions are consistent for dipole sources. That is, (6.13) implies

$$\eta 3 = E_\rho^s(\rho,\phi,-d)/H_\phi^s(\rho,\phi,-d) = - E_\phi^s(\rho,\phi,-d)/H_\rho^s(\rho,\phi,-d) \ . \tag{6.14}$$

For electric dipoles, (5.13) and (5.14) give

$$\eta 3 = Z_0 \left[\frac{jk_oR + 1 - k_o^2R^2}{jk_oR\ (jk_oR + 1)}\right] \ , \tag{6.15}$$

The reader can verify that (6.1) with $H1^s_\rho(\rho,\phi,0)$ and $H1^s_\phi(\rho,\phi,0)$ given by (6.4) and (6.5) is in good agreement with corresponding expressions obtained by Bannister [29] using the quasi-static approximation for horizontal electric and magnetic dipoles above a conducting half-space. However, unlike the quasi-static approximation, equation (6.1) is not limited by the assumption that the distance between the source and the observation point is small compared to the wavelength of the field in free space (λ).

6.2 Infinite Plane Sheet of Uniform Thickness

By keeping d finite and letting $W,H \longrightarrow \infty$ as in the preceding section, we transform the generalized shield into an infinite plane sheet of uniform thickness (figure 3). The fields at a point $P'(\rho,\phi,-d)$ on the inside surface of the sheet (the surface farther away from the source) are given by (4.23). In cylindrical coordinates, (4.23) becomes

$$\begin{aligned} E3_\rho(\rho,\phi,-d) &= -\,2\,\eta 2\; H1^s_\phi(\rho,\phi,0)\; TE\; \exp(-\gamma 2 d)\;, \\ E3_\phi(\rho,\phi,-d) &= \;\;2\,\eta 2\; H1^s_\rho(\rho,\phi,0)\; TE\; \exp(-\gamma 2 d)\;, \end{aligned} \qquad (6.8)$$

$$\begin{aligned} H3_\rho(\rho,\phi,-d) &= \;\;2\; H1^s_\rho(\rho,\phi,0)\; TH\; \exp(-\gamma 2 d)\;, \\ H3_\phi(\rho,\phi,-d) &= \;\;2\; H1^s_\phi(\rho,\phi,0)\; TH\; \exp(-\gamma 2 d)\;, \end{aligned} \qquad (6.9)$$

where $\eta 2$ and $\gamma 2$ are given by (6.2) and (6.3) and TE and TH are

$$\begin{aligned} TE &= 2\,\eta 3/(\eta 2 + \eta 3)\;, \\ TH &= 2\,\eta 2/(\eta 2 + \eta 3)\;, \end{aligned} \qquad (6.10)$$

---

29 R. R. Bannister, IEEE Trans. Antennas and Propagation, AP-15 (1967), 618.

$$H2_\rho(\rho,\phi,z) = 2\, H1^s_\rho(\rho,\phi,0)\, \exp(\gamma 2 z) \ ,$$

$$H2_\phi(\rho,\phi,z) = 2\, H1^s_\phi(\rho,\phi,0)\, \exp(\gamma 2 z) \ ,$$

where

$$\eta 2 = \sqrt{\mu 2/\varepsilon 2} \cong \sqrt{j2\pi f\mu 2/\sigma 2} \quad \text{for } \sigma 2 >> 2\pi f\varepsilon' \ , \tag{6.2}$$

$$\gamma 2 = j\omega\sqrt{\mu 2\varepsilon 2} \cong \sqrt{j2\pi f\mu 2\sigma 2} \quad \text{for } \sigma 2 >> 2\pi f\varepsilon' \ , \tag{6.3}$$

and ε' and $\sigma 2$ are the real part of $\varepsilon 2$ and the conductivity respectively (equation (3.4)). In (6.1), the source terms $H1^s_\rho$ and $H1^s_\phi$ are determined by evaluating (5.14) and (5.20) at z=0. For the case of an <u>electric dipole</u> pointing in the x direction we obtain

$$\begin{aligned} H1^s_\rho(\rho,\phi,0) &= -\, p \sin\phi\, (jk_o R + 1) \cos\theta\, W(R)/R \ , \\ H1^s_\phi(\rho,\phi,0) &= -\, p \cos\phi\, (jk_o R + 1) \cos\theta\, W(R)/R \ , \end{aligned} \tag{6.4}$$

and for the case of a <u>magnetic dipole</u> with its moment pointing in the x direction

$$\begin{aligned} H1^s_\rho(\rho,\phi,0) &= m \cos\phi\, [\Omega(jk_o R + 1) + \cos^2\theta k_o^2 R^2]\, W(R)/R^2 \ , \\ H1^s_\phi(\rho,\phi,0) &= m \sin\phi\, (jk_o R + 1 - k_o^2 R^2)\, W(R)/R^2 \ , \end{aligned} \tag{6.5}$$

where

$$\left.\begin{aligned} \Omega &= 2\sin^2\theta - \cos^2\theta \ , \\ \cos\theta &= -\, D/R \ , \\ \sin\theta &= \rho/R \ , \end{aligned}\right\} \tag{6.6}$$

$$\left.\begin{aligned} W(R) &= \exp(-jk_o R)/4\pi R \ , \\ R &= \sqrt{\rho^2 + D^2} \ . \end{aligned}\right\} \tag{6.7}$$

6. PROPAGATION OF ELECTROMAGNETIC FIELDS THROUGH STRUCTURES COMPOSED OF GOOD CONDUCTORS

With the results of sections 4 and 5, we can easily obtain expressions for the fields penetrating any structure derivable from the generalized shield in figure 5 when that structure is exposed to electric and magnetic dipoles, small rectangular loops, and any other source whose fields tangent to the surface of the structure are known. Since the number of combinations of sources and structures that can be treated in this way is quite large, we will not attempt to discuss them all here. Instead, we will limit ourselves to several that are related to to classical electromagnetic propagation and shielding problems.

6.1 Uniform Half-Space

By eliminating all sheets except ES1 in figure 5, by eliminating all slots in ES1, and by letting $H,W,d \longrightarrow \infty$, we can transform the generalized shield M2 into a uniform half-space with a plane interface separating it from another half-space M1 (figure 2). If M1 is free space with elementary electric and magnetic dipoles as described in section 5.1, then this combination of source and structure is the one considered by Sommerfeld[28] and his followers[27] who used classical analytical techniques to obtain approximate solutions for the fields in M2. Our solution, based on the impedance boundary condition, is given by (4.19). Since the half-space is isotropic, (4.19) can be written directly in terms of cylindrical coordinates as follows:

$$\begin{aligned} E2_\rho(\rho,\phi,z) &= -\,2\,\eta 2\, H1^s_\phi(\rho,\phi,0)\, \exp(\gamma 2 z)\ , \\ E2_\phi(\rho,\phi,z) &= \quad 2\,\eta 2\, H1^s_\rho(\rho,\phi,0)\, \exp(\gamma 2 z)\ , \end{aligned} \tag{6.1}$$

---

27 A. Banos, Jr. Dipole Radiation in the Presence of a Conducting Half-Space, Pergamon Press, Oxford, U.K., (1966).

28 A. Sommerfeld, Ann. Physik 28,665, (1909).

the center position y = 0 that is not present in figure 8(b). This asymmetry is rather slight for the loop height chosen, but it would certainly become much more pronounced if h were significantly reduced.

The effect of increasing D on $|H_x|$ in the x,y plane is very striking in this case. The figure shows that the field at y = 0 is 8 times larger when D = 18 in. than it is when D = 36 in.This implies that $|H_x|$ varies like z^{-3} along the z axis. The figure also shows that the very sharp peak occuring at y = 0 for D = 18 in. is eliminated when the loop is moved to the point where D = 36 in. And, similar results are obtained when $|H_x|$ is plotted along the x axis. The relatively small variation in $|H_x|$ along the x and y axes when D = 36 in. indicates that a virtually uniform field distribution over a sizable surface area (at least 7 X 7 ft.) can be achieved in the near field of a small loop antenna - contrary to what one might expect.

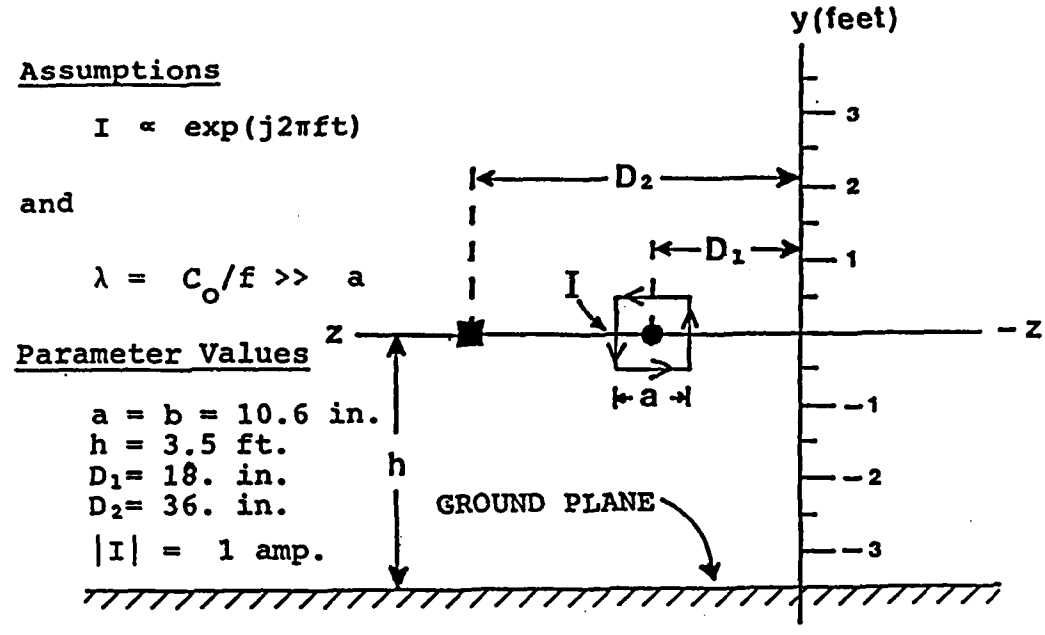

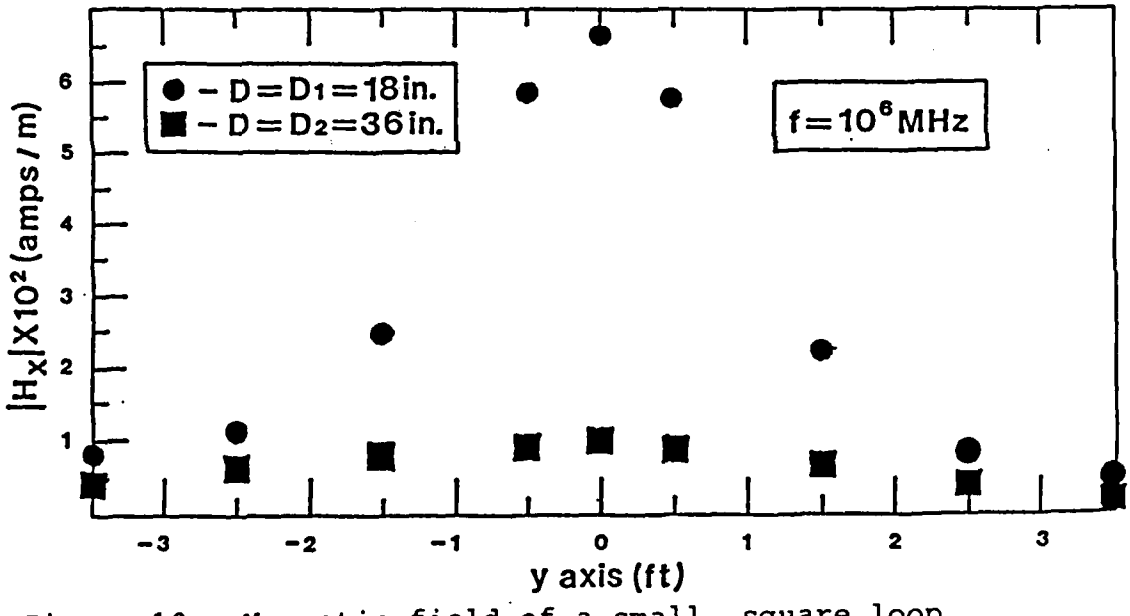

Figure 10. Magnetic field of a small, square loop.

(a) A small, square loop carrying a uniform current I centered at $(0,0,D_1)$ and $(0,0,D_2)$ at a height h above a ground plane.

(b) A plot of $|H_x|$ along the y axis for the two loop positions shown in (a).

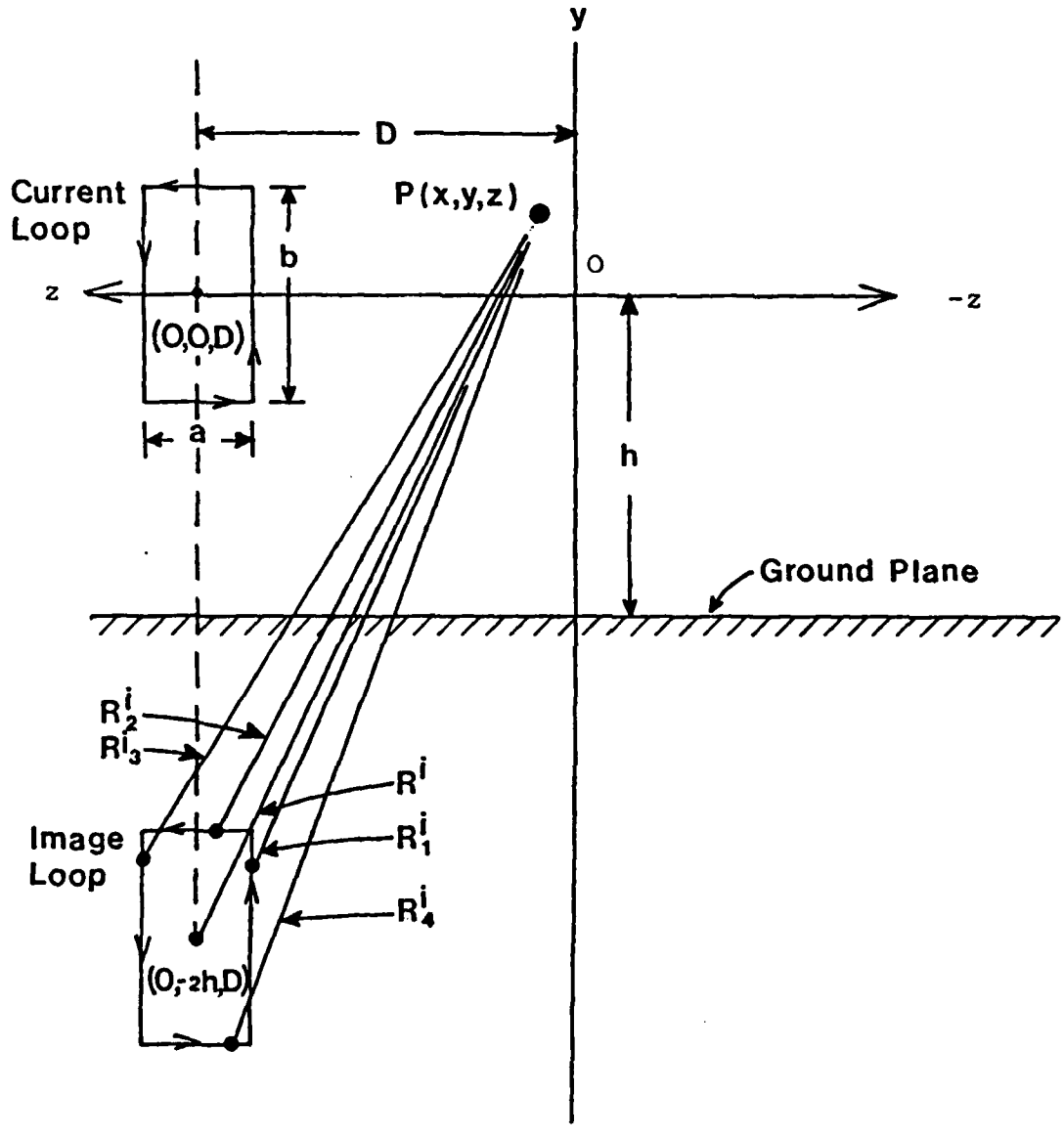

Figure 9. A rectangular current loop above a perfectly conducting ground plane with its image centered at (0,-2h,D).

as the observation point moves to more distant points on the y axis. Thus the calculations demonstrate that the use of the dipole approximation for small antennas need not be limited to situations where the distance to the observation point is large compared to the size of the antenna.

Figure 8(c) shows how the loop and dipole fields at the point x = y = z = 0 vary as functions of the source frequency f. Here $|H_x|$ is seen to be virtually independent of frequency for both loop and dipole fields over the range 0 to 10 MHz. Between 10 and 100 MHz, the loop field begins to increase linearly with f, while the dipole field shows a slight dip. However, above 100 MHz the dipole field increases rapidly and overtakes loop field which maintains a linear variation up to the resonant frequency of the loop (280 MHz) where assumption (5.23) breaks down. In view of these results, use of the dipole approximation would appear to be inadvisable at frequencies greater than 10 MHz. On the other hand, the loop equations appear to give reasonable results up to 100 MHz is this case.

5.3.2 Effect of a Perfectly Conducting Ground Plane Parallel to the x,y Plane on Magnetic Fields in the x,y Plane for Two Loop Positions

By using equation (5.39) to compute the magnetic fields from a loop and its image as shown in figure 9 and by adding the loop and image fields at an observation point P(x,y,z), the effect of a ground plane parallel to the x,y plane on the loop field can be computed. This has been done for the arrangement shown in figure 10(a) where the same current loop used in the preceding section is now located with its center at a height of 3.5 ft. above a ground plane. The results are shown in figure 10(b) for two loop positions D = 18 in. and D = 36 in. where once again we plot the magnitude of H_x along the y axis. The effect of the ground plane is to introduce an asymmetry with respect to

Assumptions

$I = \exp(j2\pi ft)$

and

$\lambda = c_o/f >> a$

Parameter Values

$a = b = 10.6$ in.

$a^2 = 112$ in.^{2}

$D = 18$ in.

$|I| = 1$ amp

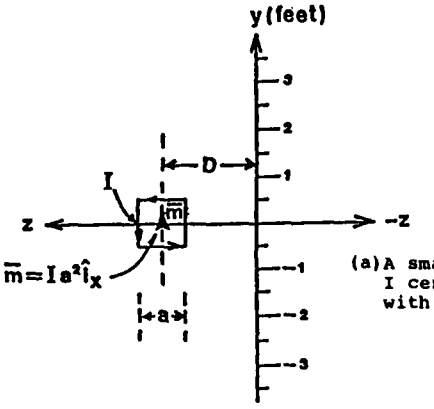

(a) A small, square loop carrying a uniform current I centered at (0,0,D) and a magnetic dipole with current moment $\bar{m} = I\,a^2\hat{i}_x$ at (0,0,D).

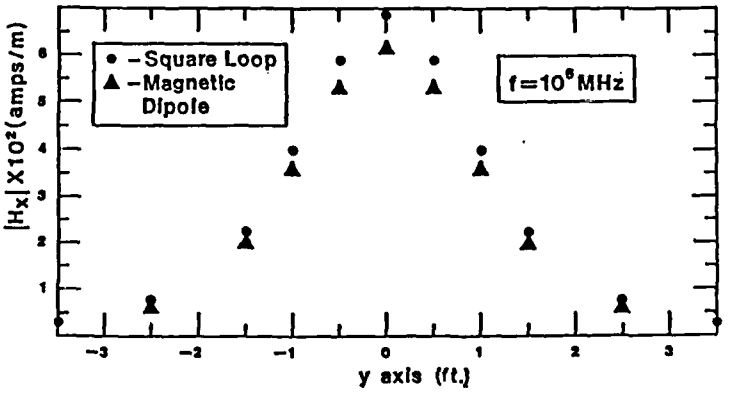

(b) A plot of $|H_x|$ along the y ax for the loop • and dipole ▲ shown in (a) where f = 10^6MHz.

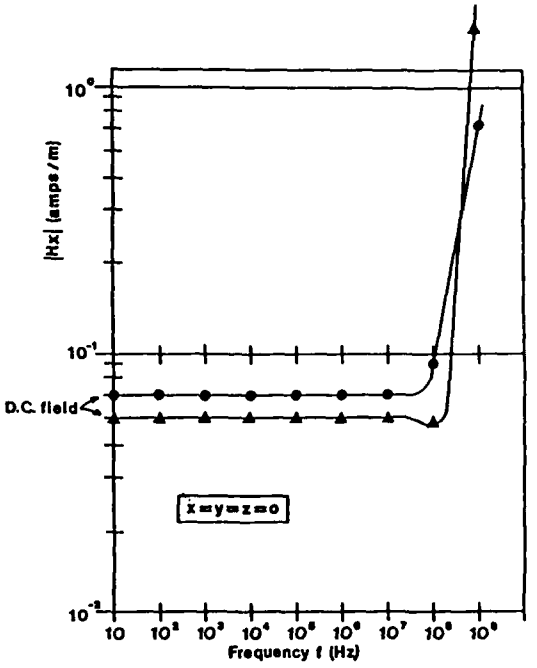

(c) A plot of $|H_x|$ versus frequency at (0,0,0) for the loop • and dipole ▲ shown in (a).

Figure 8. Comparison of loop and dipole fields.

and K1, K2, K3, and K4 are as defined previously in (5.38). With (5.39), the rectangular components H_x and H_y can be computed with (5.16) as in the case of the dipole fields.

5.3 Sample Source Field Calculations for Magnetic Dipoles and Square Loops

5.3.1 Comparison of Loop and Dipole Fields

With the equations given in the preceding sections, we can investigate the question of how well an elementary magnetic dipole approximates a small loop antenna when the distance between the antenna and the observation point is not large compared to the dimensions of the antenna. We will do this for the arrangement shown in figure 8(a). In the figure, the symbol ▲ indicates the position of a magnetic dipole on the z axis at a distance D = 18 inches from the x,y plane. Centered on the same position is a square loop antenna 10.6 inches on a side.The loop carries a uniform current I with $|I| = 1$ amp, and the magnetic dipole moment m is defined by $m = |I|a^2 = 112$ amp-in^2 $= .072$ amp-m^2 in accordance with (5.22). With this arrangement, the dominate magnetic field component in the x,y plane is H_x which can be computed with equations (5.20) and (5.16) for the dipole and equations (5.39) and (5.16) for the loop. Figures 8(b) and 8(c) show the results of one set of calculations using these equations. Figure 8(b) is a plot of $|H_x|$ along the y axis where the loop and dipole fields are indicated by ● and ▲ respectively. These curves show that the magnetic dipole is a surprisingly good approximation to the loop even when the distance to the observation point is approximately equal to the dimensions of the loop. For these calculations there is a maximum difference between the two fields of 12%. This occurs at $y = 0$, and, as one would expect, the difference between the fields decreases

(6.26) by making the following substitutions

$$E3_x(0,0,-d) \longrightarrow E3_y(0,0,-d) \ ,$$

$$H3_y(0,0,-d) \longrightarrow H3_x(0,0,-d) \ , \qquad (6.29)$$

$$H1^s_y(0,0,0) \longrightarrow H1^s_x(0,0,0) \ .$$

where $H1^s_y(0,0,0)$ is the source field from the electric dipole (6.4). Since the maximum response of a slot in a plane is always obtained when the incident magnetic field is aligned parallel to its longest dimension, equation (6.26) will always give the largest field that a slot of a given size can transmit when it is exposed to a magnetic dipole. Similarly, the equations derived from (6.26) using (6.29) will always give the largest field that a slot of a given size can transmit when it is exposed to an electric dipole.

6.4 Single Walled Continuous Enclosure in the Form of a Rectangular Parallelepiped

If a sixth plane sheet is added to the generalized shield (figure 5) to form the continuous (no slots) enclosure shown in figure 12, then the fields reaching an interior point $P'(x,y,-d)$ from the source S are given by (4.22) and (4.23) where $\eta 2$ is the intrinsic impedance of the material comprising the enclosure (6.2) and $\eta 3$ is the impedance at $z = -d$ looking into M3. As in the preceding examples, it is necessary to specify $H1^s_x(x,y,0)$ and $H1^s_y(x,y,0)$ (or $H1^s_\rho(\rho,\phi,0)$ and $H1^s_\phi(\rho,\phi,0)$) as well as $\eta 3$ in order to give explicit meaning to these formal expressions.

For electric and magnetic dipoles, the source fields are again obtained by evaluating (6.4) and (6.5). Similarly, for a rectangular loop antenna, the source fields would be obtained

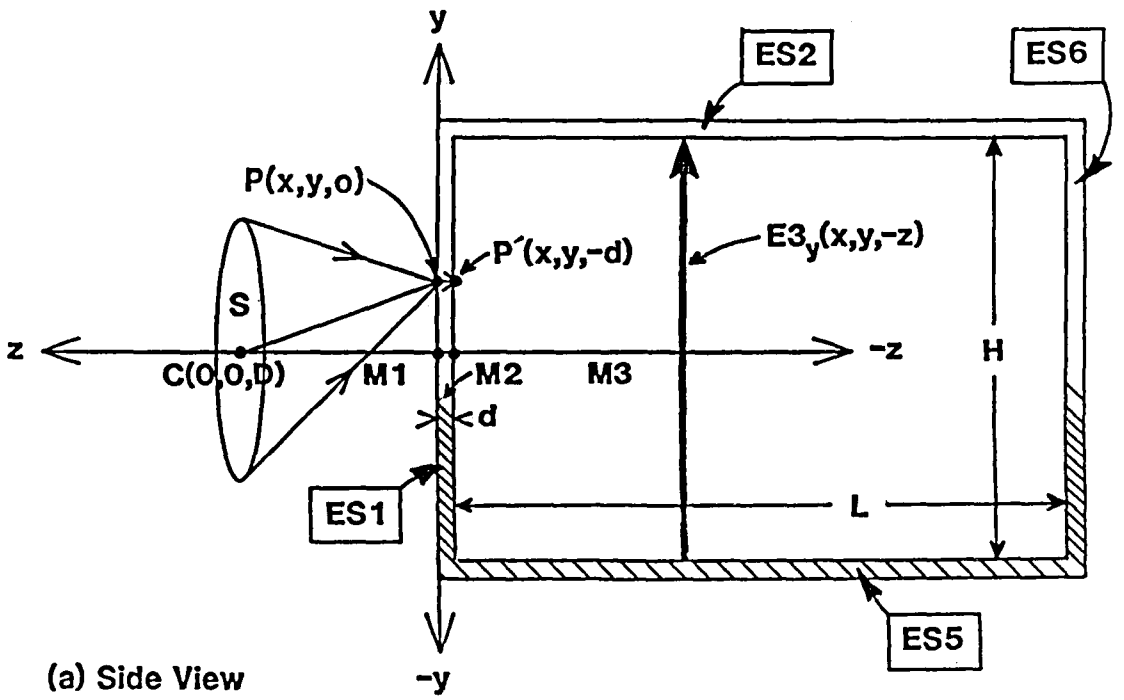

(a) Side View

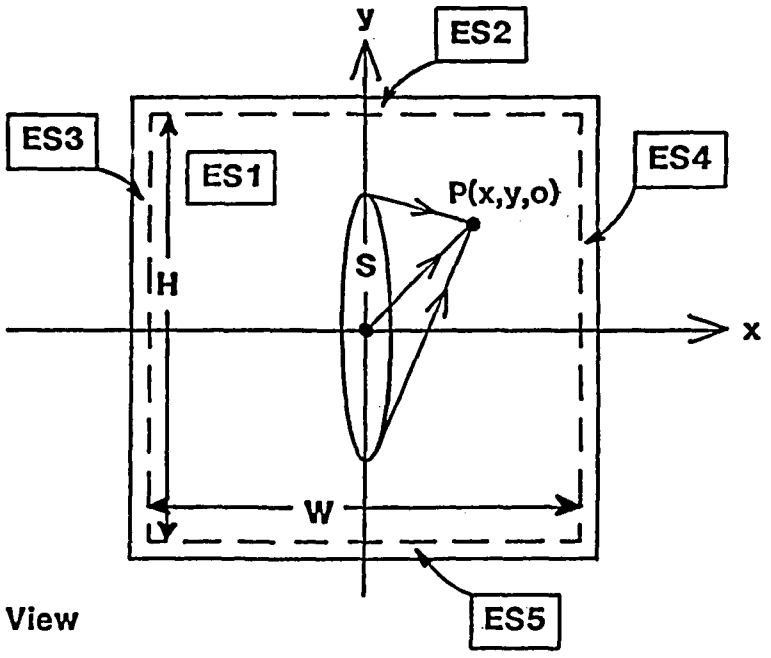

(b) Front View

Figure 12. A source S illuminating a continuous enclosure in the form of a rectangular parallelepiped.

by evaluating (5.39) at z = 0.In this way,the formal expressions can be used to represent the transmitted field of any source whose magnetic field components tangent to ES1 are known.

To evaluate $\eta 3$, we first note that M3 now occupies a finite volume rather than a half-space as in the case of the infinite plane sheet considered in the preceding sections. Consequently, the fields in M3 will not satisfy a radiation condition like the one satisfied by the source field in M1; and, in general, $\eta 3$ will be unrelated to the wave impedance of the source field. In this case, the structure of the fields in M3 will be determined primarily by the geometry of the enclosure and by its size relative to the wavelength of the source field (λ). Since the thin walled parallelepiped in figure 12 is equivalent to a section of rectangular waveguide closed at both ends by good conductors, $\eta 3$ will be determined by one or more of the waveguide modes that this structure can support. There are, of course, a doubly infinite number of such modes so that determining $\eta 3$ in the general case is a formidable problem. Fortunately, in many cases of interest, there is a single dominant mode that can account very well for the principal features of the fields in M3. This is the TE_{10} mode[30] which has the following important properties:

* The cutoff frequency is independent of one of the dimensions of the cross section (W or H).
* The polarization of the field is definitely fixed: the electric field passing from top to bottom of M3 as shown in figure 12(a) if $E3_y$ is the dominant electric field component at z = - d or from side to side if $E3_x$ is the dominant field component at z = - d.

---

30 S. Ramo, J. R. Whinnery, and T. Van Duzer, Fields and Waves in Communications Electronics, John Wiley and Sons, Inc., New York, p. 425, (1965).

* For a given frequency and H to W ratio, attenuation due to "copper" losses in the walls is less for the TE_{10} mode than for other modes.

Using these and other properties of the TE_{10} mode, we can construct an appropriate expression for $\eta 3$ that can be used in (4.22) and (4.23).

To illustrate this process, we consider the case where a source such as the x directed magnetic dipole or the rectangular loop antenna produces a magnetic field incident on ES1 with a dominant $H1_x^s$ component as shown in figure 8. In this case, the dominant electric field component at z = - d will be $E3_y$. That is, the source will couple to the vertically polarized TE_{10} mode in M3. If we now adopt the usual assumption in waveguide theory that wall losses can be ignored in first order approximations when the waveguide is composed of a good conductor (metal), then the characteristic impedance Z_{TE} and propagation constant $\gamma 3$ of the vertically polarized TE_{10} mode are given by the following:[30]

$$Z_{TE} = j\omega Z_0/\omega_c G \ , \tag{6.30}$$

$$\gamma 3 = k_c G \ , \tag{6.31}$$

where

$$G = \sqrt{1 + (j\omega/\omega_c)^2} \ , \tag{6.32}$$

$$\omega_c = 2\pi f_c \ , \tag{6.33}$$

$$f_c = C_o/2W \ , \tag{6.34}$$

$$k_c = 2\pi f_c/C_o \ , \tag{6.35}$$

---

30 S. Ramo, J. R. Whinnery, T. Van Duzer, Fields and Waves in Communications Electronics, John Wiley and Sons, Inc., New York, pages 409 and 425, (1965).

With these expressions, the impedance at z = - d looking into M3 can be approximated as follows:

$$\eta 3 = Z_{TE} \tanh(\gamma 3\, L) \ , \tag{6.36}$$

where (6.36) assumes a perfectly reflecting plane at z = -L -d.[30] For frequencies below the cutoff frequency ($f < f_c$), $\gamma 3$ is real and positive, and Z_{TE} and $\eta 3$ are both imaginary (inductive). In this case, the fields in M3 attenuate exponentially as one moves away from ES1. When $f > f_c$, $\gamma 3$ is imaginary, and Z_{TE} is real. The fields then propagate into M3 without attenuation and are reflected between ES1 and ES6 to form standing waves. At much higher frequencies where $f >> f_c$, $Z_{TE} \longrightarrow Z_0 = 120\pi$(ohms). By regarding $\gamma 3$ as a complex variable and using the hyperbolic tangent in (6.36) to represent reflections of the complex field, we are able to write $\eta 3$ as a single expression over the entire range of frequencies. This will prove to be very convenient in later sections when we consider transient fields.

With $\eta 2$ given by (6.2) and $\eta 3$ given by (6.36), we have the following expressions from (4.22) and (4.23) for the vertically polarized TE_{10} field at P´(x,y,-d) due to a source that produces a dominant magnetic field component $H1_x^s(x,y,0)$ at P(x,y,0):

$$E3_y(x,y,-d) = 2\,\eta 2\, H1_x^s(x,y,0)\ TE\ \exp(-\gamma 2\ d) \ ,$$
$$H3_x(x,y,-d) = 2\ H1_x^s(x,y,0)\ TH\ \exp(-\gamma 2\ d) \ , \tag{6.37}$$

where

$$TE = 2\ \ \eta 3/(\eta 2 + \eta 3) \ ,$$
$$TH = 2\ \ \eta 2/(\eta 2 + \eta 3) \ , \tag{6.38}$$

---

30 S. Ramo, J. R. Whinnery, T. Van Duzer, Fields and Waves in Communications Electronics, John Wiley and Sons, Inc., New York, Pages 46-48, (1965).

and

$$\gamma 2 = j\omega \sqrt{\mu 2 \varepsilon 2} \cong \sqrt{j\omega \mu 2 \sigma 2} \ . \tag{6.39}$$

The reader can easily verify that the horizontally polarized TE_{10} mode fields at $P'(x,y,-d)$ due to a source generating a dominant $H1_y^s(x,y,0)$ component over the surface of ES1 can be obtained from (6.37) with the following transformation:

$$\begin{aligned} &E3_x(x,y,-d) \longrightarrow E3_y(x,y,-d) \ , \\ &H3_y(x,y,-d) \longrightarrow H3_x(x,y,-d) \ , \\ &H1_y^s(x,y,0) \longrightarrow H1_x^s(x,y,0) \ , \\ &C_o/2H \longrightarrow f_c \quad \text{(See equation (6.4))} \ . \end{aligned} \tag{6.40}$$

For example, this transformation could be used to obtain the horizontally polarized TE_{10} fields at $P'(x,y,-d)$ due to an x directed electric dipole located close to ES1 where $H1_y^s(x,y,0)$ is computed from (5.14).

6.5 Single Walled Parallelepiped with a Narrow Rectangular Slot in One Side

When a continuous single walled parallelepiped is rendered discontinuous by a narrow rectangular slot, the fields that penetrate the slot will share some of the properties of the fields described in the two preceding sections. In the case of an enclosure with a horizontal slot as shown in figure 13, the field at $P'(0,0,-d)$ due to a source field $H1_x^s(0,0,0)$ at $P(0,0,0)$ will couple to the vertically polarized TE_{10} mode. Equations (4.24) and (4.25) then give

$$\begin{aligned} E3_y(0,0,-d) &= 2\ j\omega L_s\ H1_x^s(0,0,0)\ TE\ \exp(-\mu_o d/L_s) \ , \\ H3_x(0,0,-d) &= 2\ H1_x^s(0,0,0)\ TH\ \exp(-\mu_o d/L_s) \ , \end{aligned} \tag{6.41}$$

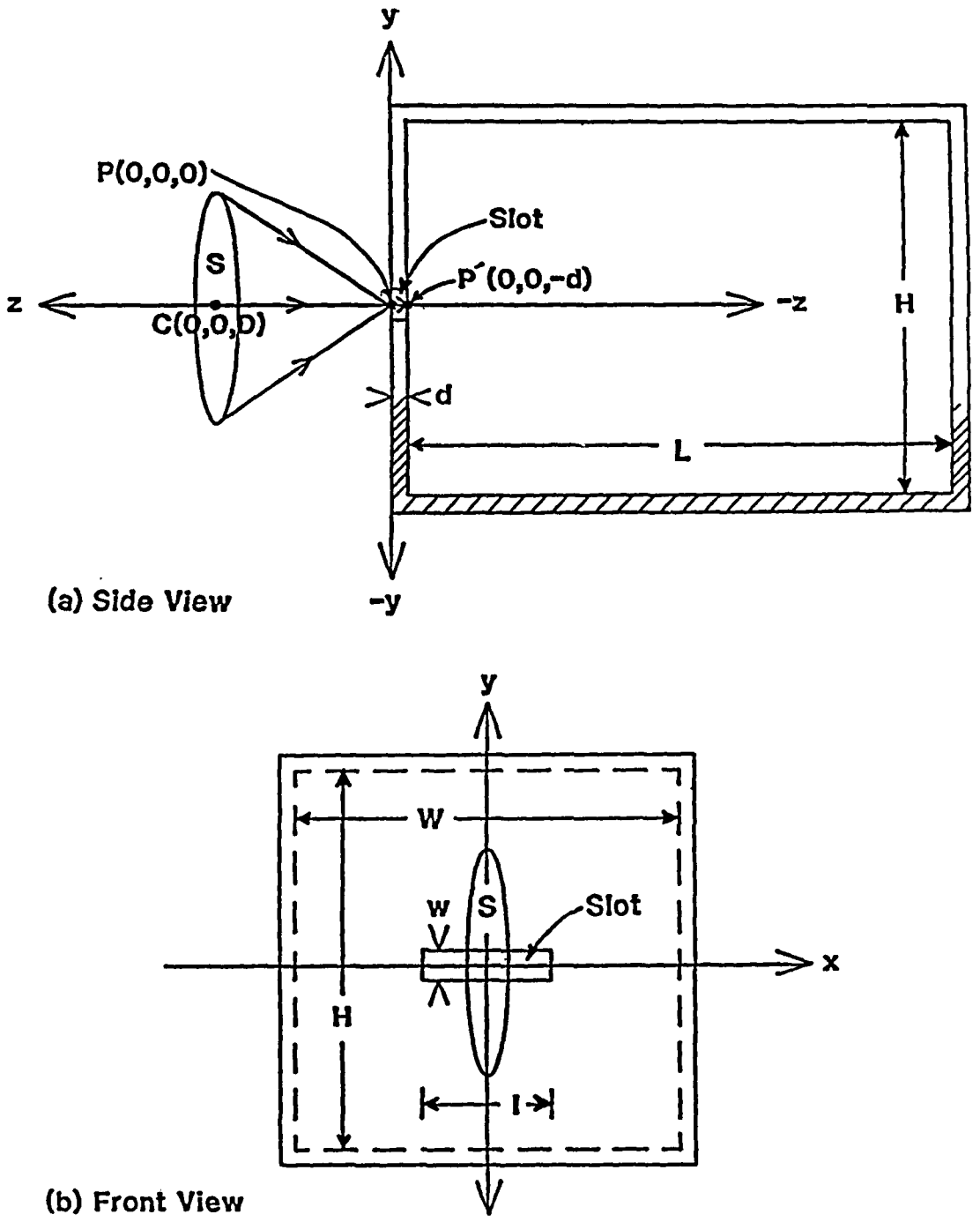

Figure 13. A source S illuminating an enclosure in the form of a rectangular parallelepiped with a slot in one face.

for an air filled slot where L_s is the slot inductance (6.25),

$$TE = 2\,\eta 3/(j\omega L_s + \eta 3)\ , \qquad (6.42)$$

$$TH = 2\,j\omega L_s/(j\omega L_s + \eta 3)\ ,$$

and $\eta 3$ is given by (6.36).

As with the expressions obtained in preceding sections, equations (6.41) can be easily adapted to other related structures such as a vertical slot in an otherwise continuous parallelepiped.

7. SHIELDING EFFECTIVENESS OF METALLIC STRUCTURES

7.1 Definitions of Shielding Effectiveness

There are two definitions of shielding effectiveness in current use which attempt to provide a figure of merit for the shielding properties of metallic structures. One of these, the theoretical definition, derives from Schelkunoff's shielding theory as described in section 2. The other, which we can call the experimental definition, has been promulgated in many public and private shielding standards such as MIL-STD-285[1] and IEEE 299.[31] As implied by these names, the first is used primarily in theoretical investigations; while the second is used in attempts to measure the effectiveness of electromagnetic shields in the laboratory and in the field.

Both definitions express the shielding effectiveness (SE) in terms of the ratio of the magnitude of an unshielded field component to the magnitude of the same field component when the shield is in place, and both definitions express the ratio of unshielded to shielded field components in terms of the same logarithmic scale. However, the definitions differ in the way the shielded and unshielded field components are specified, and the difference will contribute to the discrepancies between shielding measurements and theory noted in section 2. The difference between the definitions is illustrated in figure 14 where (a) and (b) describe the fields used in the theoretical definition and (c) and (d) refer to the experimental definition.

---

1 Anonymous, MIL-STD-285 "Method of Attenuation Measurements for Enclosures, Electromagnetic Shielding, for Electronic Test Purposes, Dept. of Defense, (25 June 1956).

31 Anonymous, Proposed IEEE Recommended Practice for Measurement of Shielding Effectiveness of High Performance Shielding Enclosures, IEEE 299, IEEE Inc., NY, NY, (June 1969).

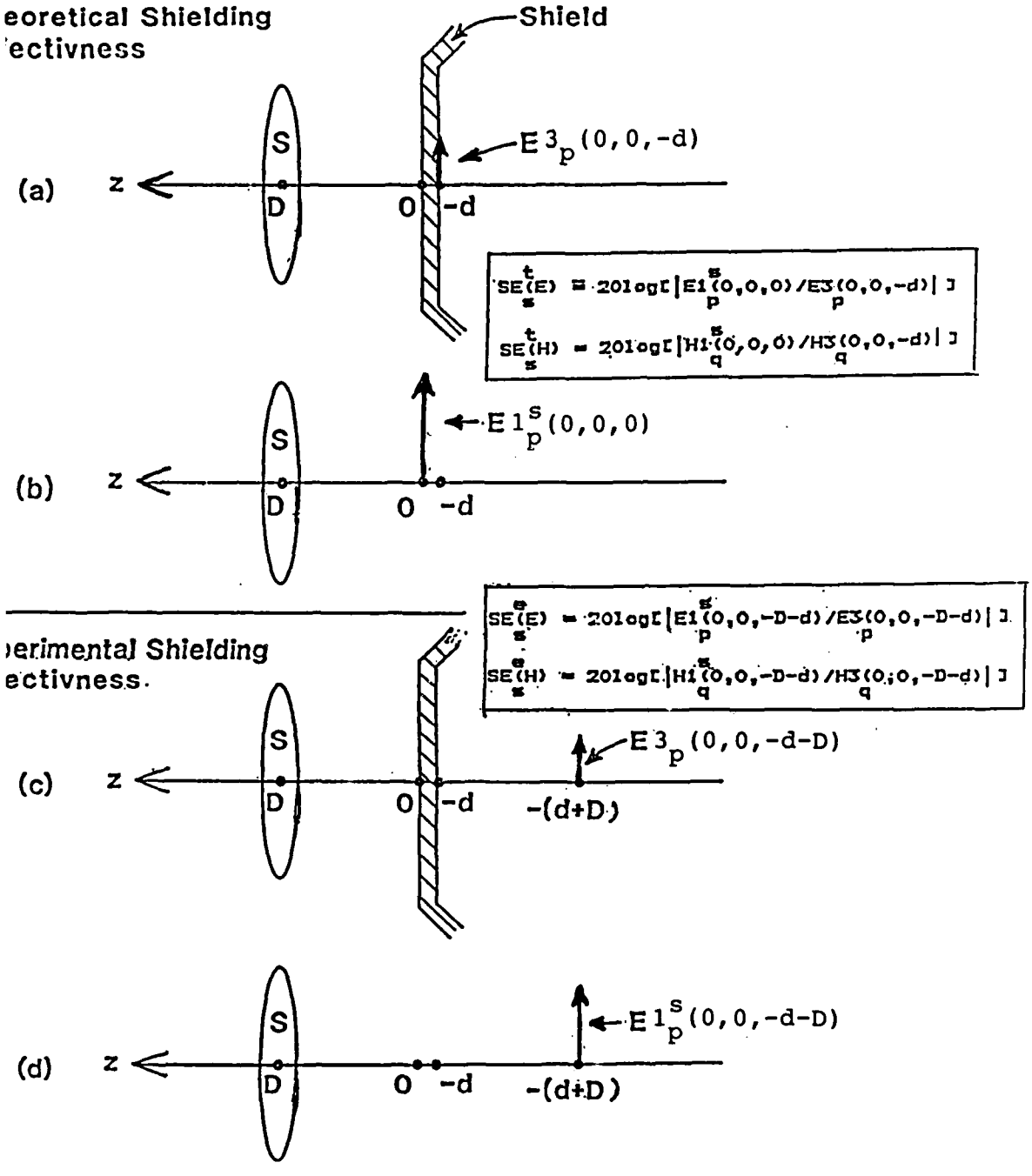

igure 14. Definitions of shielding effectiveness-
Theoretical definition: (a) - (b)
Experimental definition: (c) - (d)

n (a), a source S located at a distance D from the surface roduces a shielded electric field component $E3_p(0,0,-d)$ on the nside surface of the shield, and in (b) the same source at the ame location produces an unshielded electric field component $E1_p^s(0,0,0)$ at P(0,0,0) when the shield is removed. The theoretical definition of the shielding effectiveness against electric ields is then

$$SE_s^t(E) \equiv 20\log[|E1_p^s(0,0,0)/E3_p(0,0,-d)|] , \qquad (7.1)$$

where p denotes one of two orthogonal field components in a plane perpendicular to the z axis. Similarly, the shielding effectiveness of the same structure against magnetic fields from S is

$$SE_s^t(H) = 20\log[|H1_q^s(0,0,0)/H3_q(0,0,-d)|] , \qquad (7.2)$$

where q, like p, denotes one of the orthogonal components transverse to z. In figure 14(c) and (d), the same source and shield placed at the same positions relative to the z axis produces a shielded electric field component $E3_p(0,0,-D-d)$ at P'(0,0,-D-d) and an unshielded component $E1_p^s(0,0,-D-d)$ at the same point when the shield is removed. With these fields, the experimental definition of shielding effectiveness is written

$$SE_s^e(E) = 20\log[|E1_p^s(0,0,-D-d)/E3_p(0,0,-D-d)|] . \qquad (7.3)$$

And, for magnetic fields,

$$SE_s^e(H) = 20\log[|H1_q^s(0,0,-D-d)/H3_q(0,0,-D-d)|] . \qquad (7.4)$$

Since $E1_p^s(0,0,0) \neq E1_p^s(0,0,-D-d)$ and $E3_p(0,0,-d) \neq E3_p(0,0,-D-d)$, it is clear that, in general, $SE_s^t(E) \neq SE_s^e(E)$. And by the same token, $SE_s^t(H) \neq SE_s^e(H)$. Thus even under ideal circumstances, the two definitions will not give identical

ults. The question then arises as to how much of a discrep-
y is built into these definitions. Most investigators would
bably say that the discrepancy is negligible (<3 dB) basing
ir argument on the fact that the experimental definition as
is usually applied requires D to be relatively small. For
mple, MIL-STD-285 and IEEE 299 both describe shielding effec-
eness measurements using (7.4) in which the source and the
ld sensor are coplanar circular loops 12 inches in diameter
ated symmetrically on either side of the shield with their
ters at a distance D = 18 inches from the wall. When D is
s small, it can be argued that $E3_p$ will change at very nearly
same rate with respect to z that $E1_p^s$ changes so that
ir ratio will be virtually constant near the wall. This
lies:

$$SE_s^t(E) \cong SE_s^e(E) ,$$
$$SE_s^t(H) \cong SE_s^e(H) . \qquad (7.5)$$

ortunately, this argument is not always valid so that in some
es (7.5) is open to question. For example, it was pointed
in the preceding section that $H3_p$ inside an enclosure decreas-
exponentially with -z as the observation point moves away
m ES1 when the source frequency is below the cutoff frequency,
it was shown in section 5.2 that the source field $H1_p^s$ varies
e $1/z^3$ at points close to the source. Hence, $H1_p^s/H3_p$ could
y by a significant amount at points close to ES1 in this
e. It was also pointed out that standing waves could occur
an enclosure at frequencies above cutoff. $H3_p$ may then
rease at points in the interior leading to a much smaller
ue of shielding effectiveness as determined using the experi-
tal definition compared to that obtained with the theoretical
inition. For measurements made in accordance with MIL-STD-285

IEEE 299, the difference due to standing waves would be more
n 18 dB.

In the following, we will accept (7.5) as a working approxi-
ion while recognizing that in some cases significant differ-
es between the theoretical and experimental shielding effec-
eness of a given structure may occur solely because of the way
se quantities are defined. To eliminate such differences, it
ld be necessary to change one or the other of these defini-
ns. On the theoretical side, this could be done by extrapol-
ng the fields from $z = -d$ out to $z = -D-d$ and applying
experimental definition to the computed fields. Conversely,
the experimental side, one could measure the fields at $z = -d$
apply the theoretical definition to the measured fields.
ere are, of course, problems associated with both procedures,
a discussion of these problems is beyond the scope of the
sent report.

7.2 Shielding Effectiveness of Plane Sheets

In this section, we will obtain theoretical expressions
r the shielding effectiveness of uniform and slotted sheets using
e transmitted fields given in Sections 6.2 and 6.3. These
pressions will show that

$$SE_s^t \equiv SE_s^t(E) = SE_s^t(H) \quad , \tag{7.6}$$

ere SE_s^t is formally identical to Schelkunoff's Shielding Form-
a (2.16).

7.2.1 Uniform Sheets

The shielding effectiveness of a uniform sheet
n be obtained by evaluating equations (6.8) and (6.9) at
(0,0,-d) and substituting these expressions into (7.1) and
.2). Starting with $E3_\rho(0,0,-d) = E3_x(0,0,-d)$ and using (6.8)

7.1), we obtain

$$SE_s^t(E) = 20\log\left[\left|\frac{2\eta 2\ H1_y^s(0,0,0)\ TE\ \exp(-\gamma 2\, d)}{E1_x^s(0,0,0)}\right|\right] , \quad (7.7)$$

$E = 2\eta 3/(\eta 2 + \eta 3)$,

$1_x^s(0,0,0)/H1_y^s(0,0,0) = \eta 1$ by definition and $\eta 3 \cong \eta 1$ by
). Hence, $TE = 2\eta 1/(\eta 2 + \eta 1)$, and (7.7) can be rewritten as
ws

$$SE_s^t(E) = 20\log\left[\left|\frac{4\eta 2\ \exp(-\gamma 2\ d)}{\eta 2 + \eta 1}\right|\right] , \quad (7.8)$$

ting the ratio and using (6.3) to replace $\gamma 2$, we obtain

$$E_s^t(E) = 20\log[|(\eta 2 + \eta 1)/4\eta 2|] + 8.686(\pi\mu 2\sigma 2\ f)^{\frac{1}{2}}d .$$

in most cases of interest, the magnitude of the wave imped-
of the source field at P(0,0,0) is much greater than the
nsic impedance of M2, that is, $|\eta 1| >> |\eta 2|$. Consequently,
) reduces to its final form

$$E_s^t(E) = 20\log(|\eta 1\ /\ 4\eta 2|) + 8.686(\pi\mu 2\sigma 2\ f)^{\frac{1}{2}}d , \quad (7.9)$$

, with a trivial change in notation, is seen to be identi-
o (2.16) for $c = 4$.

f we now start with $H3_\rho(0,0,-d) = H3_x(0,0,-d)$ and use (6.9)
.2), we can easily show that $SE_s^t(H) = SE_s^t(E)$ in this case.

That is,

$$-SE_s^t(H) = 20\log\left[\left|\frac{2\ H1_x^s(0,0,0)\ TH\ \exp(-\gamma 2\ d)}{H1_x^s(0,0,0)}\right|\right]$$

$$= 20\log\left[|2\ TH\ \exp(-\gamma 2\ d)|\right] , \qquad (7.10)$$

where

$$TH = 2\eta 2/(\eta 2 + \eta 3) .$$

But again $\eta 3 = \eta 1$; hence (7.10) becomes

$$-SE_s^t(H) = 20\log\left[\left|\frac{4\eta 2\ \exp(-\gamma 2\ d)}{\eta 1 + \eta 2}\right|\right] ,$$

which is identical to (7.8). Therefore, $SE_s^t(E) = SE_s^t(H)$.

The reader can verify that the same result is obtained if one uses $E3_\phi(0,0,-d) = E3_y(0,0,-d)$ in (7.1) or $H3_\phi(0,0,-d) = H3_y(0,0,-d)$ in (7.2).

7.2.2 Slotted Sheets

The shielding effectiveness of a sheet with a narrow rectangular slot is formally identical to (7.9); however, because of the anisotrophy of this structure, the source and its orientation with respect to the slot must be specified. Thus,the shielding effectiveness of a "horizontal" slot (Figure 4(a)) against the fields of an x directed electric dipole is obtained by using (6.21) in (7.1) and (7.2). Following the same procedure as in the preceding section, we obtain

$$SE_{ED}^t(=) = SE_{ED}^t(E) = SE_{ED}^t(H)$$

$$= 20\log\left[|\eta 1\ /\ 4\eta 2_x|\right] + 8.686\ |\mu 2_x/\eta 2_x|d , \qquad (7.11)$$

where ED identifies the electric dipole source, and (=) indicates that the dipole is oriented parallel to the slot.

Similarly, the shielding effectiveness of the same slot against the fields of an x directed magnetic dipole is obtained using (6.23) in (7.1) and (7.2). The result is

$$SE^t_{MD}(=) = SE^t_{MD}(E) = SE^t_{MD}(H)$$
$$= 20\log[|\eta 1 \,/\, 4\eta 2_y|] + 8.686|\mu 2_y/\eta 2_y|d \,, \tag{7.12}$$

where MD refers to the source and (=) again indicates that the dipole is oriented parallel to the slot. For an air filled slot where $\mu 2_y = \mu_o$ and $\eta 2_y = j\omega L_s$, $SE^t_{MD}(=)$ reduces to

$$SE^t_{MD}(=) = 20\log[|\eta 1|\,/\,4\omega L_s] + 8.686\ \mu_o d/L_s \,, \tag{7.13}$$

where L_s is the slot inductance and $\eta 1 = \eta 3$ is given by (6.16).

Comparable expressions are easily obtained for the "vertical" slot (figure 4(b)) when it is exposed to x directed dipoles.In the case, of an air filled slot exposed to an electric dipole, the result is

$$SE^t_{ED}(+) = 20\log[|\eta 1'|/4\omega L_s] + 8.686\ \mu_o d/L_s \,, \tag{7.14}$$

where (+) indicates that the dipole is oriented perpendicular to the slot and $\eta 1'$is given by (6.15).

7.3 Shielding Effectiveness of Enclosures

In this section, we will obtain theoretical expressions for the shielding effectiveness of continuous and discontinuous enclosures (figures 12 and 13) using the results of sections 6.4 and 6.5. For both of these cases, it will be seen that

$$SE^t_s(E) \neq SE^t_s(H) \,. \tag{7.15}$$

Consequently, neither $SE_s^t(E)$ nor $SE_s^t(H)$ is reducible to Schelkunoff's equation (2.16).

7.3.1 Single Walled Continuous Parallelepiped

Starting with (6.37) and following the same procedure as before, we obtain

$$SE_s^t(E) = 20\log\left[\left|\frac{\eta 1(\eta 2 + \eta 3)}{4\eta 2\eta 3}\right|\right] + 8.686(\pi\ \mu 2\ \sigma 2\ f)^{\frac{1}{2}}d\ ,$$

and (7.16)

$$SE_s^t(H) = 20\log\left[\left|\frac{\eta 2 + \eta 3}{4\eta 2}\right|\right] + 8.686(\pi\ \mu 2\ \sigma 2\ f)^{\frac{1}{2}}d\ ,$$

for the shielding effectiveness of a rectangular parallelepiped where $\eta 3$ is given by (6.36). The preceding implies

$$SE_s^t(E) - SE_s^t(H) = 20\log[|\eta 1/\eta 3|]\ . \qquad (7.17)$$

That is, the difference between the shielding effectiveness of an enclosure against electric fields and its shielding effectiveness against magnetic fields from the same source depends on the ratio of the source impedance at z = 0 to the enclosure impedance at z = -d. When $|\eta 1| > |\eta 3|$, $SE_s^t(E) > SE_s^t(H)$. And conversely, $|\eta 1| < |\eta 3|$ implies $SE_s^t(E) < SE_s^t(H)$. If $|\eta 1| = |\eta 3|$, then $SE_s^t(E) = SE_s^t(H)$, and (7.16) reduces to (7.9) since $|\eta 1| >> |\eta 2|$. That is, when the impedance of the source equals the impedance of the enclosure, the shielding effectiveness of the enclosure is equivalent to the shielding effectiveness of an infinite plane sheet.

7.3.2 Single Walled Parallelepiped with a Slot in One Side

The shielding effectiveness of a parallelepiped with a narrow slot in one face is formally identical to (7.16), but, as in the case of the slotted sheet, the orientation of the source with respect to the slot must be specified. For an enclosure with a horizontal air filled slot as shown in figure 13 exposed to an x directed magnetic dipole, the shielding effectiveness with respect to electric and magnetic fields is

$$SE^t_{MD}(E=) = 20\log\left[\left|\frac{\eta 1(\eta 2 + \eta 3)}{4\eta 2\eta 3}\right|\right] + 8.686\mu_o d/L_s \ , \tag{7.18}$$

$$SE^t_{MD}(H=) = 20\log\left[\left|\frac{\eta 2 + \eta 3}{4\eta 2}\right|\right] + 8.686\mu_o d/L_s \ ,$$

where $\eta 1$ is given by (6.16) and (6.19)

$$\eta 1 = Z_o\left[\frac{jk_oD\ (jk_oD + 1)}{jk_oD + 1 - k_o^2D^2}\right] \ , \tag{7.19}$$

$$\eta 2 = j\omega L_s \ , \tag{6.25}$$

and

$$\eta 3 = Z_{TE}\tanh(\gamma 3\ L) \ . \tag{6.36}$$

As in the case of (7.16), we have

$$SE^t_{MD}(E=) - SE^t_{MD}(H=) = 20\log[|\eta 1/\eta 3|] \ , \tag{7.20}$$

so that $SE^t_{MD}(E=)$ is greater than, less than,or equal to $SE^t_{MD}(H=)$ depending on whether $|\eta 1|$ is greater than, less than, or equal to $|\eta 3|$. When $|\eta 1| = |\eta 3|$, (7.18) reduces to (7.13). That is, when the magnitude of the source impedance equals the magnitude

of the enclosure impedance, the shielding effectiveness of the enclosure is equivalent to the shielding effectiveness of an infinite sheet with an air filled slot.

It is of interest to compare the shielding effectiveness measurements of Axford et al [9] with $SE^{t}_{MD}(H)$ based on (7.18). This is done in figure 15 where (a) shows a schematic representation of the experimental set-up and (b) is a plot of the measured and computed shielding effectiveness versus source frequency. As the figure indicates, the measurements were carried out using 12 in. diameter loops in the arrangement prescribed by MIL-STD-285 and IEEE 299 on a 9'x9'x9' shielded enclosure with a rectangular slot .5 m. long and 1/16 in. wide on one face. The walls of the enclosure consisted of steel and aluminum panels 1/4 in. thick, and the surface of the wall opposite the slot was prepared with an electromagnetic absorbing material to reduce internal reflections. With this arrangement, the measured shielding effectiveness of the slotted enclosure against magnetic fields from a loop antenna was obtained using the experimental definition (7.4).

In applying (7.18) to this enclosure, it was assumed that the absorbing material effectively eliminates internal reflections so that the enclosure impedance (6.36) reduces to

$$\eta 3 = Z_{TE} \quad \text{for} \quad f < f_c = 49 \text{ MHz} \ . \tag{7.21}$$

That is, the enclosure is equivalent to an infinitely long waveguide and the input impedance is equal to the characteristic impedance of the waveguide (6.30). The slot inductance L_s used

---

9 R. Axford, R. McCormack, and R. Mittra, Evaluation of the Applicability of Standard CW EMI/RFI Shielding Effectiveness Test Techniques to Assessment of EMP Hardness of Tactical Shelters, Construction Engineering Research Laboratories, CERL-TM-M-307, (March 1982).

(a) Experimental Set-up (Estimated)

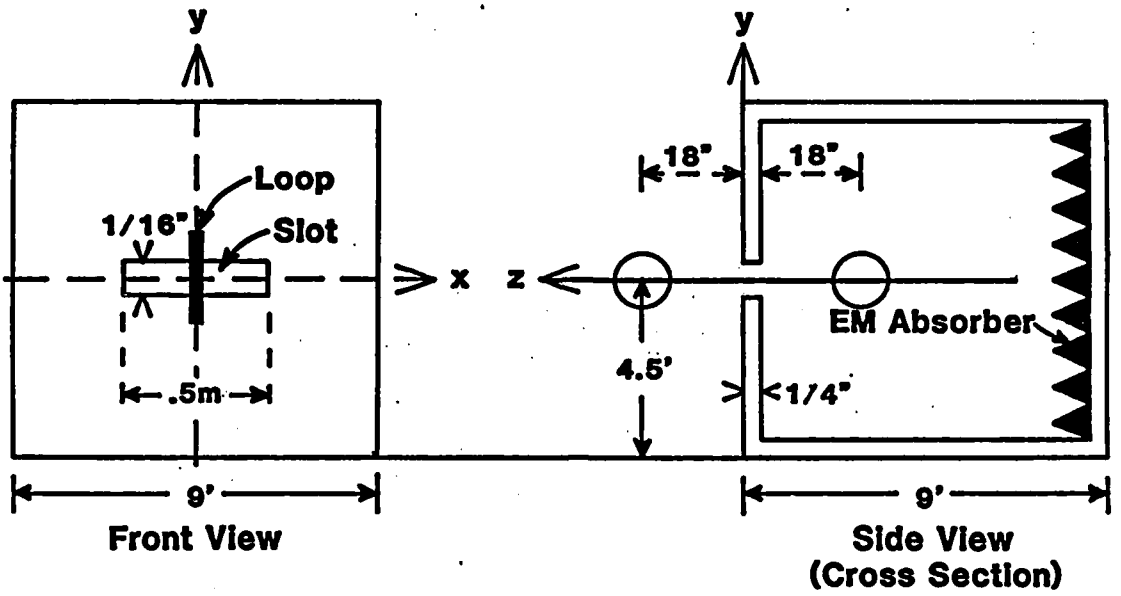

(b) Comparison of Measured and Computed Shielding Effectiveness

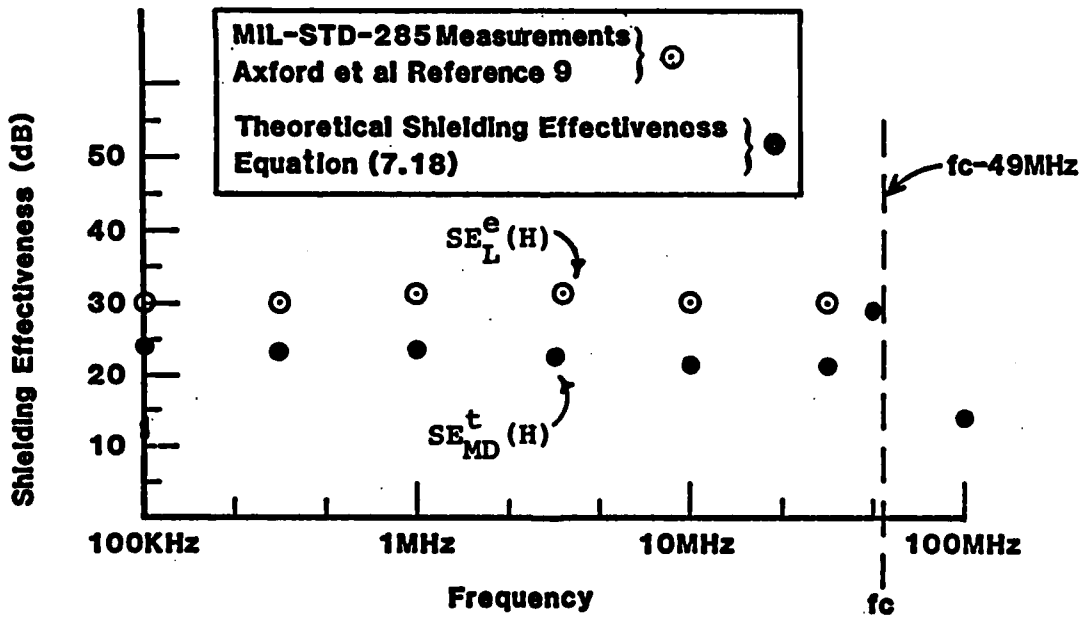

Figure 15. Measured and theoretical shielding effectiveness of an enclosure with a narrow rectangular slot in one wall. (fc = cutoff frequency).

in these calculations is 3.2×10^{-8}H (equation 6.28).

Figure 15(b) shows that the difference between the measured and theoretical shielding effectiveness ranges from 6 to 8 dB for this enclosure over more than two decades of frequency. In view of the inherent discrepancy between the discrepancy and experimental definitions os shielding effectiveness noted in section 7.1 as well as other uncertainties such as the actual effectiveness of the absorbing material used in the measurements, this must be considered good agreement.

7.4 A Modified Theoretical Definition of Shielding Effectivenss for Enclosures

In section 7.2, it was shown that the theoretical shielding effectiveness of a plane sheet (continuous or discontinuous) is characterized by a single function which is identical in form to Schelkunoff's shielding formula. That is,

$$SE_s^t = SE_s^t(E) = SE_s^t(H) \ , \qquad (7.22)$$
$$= 20\log(|\eta s/4\ \eta c|) + A \ ,$$

where ηs is the wave impedance of the source at P(0,0,0), ηc is the characteristic impedance of the sheet (Equation (6.2) or (6.25)) and A is a loss term that may depend on the frequency but is otherwise independent of the source. This result establishes the validity of the extended transmission theory of shielding described in section 2 for shields consisting of a single planar sheet. To obtain the effectiveness of a plane shield with respect to any source field, it is only necessary to specify the wave impedance of the source field in (7.22). In the case of an electric dipole, we have

$$SE_{ED}^t = SE_{ED}^t(E) = SE_{ED}^t(H) \qquad (7.23)$$
$$= 20\log(|\eta ED/4\ \eta c|) + A \ ,$$

where ηED is the wave impedance of the electric dipole at P(0,0,0) (equation (6.15)). And for the magnetic dipole,

$$SE_{MD}^{t} = SE_{MD}^{t}(E) = SE_{MD}^{t}(H)$$
$$= 20\log(|\eta MD/4\ \eta c|) + A\ , \tag{7.24}$$

where ηMD is the wave impedance of the magnetic dipole (Equation (6.16)).

The simplicity of (7.22) is a direct result of the fact that ηs is approximately equal to $\eta 3$, the impedance of the field at P´(0,0,-d) looking into M3. That is,

$$\eta s \cong \eta 3\ . \tag{7.25}$$

This, in turn, is due to the fact that the fields on both sides of the sheet satisfy the same radiation condition and approach the same wave impedance as $z \longrightarrow \pm\infty$.

In contrast to the preceding, it was seen in section 7.3 that the shielding effectiveness of an enclosure is not characterized by either $SE_s^t(E)$ or $SE_s^t(H)$ alone. That is,

$$SE_s^t \neq SE_s^t(E) \neq SE_s^t(H)\ , \tag{7.26}$$

but instead,

$$SE_s^t(E) = SE_s^t(H) + 20\log(|\eta s/\ \eta 3|)\ , \tag{7.27}$$

where ηs is again the wave impedance of the source field at P(0,0,0) and $\eta 3$ is the impedance at P´(0,0,-d) looking into the enclosure (M3). Since the structure of the fields in the enclosure is unrelated to that of the fields outside the enclosure,

$$\eta s \neq \eta 3 \equiv \eta e\ , \tag{7.28}$$

in this case. This means that the shielding characteristics of an enclosure depend on both $SE_s^t(E)$ and $SE_s^t(H)$. It follows that the shielding effectiveness of an enclosure should be defined in terms of both of these quantities. The logical choice for this definition is

$$SE_s^t \equiv (SE_s^t(E) + SE_s^t(H))/2 \ . \tag{7.29}$$

Since (7.29) reduces to (7.22) when $SE_s^t(E) = SE_s^t(H)$, this definition includes the plane sheet as a special case. Moreover, the reader can easily verify that the right side of (7.29) is determined by the ratio of the power density of the source field incident at P(0,0,0) to the power density of the transmitted field at P'(0,0,-d). That is,

$$SE_s^t = 10\log[|PD1^s(0,0,0)/PD3(0,0,-d)|] \ , \tag{7.30}$$

where

$$PD1^s(0,0,0) = E1_p^s(0,0,0)\ H1_q^s(0,0,0) \ ,$$

$$PD3(0,0,-d) = E3_p(0,0,-d)\ H3_q(0,0,-d) \ .$$

7.5 A Modified Experimental Definition of Shielding Effectiveness and Its Implications For MIL-STD-285 and IEEE 299

Since $SE_s^t(E) \neq SE_s^t(H)$, it follows from (7.5) that $SE_s^e(E) \neq SE_s^e(H)$ for enclosures. That is, the experimental shielding effectiveness of an enclosure against electric fields (7.3) is not equal to the experimental shielding effectiveness of the same enclosure against magnetic fields from the same source (7.4). Thus, the experimental shielding effectiveness of an enclosure depends on both $SE_s^e(E)$ and $SE_s^e(H)$ just as SE_s^t depends on both $SE_s^t(E)$ and $SE_s^t(H)$ as we have seen. To reflect

this fact, the experimental definition of shielding effectiveness should include both $SE_s^e(E)$ and $SE_s^e(H)$. The logical choice here (analogous to (7.29) is

$$SE_s^e = (SE_s^e(E) + SE_s^e(H))/2 \ . \qquad (7.31)$$

The reader can verify that SE_s^e is the ratio of the power density at P(0,0,-D-d) with the enclosure removed to the power density at the same point with the enclosure in place.

The clear implication of the preceding is that the shielding properties of an enclosure cannot be completely determined by measuring either $SE_s^e(E)$ or $SE_s^e(H)$ alone; yet this is precisely what virtually all shielding standards attempt to do. For example, as previously noted, both MIL-STD-285 and IEEE 299 specify shielding measurements with a source and a field sensor consisting of small loop antennas. These produce a measured value of $SE_s^e(H)$ for a loop source. But neither MIL-STD-285 or IEEE 299 provide any procedures that lead to a measured value of $SE_s^e(E)$ for the loop source. Thus, there is no way that measurements made in accordance with these standards can be related to the power density ratio for shielded and unshielded fields from the loop source.

7.6 A Generalized Schelkunoff Formula and a New Formulation of the Extended Transmission Theory of Shielding

The fact that $SE_s^t(E) \neq SE_s^t(H)$ for enclosures also has implications for the extended transmission theory of shielding. It means that, unlike the situation described in section 7.4 for plane sheets, neither $SE_s^t(E)$ nor $SE_s^t(H)$ can be reduced to Schelkunoff's equation (2.16) when the shield is in the form of an enclosure. And, since Schelkunoff's equation is the basis for the extended transmission theory of shielding, it follows that this theory as described in section 2 cannot be valid for enclo-

sures. However, with the aid of a generalized form of Schelkunoff's equation, we can reformulate the extended transmission theory in a way that includes both enclosures and plane sheets.

To obtain the generalized Schelkunoff equation, we substitute (7.16) and (7.18) into (7.29). The result (with a change in notation) is

$$SE_s^t = 10\log(|\eta s/\eta e|) + 20\log\left[\left|\frac{\eta c + \eta e}{4\ \eta c}\right|\right] + A\ , \qquad (7.32)$$

where ηs is the wave impedance of the source, ηe is the impedance looking into the enclosure, ηc is the characteristic impedance of the enclosure wall and A is the absorption term. With (7.32), we can compute the shielding effectiveness of any enclosure for which ηe, ηc, and A can be determined against the fields of any source for which ηs is known. Thus, according to the reformulated theory, the shielding problem reduces to the problem of calculating these quantities.

In applying this theory, two things must be kept in mind: First, ηe, ηc, and A can all depend on the polarization of the incident field or, in other words, the orientation of the source with respect to the enclosure and to any discontinuities that may be iluuminated. Consequently, in citing the shielding effectiveness of any enclosure, the spatial relationship between the source and the enclosure must be specified. Second, theoretical results based on (7.32) should only be compared to measurements based on the modified experimental definition of shielding effectiveness (7.31). That is, a valid test of (7.32) requires measurements of both $SE_s^e(E)$ and $SE_s^e(H)$.

7.7 A Correction Factor Relating the Shielding Effectiveness of an Enclosure as Seen by Two Sources

With (7.32), we can obtain a simple analytical relationship between the shielding effectiveness of an enclosure as

seen by one source and the shielding effectiveness of the same enclosure as seen by a second source. If $\eta S1$ is the wave impedance of the first source, then we have

$$SE^t_{S1} = 10\log(|\eta S1/\ \eta e|) + 20\log\left[\left|\frac{\eta c + \eta e}{4\ \eta c}\right|\right] + A\ ,$$

And, if $\eta S2$ is the wave impedance of a second source with the same orientation (polarization) as S1, then

$$SE^t_{S2} = 10\log(|\eta S2/\ \eta e|) + 20\log\left[\left|\frac{\eta c + \eta e}{4\ \eta c}\right|\right] + A\ ,$$

is the shielding effectiveness of the enclosure as seen by S2. Now taking the difference between SE^t_{S1} and SE^t_{S2}, we obtain

$$\Delta(S1:S2) \equiv SE^t_{S1} - SE^t_{S2}$$

$$= 10\log(|\eta S1/\ \eta S2|)\ . \qquad (7.33)$$

That is, the difference between the shielding effectiveness of an enclosure as seen by two sources with the same orientation depends only on the ratio of the wave impedance of the two sources.

With the correction factor, $\Delta(S1:S2)$, measured values of shielding effectiveness taken with one source can be analytically adjusted to give an estimate of the shielding effectiveness that would have been measured with another source. This can be very useful in cases where shielding measurements with one source are difficult or impossible as they are with a plane wave EMP sources where $\eta S1 = 120\pi$ ohms. In this case, the estimated shielding effectiveness of an enclosure against a plane wave EMP field is

earth's surface where θ and ϕ , like ρ, are coordinates referred to a burst, centered sheprical system and the superscript c denotes the fact that the direct Compton current is the source of these fields. Additional and even larger fields E_θ^r and B_ϕ^r are generated by current loops formed when Compton currents in the air are returned through the ground to re-establish charge neutrality in the source region. The net vertical electric field E_θ and azimuthal magnetic field B_ϕ near ground level are equal to the sum of these fields: $E_\theta = E_\theta^c + E_\theta^r$, $B_\phi = B_\phi^c + B_\phi^r$.

E_ρ and B_ϕ are the largest fields generated in the source region. Peak fields occur close to the burst point above ground level, and both fields decrease rapidly with increasing distance from the burst point. The time history of E_ρ is characterized by a rapid rise to a maximum at t = 50 ns followed by a 50 ns decay to a plateau that is maintained for 10-20 μs before the final decay. As shown in figure 18(b)[35], B_ϕ has a narrow early peak (B_ϕ^c) followed by a much broader late peak (B_ϕ^r). The rise time of the early peak is approximately the same as that of E_ρ. The late peak occurs at approximately 7 μs and is followed by a gradual decay out to 70 μs. An analytical approximation to the waveform in figure 18(b) can be written as follows

$$B_\phi(t) = B_\phi^c(t) + B_\phi^r(t) \quad , \tag{8.23}$$

where

$$\begin{aligned} B_\phi^c &= A_1[\exp(-\alpha_1 t) - \exp(-\alpha_2 t)] \quad , \\ B_\phi^r &= A_2[\exp(-\alpha_3 t) - \exp(-\alpha_4 t)] \quad , \end{aligned} \tag{8.24}$$

35 T. Wyatt, Harry Diamond Laboratories, Washington, D.C., Private Communication, (June 1984).

(a)

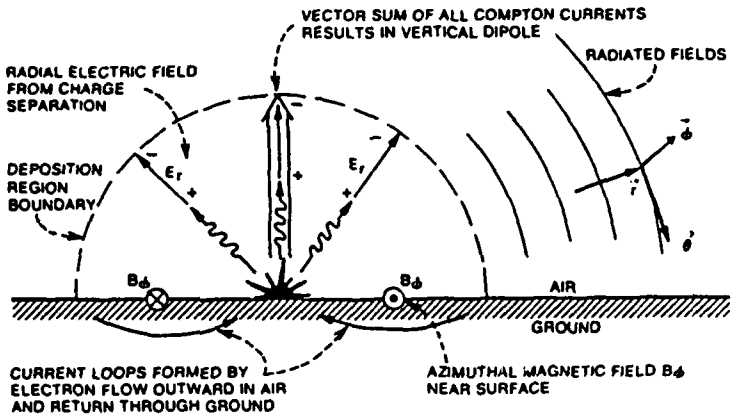

(b)

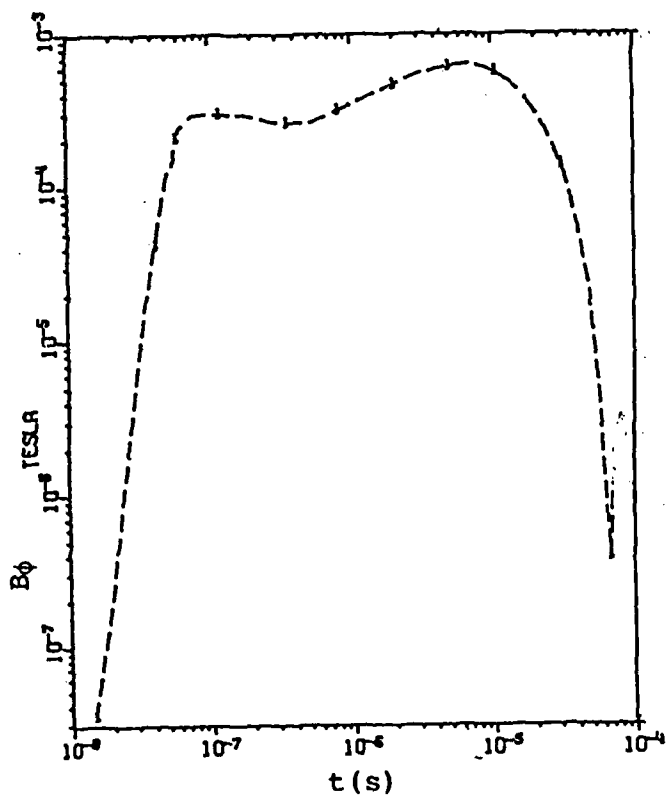

Figure 18. Source region currents and fields.

(a) Schematic representative of source region currents and fields (Adapted from ref.34).

(b) Source region magnetic field B_ϕ versus time (Reproduced from ref.35).

bining the most important features of the entire range of HA EMP waveforms has been constructed for use in studies that attempt to determine the vulnerability of military systems to interference or damage from these fields. This field is in the form of a plane wave where the electric and magnetic components are given by[34]

$$e(t) = Z_o\, h(t) , \qquad (Z_o = 120\pi \text{ ohms})$$
$$= 5.25\times10^4 [\exp(-4\times10^6 t) - \exp(-4.76\times10^8 t)] \text{ (V/m)} . \tag{8.22}$$

The reader can verify that (8.22) gives peak fields of 5×10^4 V/m and 140 A/m at $t = 5$ ns. The similarity between the fields given by (8.22) and the field shown in figure 17 suggests that the waveform of the HA EMP field can be simulated over a limited area by a loop antenna driven with an appropriately designed current pulse.

Source Region EMP (SREMP). When a nuclear weapon is detonated on or within a few kilometers above the surface of the earth, the EMP source region will consist of a truncated sphere 3 to 6 kilometers in diameter as shown in figure 18(a). In the air, Compton currents will generate a radial electric field E_ρ; however, below the surface of the earth this current and field will be greatly reduced owing to the high conductivity of earth relative to that of the ionized air in the source region. The result will be an asymmetric distribution of Compton currents. The vector sum of this unbalanced distribution of currents is a vertical electric dipole at the burst point capable of radiating electric and magnetic fields beyond the source region. Within the source region, the vertical dipole generates a vertical electric field E_θ^c and an azimuthal magnetic field B_ϕ^c at the

34 Bell Laboratories, EMP Engineering and Design Principles, Whippany, N.J., (1975).

and for this reason, as well as others, we will not attempt to carry out such calculations here. Instead, we will give descriptions of two important types of EMP fields based on calculations carried with three dimensional, time dependent computer codes that are designed to give self-consistent solutions for the Compton current and its fields.

High Altitude EMP (HA EMP). When a nuclear explosion occurs at an altitude above 40 km, the density of the atmosphere is so small that gamma rays are not scattered in the vicinity of the burst point. Instead, they travel radially in a spherical shell until a portion of the shell reaches an altitude of 20-40 km where the density is such that the Compton process is important. The resulting distribution of Compton currents defines a pancake-shaped EMP source region 20 km thick with a lateral extent limited by the curvature of the earth. Within this region, high energy recoil electrons spiralling around geomagnetic field lines comprise a component of the Compton current transverse to the gamma ray flux. This Compton current is equivalent to an array of elementary magnetic dipoles whose vector sum is capable of producing a peak electric field of 50×10^3 V/m at the surface of the earth. Since the direction of the net magnetic dipole moment of this array is determined by the geomagnetic field vector in the source region, the orientation of the dipole moment is not fixed with respect to the surface of the earth. Rather, it is a function of the altitude and geographical coordinates of the source region. This means that the HA EMP field incident at a point on the surface of the earth depends in a complicated way on the coordinates of that point and the coordinates of the source region.

Since the geometry of the source region cannot be accurately known prior to a detonation, the incident EMP field at a point is unpredictable. For this reason,a composite HA EMP field com-

P(0,0,0). The figure shows that $h1_x^s(0,0,0;t)$ reaches its peak in 6 ns (6×10^{-9}s) compared to 10 ns for the loop current itself. This indicates that the second term in (8.21) which arises from the $j\omega r_2 D/C_0$ term in (8.18) can have a significant effect on the rise time of $h1_x^s(0,0,0;t)$ if the derivative of i(t) is large enough, although the general character of the magnetic field will be the same as the loop current source. In view of figure 8(c), this in an expected result.

8.3 EMP Sources

An EMP field is generated by an intense pulse of gamma rays from a nuclear explosion.[33] Gamma rays traveling radially away from the burst point ionize ambient matter by Compton scattering and produce a flux of recoil electrons moving in the same direction. This electron flux constitutes a transient current called the Compton current that is the proximate source of all EMP fields. The volume through which Compton currents flow following a detonation is called the deposition or EMP source region.

The spatial and temporal characteristics of the EMP field are determined by the corresponding characteristics of the Compton current in much the same way that $h1_x^s(0,0,0;t)$ was determined by i(t) in the preceding section. Once the Compton current is known, the electromagnetic field can be computed from Maxwell's equations using the same techniques employed in section 5. However, in this case, the problem is greatly complicated by the fact that the Compton current itself is strongly affected by the fields it produces. That is, the problem is inherently nonlinear. This fact places the problem of computing Compton currents and EMP fields beyond the scope of this study,

---

33 C. L. Longmire, IEEE Trans. Ant. Propt., AP-16, No.1,(1978).

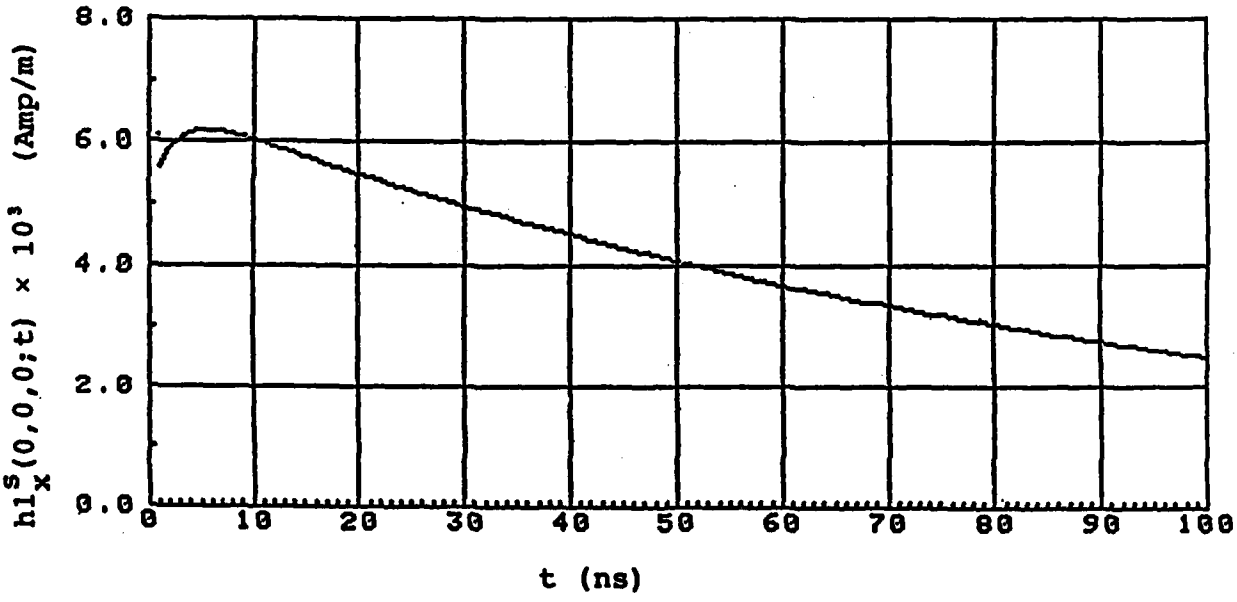

Figure 17. Loop magnetic field at O versus time.

With $I(j\omega)$ replacing I in (5.39), we obtain the following expression for the dominant magnetic field component at P(0,0,0) due to i(t) on the loop

$$H1_x^s(0,0,0) = H1_\rho^s(0,0,0) = I(j\omega)\ G(0,0,0;j\omega)\ , \tag{8.17}$$

where

$$G(0,0,0;j\omega) = \exp(j\omega D/C_0)\ [r_1 + j\omega r_2 D/C_0]/4\pi\ , \tag{8.18}$$

and r_1 and r_2 are functions of D (the distance between the geometric center of the loop and the observation point), a (the length of one side of the loop), and h (the distance between the center of the loop and the ground plane). When

$$D = 18"\ ,\ a = 10.6"\ ,\ h = 3.5'\ , \tag{8.19}$$

we obtain

$$r_1 = .076\ m^{-1},\ r_2 = .105\ m^{-1}\ , \tag{8.20}$$

from equation (5.39).

The inverse Laplace transform of equation (8.17) with $I(j\omega)$ given by (8.16) and $G(0,0,0;j\omega)$ given by (8.18) is the transient magnetic field $h1_x^s(0,0,0;t)$ incident at P(0,0,0) when the loop is driven by a current pulse in the form of equation (8.15). In this case, the inverse can be evaluated exactly using tabulated transforms. The result is

$$h1_x^s(0,0,0;t) = r_1 i(t-D/C_0)/(4\pi) + (r_2 D/4\pi C_0)\left[\frac{\partial i(t-D/C)}{\partial t} + A_0(\alpha_1 - \alpha_2)\right]\ , \tag{8.21}$$

for $t \geq D/C$. Figure 17 is a plot of $h1_x^s(0,0,0;t)$ using the parameters specified by (8.15), (8.19), and (8.20). In this figure, and in all subsequent figures, the time delay D/C_0 has been dropped so that t = 0 corresponds to the arrival of the field at

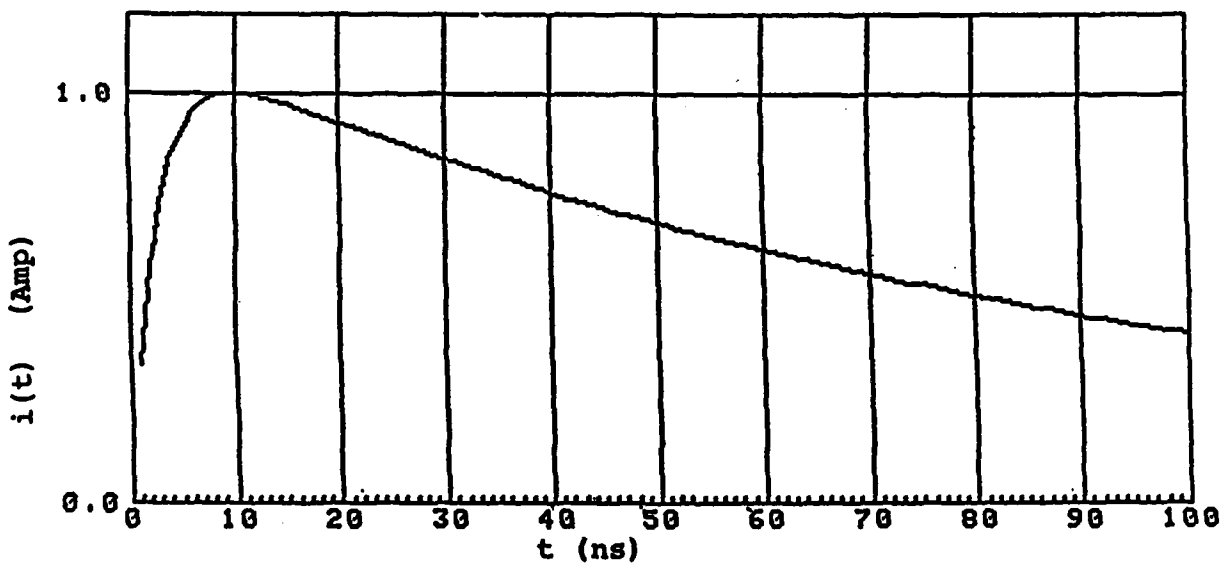

Figure 16. Loop current i(t) versus time.

When the source is defined in terms of an incident magnetic field $h_x^s(t)$ at P(0,0,0) on continuous and slotted enclosures as in (8.7) and (8.8), then the transmitted fields are

$$h3_x(0,0,-d;t) = L^{-1}[H_x^s(j\omega)\ T1(-d;j\omega)] \ , \tag{8.13}$$

and

$$h3_x(0,0,-d;t) = L^{-1}[H_x^s(j\omega)\ T2(-d;j\omega)] \ . \tag{8.14}$$

In the following sections, we will evaluate $I(j\omega)$ and $H_x^s(j\omega)$ for a specified loop current $i(t)$ and magnetic field $h_x^s(t)$. We will then use $I(j\omega)$ to obtain the frequency domain expressions in (8.3), (8.5), and (8.6). And, we will use $H_x^s(j\omega)$ to obtain the corresponding expression in (8.7). Finally, we will evaluate the inverse Laplace transforms in (8.10)-(8.13) to obtain explicit time domain representations of the incident and transmitted fields from these transient fields.

8.2 A Small Loop Antenna Carrying a Current Pulse

If the square loop antenna shown in figure 10(a) is driven with the current pulse $i(t)$ shown in figure 16, then $i(t)$ can be represented analytically as follows

$$i(t) = A_0[\exp(-\alpha_1 t) - \exp(-\alpha_2 t)] \ , \tag{8.15}$$

where

$$A_0 = 1.14\ A \ , \ \alpha_1 = 10^7\ s^{-1} \ , \ \alpha_2 = 3.72\times10^8\ s^{-1} \ ,$$

and $I(j\omega)$ can be computed from (8.15) using a tabulated Laplace transform.[32] The result is

$$I(j\omega) = L[i(t)] = A_0[1/(\alpha_1 + j\omega) - 1/(\alpha_2 + j\omega)] \ . \tag{8.16}$$

---

32 G. Doetsch, Guide To Applications of Laplace Transforms, D. Van Nostrand Company LTD., London, (1961).

for the fields transmitted by continuous and slotted enclosures from this source. For the continuous enclosure, we obtain

$$H3_x(0,0,-d) = H_x^s(j\omega)\ T1(-d;j\omega)\ , \tag{8.7}$$

and for the slotted enclosure

$$H3_x(0,0,-d) = H_x^s(j\omega)\ T2(-d;j\omega)\ . \tag{8.8}$$

where T1 and T2 are again determined from (6.37) and (6.41) respectively.

Frequency domain expressions such as (8.3), (8.4), (8.5), (8.6), and (8.7) are sufficient for many problems involving transient sources; however, for others, there is no substitute for time domain representations of the incident and transmitted fields. These can be obtained by applying the inverse Laplace transform $L^{-1}[\ ]$ to the appropriate frequency domain expression where

$$L^{-1}[F(j\omega)] \equiv \frac{1}{2\pi} \int_{-j\infty}^{j\infty} \exp(j\omega t)\ F(j\omega)\ d\omega\ . \tag{8.9}$$

Thus, from (8.3) we obtain the transient magnetic field incident at P(x,y,0) from a loop antenna carrying the current i(t)

$$h1_x^s(x,y,0;t) = L^{-1}[I(j\omega)\ G(x,y,0;j\omega)]\ . \tag{8.10}$$

From (8.5) we obtain the transient field transmitted to the interior of a continuous enclosure from this source

$$h3_x(x,y,-d;t) = L^{-1}[I(j\omega)\ G(x,y,0;j\omega)\ T1(-d;j\omega)]\ . \tag{8.11}$$

And, from (8.6) we obtain the transient field transmitted to the interior of a slotted enclosure from the same source

$$h3_x(0,0,-d;t) = L^{-1}[I(j\omega)\ G(0,0,0;j\omega)\ T2(-d;j\omega)]\ . \tag{8.12}$$

When these transforms are evaluated, $I(j\omega)$ and $H_x^s(j\omega)$ can be used with our previous results to give frequency domain expressions for the fields incident on and transmitted by an electromagnetic shield from a transient source. In the case where $i(t)$ is a current on a loop antenna such as the one described in section 5.2, we can obtain the magnetic field in the x,y plane due to this transient source by substituting $I(j\omega)$ for I in equation (5.39). This field can be used in turn in equation (6.37) to give expressions for the fields transmitted through the wall of a continuous enclosure. It can also be used in (6.41) to give the fields transmitted by a slotted enclosure. This process can be summarized as follows:

$$H1_x^s(x,y,0) = I(j\omega)\ G(x,y,0;j\omega)\ , \tag{8.3}$$

where $G(x,y,0;j\omega)$ is determined from (5.39). And ,

$$H3_x(x,y,-d) = H1_x^s(x,y,0)\ T1(-d,j\omega)\ , \tag{8.4}$$

where $T1(-d,j\omega)$ is determined by (6.37). Thus ,

$$H3_x(x,y,-d) = I(j\omega)\ G(x,y,0;j\omega)\ T1(-d;j\omega)\ , \tag{8.5}$$

is the frequency domain expression for the fields transmitted by a continuous enclosure in terms of the transient source $I(j\omega)$. In the case of a slotted enclosure exposed to the same source, the transmitted field at $P'(0,0,-d)$ is

$$H3_x(0,0,-d) = I(j\omega)\ G(0,0,0;j\omega)\ T2(-d;j\omega)\ , \tag{8.6}$$

where $T2(-d;j\omega)$ is determined by (6.41).

If $h_x^s(t)$ is the magnetic field incident on an enclosure at $P(0,0,0)$ from a remote, but otherwise unspecified transient source, $H_x^s(j\omega)$ can be substituted directly for $H1_x^s(x,y,0)$ and $H1_x^s(0,0,0)$ in equations (6.37) and (6.41) to give expressions

8. TRANSIENT ELECTROMAGNETIC SOURCES

8.1 Theory

In preceding sections, we developed a shielding theory directly applicable to electromagnetic sources with a harmonic time variation. However, many shielding problems originate from transient rather than harmonic sources. Transient sources can produce intense fields that change with time in a much more complicated way than the simple sinusoidal variation ($\exp(j\omega t)$) of harmonic sources. In general, a transient source is a distribution of natural or man made currents, voltages, or fields that are zero prior to an instant of time t_0, increase in magnitude to one or more peak values for $t > t_0$, and approach a steady state value (usually zero) as $t \longrightarrow \infty$. Lightning and EMP are two types of transient sources that produce electric and magnetic fields with complicated time histories. Examples of the latter will be described in section 8.3.

To compute the transmitted fields from a transient source using the results of sections 4, 5, and 6, it is necessary first to represent the transient source as an equivalent harmonic source. This transformation from the "time domain" to the "frequency domain" is accomplished by applying the Laplace transform $L[\ ]$

$$L[f(t)] = \int_0^\infty \exp(j\omega t)\ f(t)\ dt\ , \tag{8.1}$$

to the source function. Thus, if $i(t)$ and $h_x^s(t)$ are source functions describing a transient current and magnetic field component, the equivalent harmonic sources are

$$I(j\omega) = L[i(t)]\ ,$$

and (8.2)

$$H_x^s(j\omega) = L[h_x^s(t)]\ .$$

(7.37), and (7.38) can be used in place of (7.33) to analytically adjust measured values of shielding effectiveness taken with one source to give an estimate of the shielding effectiveness that would have been measured with another source. In the case where the other source is an EMP field, this gives:

$$SE_{EMP}^{(estimated)}(E) = SE_{S2}^{e}(E) + \delta(EMP;S2) \ , \tag{7.39}$$

$$SE_{EMP}^{(estimated)}(H) = SE_{S2}^{e}(H) \ . \tag{7.40}$$

The reader can easily verify that (7.39) and (7.40) are equivalent to (7.34).

$$SE_{EMP}^{(estimated)} = SE_{S2}^{e} + \Delta(SEMP:S2) \quad , \tag{7.34}$$

where

$$\Delta(SEMP:S2) = 10\log(120\pi/|\eta S2|). \tag{7.35}$$

Equation (7.33) differs by a factor of 2 from the correction factor δ given by (5.12) in Monroe[2]:

$$\delta(S1;S2) = 2\Delta(S1;S2) = 20\log(|\eta S1/\eta S2|) \ . \tag{7.36}$$

This difference is due to the fact that (7.36) is based on (2.16) which, as we have seen, is valid for plane sheets but not for enclosures except for the special case where the wave impedance of the source is equal to the wave impedance of the enclosure. Nevertheless, δ also plays an important role in characterizing the shielding of enclosures. In fact, equations (7.16) and (7.18) show that δ is equal to the difference in the shielding effectiveness of a continuous or slotted enclosure against electric fields from S1 and S1. That is,

$$\delta(S1;S2) = SE_{S1}^{t}(E) - SE_{S2}^{t}(E) \ . \tag{7.37}$$

But (7.16) and (7.18) also show

$$SE_{S1}^{t}(H) = SE_{S1}^{t}(H) \ . \tag{7.38}$$

That is, the shielding effectiveness of an enclosure against magnetic fields is the same for any two sources. Hence, (7.36),

---

2 R. L. Monroe, EMP Shielding Effectiveness and MIL-STD-285, Harry Diamond Laboratories, HDL-TR-1636, (July 1973).

and

$$A_1 = 3.12\times10^{-4}\,T \ ,$$

$$\alpha_1 = 1.20\times10^{6}\ s^{-1} \ , \tag{8.25}$$

$$\alpha_2 = 5.10\times10^{7}\ s^{-1} \ ,$$

$$A_2 = 14.9\times10^{-4}\,T \ ,$$

$$\alpha_3 = 7.90\times10^{4}\ s^{-1} \ , \tag{8.26}$$

$$\alpha_4 = 2.50\times10^{5}\ s^{-1} \ .$$

Converting (8.23) to more convenient units (A/m) and reverting to our previous notation, we obtain

$$h^s_\phi(t) = B_\phi(t)/\mu_0 \ . \tag{8.27}$$

Transforming the latter gives the following frequency domain expression for the source region magnetic field

$$H^s_\phi(j\omega) = H^c_\phi(j\omega) + H^r_\phi(j\omega) \ , \tag{8.28}$$

where

$$H^c_\phi(j\omega) = (A_1/\mu_0)[1/(\alpha_1 + j\omega) - 1/(\alpha_2 + j\omega)] \text{ A/m} \ ,$$

$$H^r_\phi(j\omega) = (A_2/\mu_0)[1/(\alpha_3 + j\omega) - 1/(\alpha_4 + j\omega)] \text{ A/m} \ . \tag{8.29}$$

The reader can verify that the first term in (8.23) and (8.28) accounts for the first peak in figure 18(b) and the second term accounts for the second peak.

9. TRANSIENT MAGNETIC FIELDS INSIDE METALLIC ENCLOSURES FROM EXTERNAL ELECTROMAGNETIC SOURCES

In this section, we will calculate the magnetic fields transmitted to the interiors of metallic enclosures when an outside surface is exposed to magnetic fields from an external transient source. We will consider three combinations of enclosure and source: a slotted enclosure exposed to fields from a square loop antenna, a continuous enclosure exposed to the same source, and a continuous enclosure exposed to a SREMP field. For each combination, we obtain a frequency domain expression for the transmitted field at the point P′(0,0,-d) inside the enclosure using the results of sections 5, 6, and 8. We then evaluate the inverse Laplace Transform of this expression using an analytical approximation technique. This technique produces a closed form expression for the transient magnetic field as a function of time. Using this expression, we plot the field for a representative set of input parameters and interpret the result. In all cases, the source function is a sum of terms each of which has the form A exp(-αt) where A and α are real.

9.1 A Rectangular Parallelepiped With a Slot in One Face Exposed to Fields From, a Square Loop Antenna

Figure 19 shows the arrangement that the calculations attempt to describe. A small square loop antenna is located with its geometric center C(0,0,D) at a height h above a ground plane and a distance D from the outside surface of a metallic enclosure. The perimeter of the loop is 4a, and the inside dimensions of the enclosure are H, W, and L. The thickness of the enclosure wall is d. A narrow, air filled, rectangular slot with its length parallel to the ground plane penetrates the enclosure wall facing the antenna. The length and width of the slot are l and w respectively.

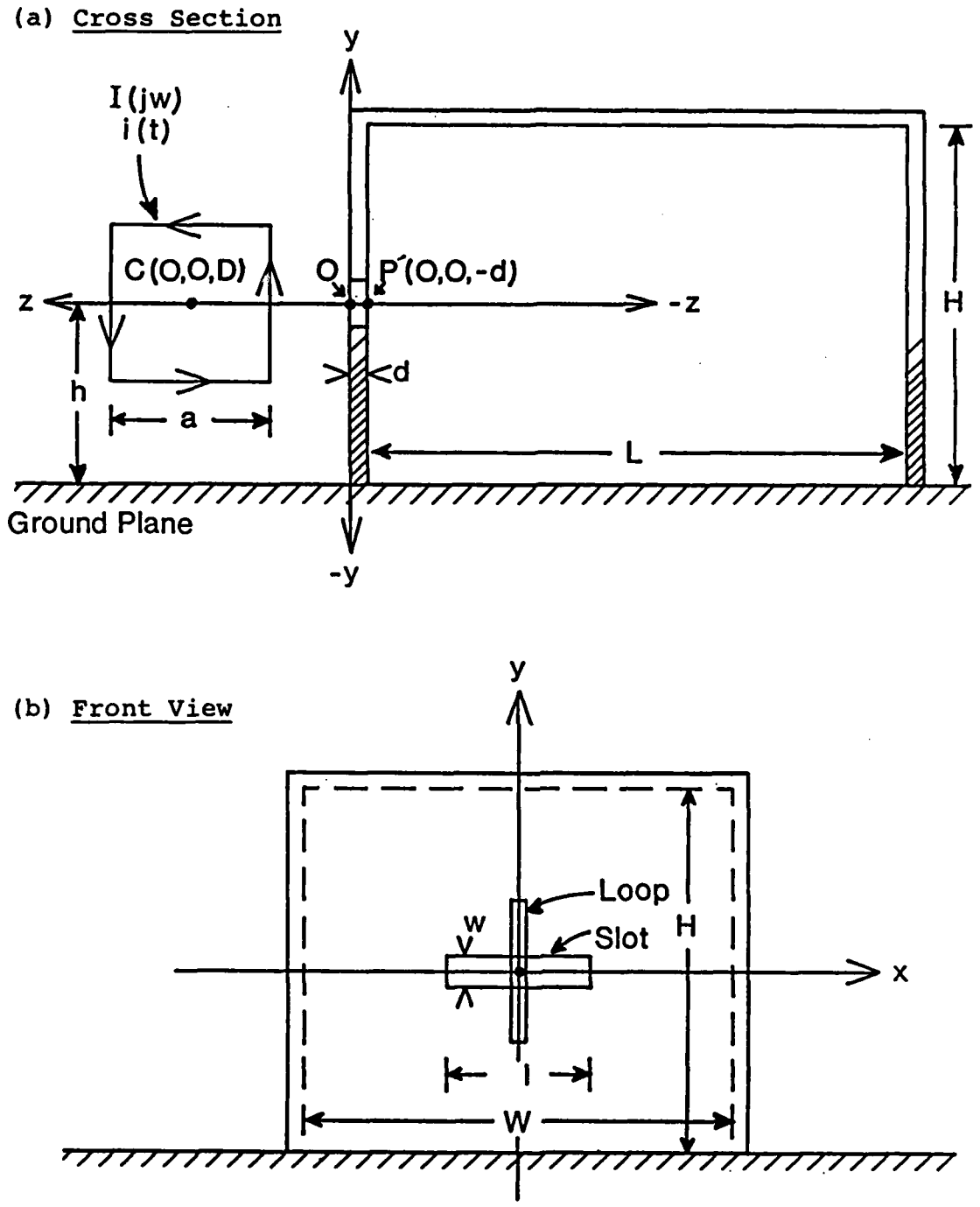

Figure 19. A rectangular parallelepiped with a horizontal slot exposed to fields from a square loop antenna carrying a transient current i(t).

This arrangement is identical to the one shown in figure 13 except that the enclosure now rests on a ground plane and the generalized source is replaced by the loop antenna. The loop antenna is identical to the one described in figure 10(a) which was shown in section 5.3 to produce a magnetic field at O with a dominant component in the x direction. It was also shown in section 5.3 that the ground plane has little effect on the field at O if $a < D < h$.

If the loop antenna in figure 19 is driven by a transient current i(t) in the form of equation (8.15), then the frequency domain representation of this current is given by (8.16), and the resulting magnetic field at O can be obtained from (8.17) and (8.18). With the aid of (8.16), (8.17), (8.18), (6.14), and (8.6), the frequency domain representation of the magnetic field transmitted through the slot at $P'(0,0,-d)$ can be written as follows

$$H3_x(0,0,-d) = I(j\omega)\ G(0,0,0;j\omega)\ T2(-d;j\omega)\ , \tag{9.1}$$

where

$$I(j\omega) = A_0[1/(\alpha_1 + j\omega) - 1/(\alpha_2 + j\omega)]\ , \tag{9.2}$$

$$G(0,0,0;j\omega) = \exp(j\omega D/C_0)[r_1 + j\omega r_2 D/C_0]/4\pi\ , \tag{9.3}$$

$$T2(-d;j\omega) = 4j\omega L_s \exp(-\mu_0 d/L_s)/(j\omega L_s + \eta 3)\ , \tag{9.4}$$

and

$$\eta 3 = Z_{TE}\tanh(\gamma 3\ L)\ , \tag{9.5}$$

where

$$Z_{TE} = \frac{j\omega Z_0}{\omega_c\sqrt{1 + (j\omega/\omega_c)^2}}\ , \tag{9.6}$$

$$\gamma 3 = k_c \sqrt{1 + (j\omega/\omega_c)^2} \ , \tag{9.7}$$

and

$$\omega_c = 2\pi f_c \ , \quad f_c = C_0/2W \ , \quad k_c = \omega_c/C_0 \ . \tag{9.8}$$

Equation (9.1) can be written in a somewhat more convenient form as the difference of two terms

$$H3_x(0,0,-d) = H_1(j\omega) - H_2(j\omega) \ , \tag{9.9}$$

where

$$\begin{aligned} H_1(j\omega) &= I_1(j\omega)\ G(0,0,0;j\omega)\ T2(-d;j\omega) \ , \\ H_2(j\omega) &= I_2(j\omega)\ G(0,0,0;j\omega)\ T2(-d;j\omega) \ , \end{aligned} \tag{9.10}$$

and

$$\begin{aligned} I_1(j\omega) &= A_0/(\alpha_1 + j\omega) \ , \\ I_2(j\omega) &= A_0/(\alpha_2 + j\omega) \ . \end{aligned} \tag{9.11}$$

The transient magnetic field at $P'(0,0,-d)$ can then be obtained as the difference between two functions of t by taking the inverse Laplace transform of (9.9)

$$h3_x(0,0,-d;t) = L^{-1}[H3_x(0,0,-d)] = h_1(t) - h_2(t) \ , \tag{9.12}$$

where

$$h_1(t) = L^{-1}[I_1(j\omega)\ G(0,0,0;j\omega)\ T2(-d;j\omega)] \ , \tag{9.13}$$

$$h_2(t) = L^{-1}[I_2(j\omega)\ G(0,0,0;j\omega)\ T2(-d;j\omega)] \ . \tag{9.14}$$

Thus the problem of calculating the transmitted field reduces to the problem of evaluating $h_1(t)$ and $h_2(t)$. Moreover, any technique that yields $h_1(t)$ will also give $h_2(t)$ and vice versa,

since (9.13) and (9.14) are formally identical.

To compute $h_1(t)$ and $h_2(t)$, we reduce the bracketed terms in (9.13) and (9.14) by suitable rearrangements and approximations to expressions for which the inverse Laplace transform can be obtained explicitly by elementary means using tabulated functions. Since the inverse transforms of $I_1(j\omega)$, $I_2(j\omega)$ and $G(0,0,0;j\omega)$ are well known, this means that only $T2(-d;j\omega)$ must be modified. To this end, we rewrite $T2(-d;j\omega)$ as follows:

$$T2(-d;j\omega) = \frac{4\ L_s \exp(-\mu_0 d/L_s)}{L_s + \dfrac{Z_0 \tanh(\gamma 3\ L)}{\omega_c\sqrt{1 + (j\omega/\omega_c)^2}}} \quad . \tag{9.15}$$

Now, in most cases of interest

$$L_s << \left| \frac{Z_0 \tanh(\gamma 3\ L)}{\omega_c\sqrt{1 + (j\omega/\omega_c)^2}} \right| ,$$

so that (9.15) reduces to

$$T2(-d;j\omega) = \frac{4L_s \exp(-\mu_0 d/L_s)\,\omega_c \sqrt{1 + (j\omega/\omega_c)^2}}{Z_0\ \tanh(\gamma 3\ L)} \quad . \tag{9.17}$$

But

$$\sqrt{1 + (j\omega/\omega_c)^2} \cong 1 + \frac{(j\omega/\omega_c)^2}{j\omega/\omega_c + k} \quad , \tag{9.18}$$

where

$$k = 1.25 \quad . \tag{9.19}$$

And $\coth(\Upsilon 3\ L) = 1/\tanh(\Upsilon 3\ L)$ is a meromorphic function[36] of $j\omega$ with the following uniformly convergent partial fraction expansion

$$\coth(\Upsilon 3\ L) = f_0 + 2(j\omega)^2 \sum_{n=0}^{\infty} \frac{R_n}{j\omega_n \left[(j\omega)^2 - (j\omega_n)^2\right]} , \qquad (9.20)$$

where

$$f_0 = \frac{\exp(k_c L) + \exp(-k_c L)}{\exp(k_c L) - \exp(-k_c L)} , \qquad (9.21)$$

$$R_n = \left(\frac{C_0}{L}\right) \frac{n\pi C_0}{\left[(n\pi C_0)^2 + (\omega_c L)^2\right]^{1/2}} , \qquad (9.22)$$

$$\omega_n = \left[(n\pi C_0/L)^2 + \omega_c^2\right]^{1/2} . \qquad (9.23)$$

Substituting (9.18) and (9.20) into (9.17), we obtain

$$T2(-d;j\omega) = \left[\frac{4\omega_c L_s}{Z_0}\right] \exp(-\mu_o d/L_s) \left[1 + \frac{(j\omega/\omega_c)^2}{(j\omega/\omega_c + k)}\right] \times \left[f_0 + 2(jw)^2 \sum_{n=1}^{\infty} \frac{R_n}{j\omega_n \left[(j\omega)^2 - (j\omega_n)^2\right]}\right] . \qquad (9.24)$$

---

36 E. C. Titchmarsh, The Theory of Functions, 2nd Ed., Oxford University Press, Section 3.2, (1939).

Combining (9.24) with (9.3) and (9.11) gives

$$I_1(j\omega)\ G(0,0,0;j\omega)\ T2(-d;j\omega) =$$

$$A\ \exp(j\omega D/C_0)\left[\frac{r_1 + j\omega r_2 D/C_0}{\alpha_1 + j\omega}\right]\left[1 + \frac{(j\omega/\omega_c)^2}{j\omega/\omega_c + k}\right]$$

$$\times\left[f_0 + 2(j\omega)^2 \sum_{n=1}^{\infty} \frac{R_n}{j\omega_n\left[(j\omega)^2 - (j\omega_n)^2\right]}\right], \tag{9.25}$$

where

$$A = A_0\ \omega_c\ L_s\ \exp(-\mu_0 d/L_s)/\pi Z_0\ . \tag{9.26}$$

Now the right side of equation (9.25) is a uniformly convergent series, and each term in this series is a function of $j\omega$ whose inverse Laplace transform can be obtained explicitly by elementary means using tabulated functions. We can therefore substitute (9.25) into (9.13), and carry out a term by term[32] inverse Laplace transformation to obtain $h_1(t)$. The result after a lengthy calculation is

$$h_1(t) = A\ \omega_c\left[f_0\ (L_1\exp(-\alpha_1 t) + L_2\exp(-k\omega_c t) - L_1 - L_2) + \sum_{n=1}^{\infty} 2R_n f_n(t)\right], \tag{9.27}$$

---

32 G. Doetsch, Guide to Applications of Laplace Transforms, D. Van Nostrand Company LTD., London, Chapter 7, (1961).

where $t = t' - D/C_0$ is the retarded time

$$f_n(t) = M_1\cos(\omega_n t) + M_2\sin(\omega_n t) + M_3\exp(-\alpha_1 t) + M_4\exp(-k\omega_c t) \quad , \tag{9.28}$$

and

$$L_1 = \left(\beta - \eta\alpha_1 + \theta\alpha_1^2 - \zeta\alpha_1^3\right) \Big/ (k\omega_c - \alpha_1) \quad ,$$

$$L_2 = -\left(\beta - \eta k\omega_c + \theta(k\omega_c)^2 - \zeta(k\omega_c)^3\right) \Big/ (k\omega_c - \alpha_1) \quad , \tag{9.29}$$

$$\left.\begin{aligned} \beta &= r_1 k \quad , \\ \eta &= r_1/\omega_c + r_2 kD/C_0 \quad , \\ \theta &= r_1/\omega_c^2 + r_2 D/(C_0\omega_c) \quad , \\ \zeta &= r_2 D/(C_0\omega_c^2) \quad , \end{aligned}\right\} \tag{9.30}$$

$$\left.\begin{aligned} M_1 &= -M_3 - M_4 \quad , \\ M_2 &= \frac{L_1\omega_n}{\alpha_1^2 + \omega_n^2} + \frac{L_2\omega_n}{(k\omega_c)^2 + \omega_n^2} \quad , \end{aligned}\right\} \tag{9.31}$$

$$M_3 = - L_1\alpha_1/(\alpha_1^2 + \omega_n^2) \ ,$$

$$M_4 = - L_2 k\omega_c/((k\omega_c)^2 + \omega_n^2) \ , \qquad (9.32)$$

and all other quatities are as previously defined.

When α_2 replaces α_1 in (9.27)-(9-32), $h_1(t)$ is transformed into an expression for $h_2(t)$. This expression combined with $h_1(t)$ in (9.12) then determines $h3_x(0,0,-d;t)$. Because of its great length, we will not write out $h3_x(0,0,-d;t)$ in detail here.

Figure 20 is a plot of $h3_x(0,0,-d;t)$ based on $h_1(t)$ and $h_2(t)$ as determined by (9.27)-(9.32) using a twenty term approximation for the infinite series for the case where the loop antenna in figure 19 is driven by the transient current shown in figure 16. In this case, the current is characterized by the following:

$A_0 = 1.14$ A. , $\alpha_1 = 10^7\,s^{-1}$, $\alpha_2 = 3.72\times10^8 s^{-1}$,

and the remaining input parameters are

$a = 10.6"$, $D = 18"$, $h = 3.5'$,

$r_1 = .076\ m^{-1}$, $r_2 = .105\ m^{-1}$ (from equation (5.39)) ,

$d = .25"$, $L = W = H = 9'$,

$1 = .5$ m , $w = .063"$,

$L_s = 3.2\times10^{-8}$ henrys (equation (6.28)) .

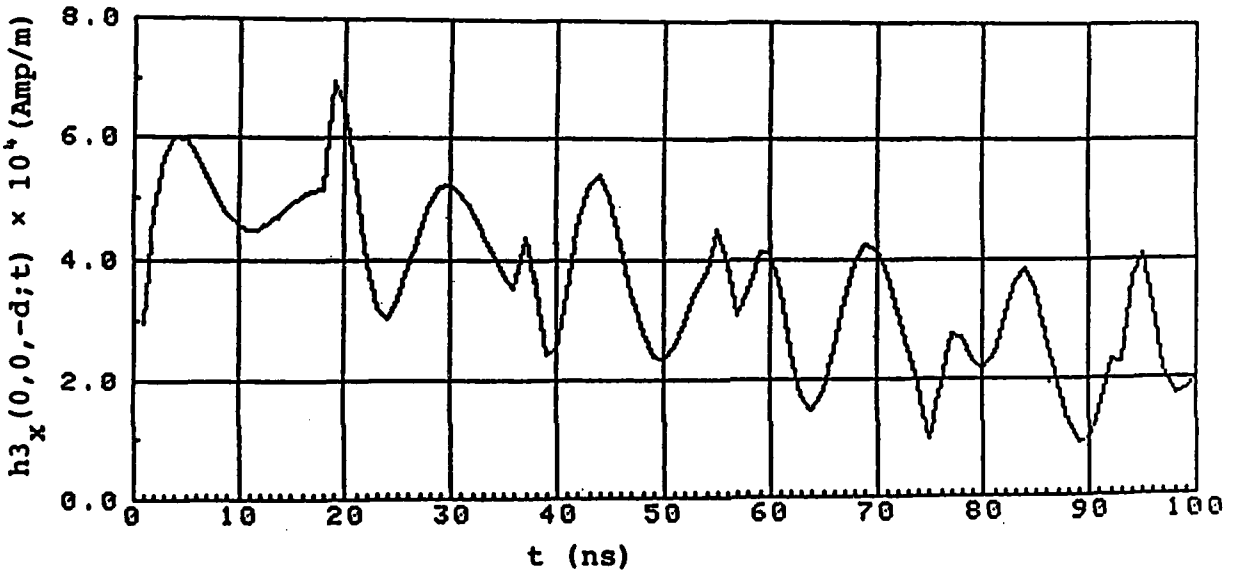

Figure 20. Magnetic field inside a slotted enclosure exposed to transient fields from a square loop antenna.

The transmitted magnetic field depicted in fig. 20 exhibits a fair degree of complexity, but the source of this complexity can be related to the characteristics of the incident field and the enclosure. For example, the early history of the transmitted field is dominated by two peaks. The first has a rise time nearly equal to the rise time of $h1_x^s(0,0,0;t)$ (See figure 17). The second peak (virtually a spike on the 1 ns time scale of the figure) is obviously related to the cutoff frequency of the enclosure f_c since it takes off at t = 18 ns which is very close to $1/f_c$ in this case. Further inspection of figure 20 shows that both of these features are repeated at intervals of 18+ ns with gradually decaying amplitudes. Since 18 ns is also the approximate round trip travel time of a reflected pulse inside the enclosure, we can interpret figure 20 as a series of internally reflected pulses riding on top of a much slower pulse. In fact, $h3_x(0,0,-d;t)$ can be written as the sum of two fields as follows:

$$h3_x(0,0,-d;t) = h_s(t) + h_p(t) \ , \qquad (9.33)$$

where $h_s(t)$ is derived from the term involving f_0 in equation (9.27) and $h_p(t)$ is derived from the series $\sum R_n f_n(t)$. Figure 21 is a plot of $h_s(t)$, and figure 22 is a plot of $h_p(t)$. Figure 21 indicates that the waveform of $h_s(t)$ is nearly identical to that of the loop current decaying smoothly to zero as $t \longrightarrow \infty$. This is clearly a nonpropagating or "static" field. Since the enclosure acts like a high pass filter, the static field is composed primarily from those frequencies in the incident field that fall below the cutoff frequency f_c = 54.6 MHz. On the other hand, $h_p(t)$ is formed almost entirely from higher frequency fields reflected between the front and back walls of the enclosure. These are propagating fields formed from frequency compo-

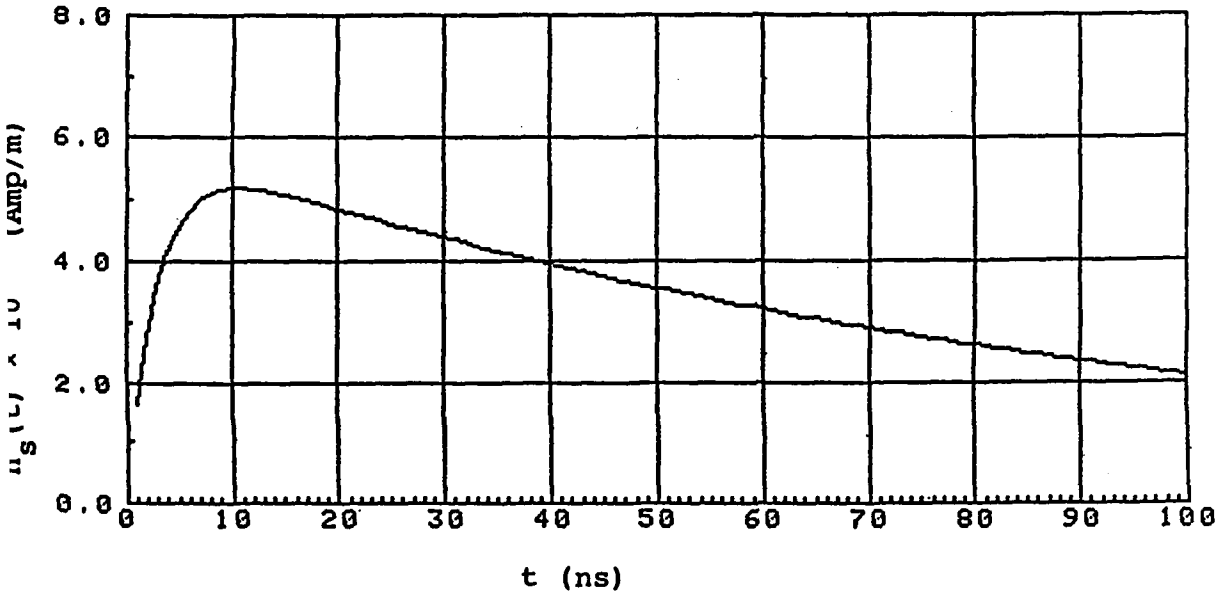

Figure 21. Static field $h_s(t)$.

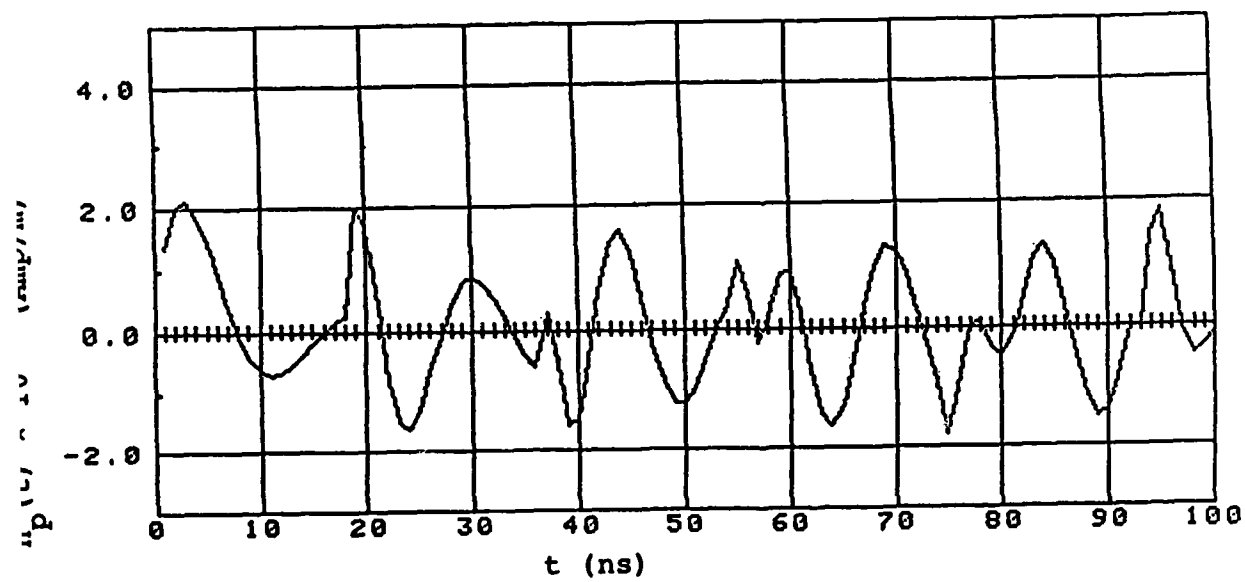

Figure 22. Propagating field $h_p(t)$.

nents of the incident field that are above f_c. Since losses in the enclosure walls are neglected in these calculations, $h_p(t)$ is undamped, and the enclosure will continue to "ring" with these fields after the static field has decayed.

The basic characteristics of $h_p(t)$ are pointed out in figure 23. Four complete repetitions of the initial pulse are shown in the figure. The exact shape of the pulse is not preserved, but certain general features are maintained from pulse to pulse. For example, the earliest part of each pulse is a nearly pure sinusoid S1, S2, S3, S4, and S5. The period of the sinusoid appears to change from pulse to pulse slowly becoming smaller at later times. After 18+ ns, the sinusoid is interrupted by a "cutoff" spike (at t = tc, 2tc, 3tc, 4tc, 5tc). The phase difference between the cutoff spike and the sinusoid changes from pulse to pulse in a way that does not appear to be entirely due to the changing period of the latter, and, as a result, the spike appears on both the positive and negative half-cycles of the sinusoid - sometimes adding to and sometimes subtracting from the field. This variation may be periodic since the last spike shown at t = 95 ns is virtually identical to the first at t = 19 ns. This would imply a 90 degree phase variation from pulse to pulse.

9.2 A Continuous, Rectangular Parallelepiped Exposed to Fields from a Square Loop Antenna

If the slotted enclosure in figure 19 is replaced by a continuous enclosure with the same shape and the loop antenna is again driven by a transient current in the form of equation (8.15), then the frequency domain expression for the magnetic field transmitted through the enclosure wall at $P'(0,0,-d)$ is

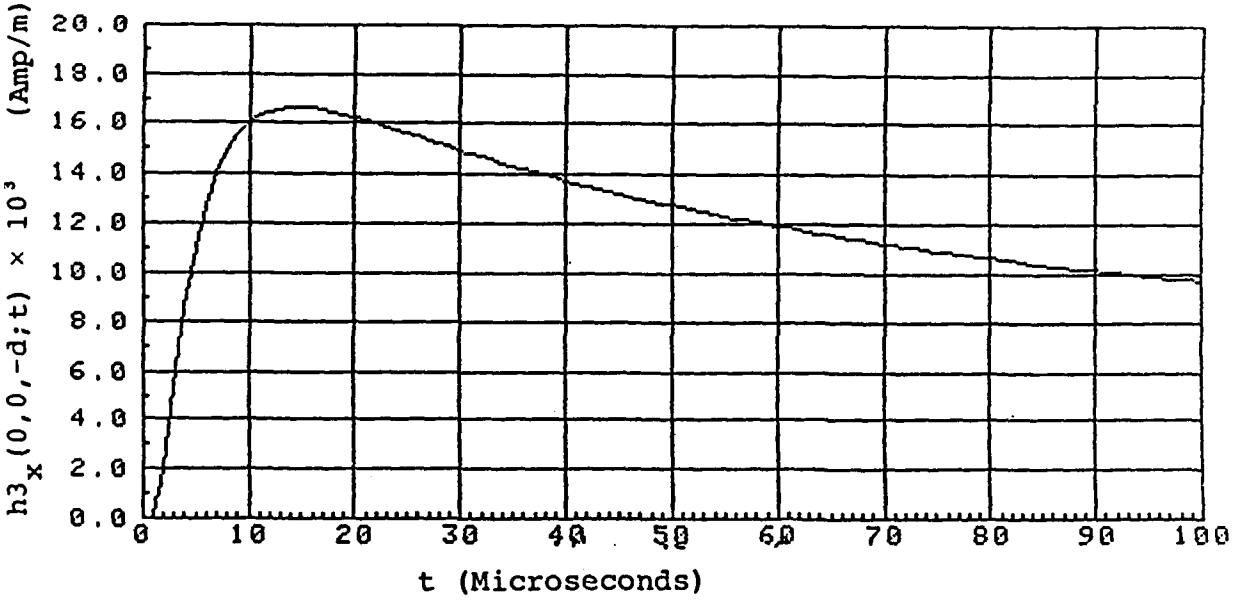

Figure 25. Magnetic field inside a continuous enclosure exposed to $h_x^c(t)$.

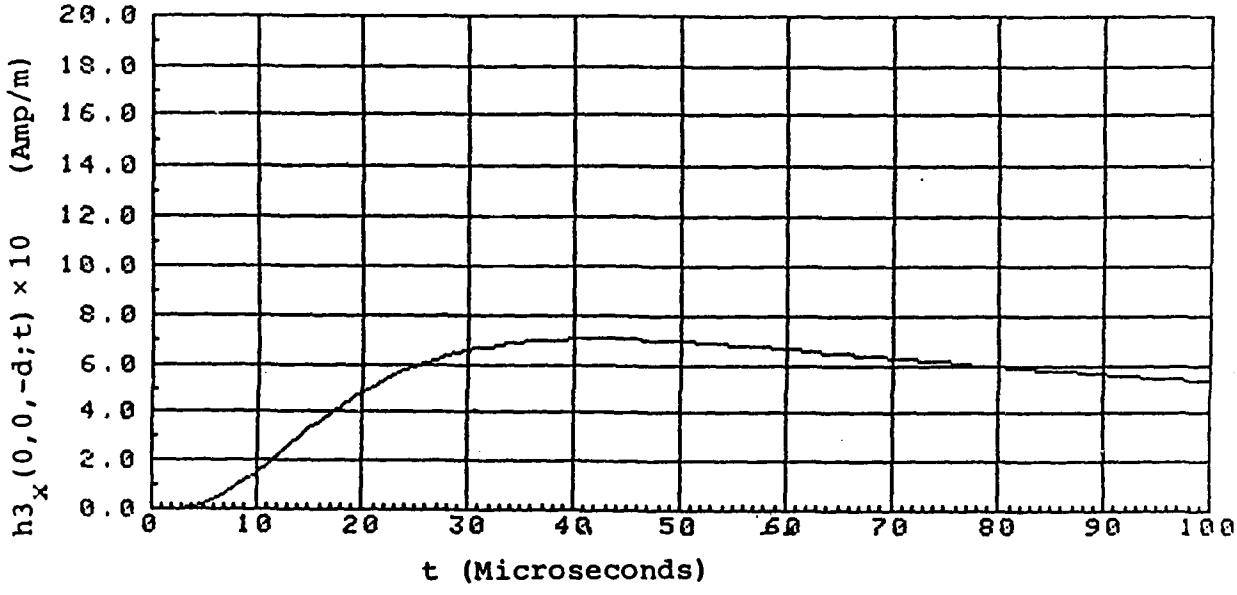

Figure 26. Magnetic field inside a continuous enclosure exposed to $h_x^r(t)$.

$$\alpha_2 = 5.10\times10^7 \ s^{-1} \ ,$$

$$h_0^r = 1.18\times10^3 \ \text{Amps/m} \ ,$$

$$\alpha_3 = 7.9\times10^4 \ s^{-1} \ , \qquad (9.64)$$

$$\alpha_4 = 2.50\times10^5 \ s^{-1} \ .$$

Since $h_x^s(t)$ is equal to the sum of two transient fields with very different amplitudes and time scales, we will compute and plot $h3_x(0,0,-d;t)$ separately for $h_x^c(t)$ and $h_x^r(t)$. The total transmitted field corresponding to the SREMP field shown in figure 18(b) will then be equal to the sum of these fields. This separation of the transmitted field into components corresponding to $h_x^c(t)$ and $h_x^r(t)$ is more than a matter of convenience; it reflects the fact that these fields are generated by distinct physical processes in the source region. Thus, $h_x^c(t)$ which accounts for the early peak in figure 18(b) is the magnetic field associated with the Compton current (vertical dipole in figure 18(a)),while $h_x^r(t)$ which accounts for the much larger late peak is the product of current loops formed by electron flow outward in the air and return in the ground. In view of this, it is a matter of some interest to know the contribution of each of these sources to the fields reaching the interior of the enclosure.

Figure 25 is a plot of the transmitted field generated by $h_x^c(t)$. Since the rise time of $h_x^c(t)$ is much smaller than the characteristic diffusion time of the enclosure wall, (9.55) is satisfied, and the curve is computed directly from equation (9.56). Thus, the form of the curve is identical to figure 20 where the peak field occurs at $t = 2T_c = 14.2$ microseconds. Figure 26 is a plot of the transmitted field produced by $h_x^r(t)$.

(9.60) to compute the magnetic field transmitted to the interior of an enclosure when it is exposed to the SREMP field described in section 8.3. These calculations will be carried out for the same aluminum enclosure we considered in the preceding section where

$$d = .032" \quad , \quad L = 138" \quad , \quad W = 81.5" \quad , \quad H = 77" \ ,$$

$$\mu 2 = 12.6\times10^{-7} \text{ henrys/m} \quad , \quad \sigma 2 = 35\times10^{8} \text{ mhos/m} \ .$$

For convenience, we assume that the z axis of our coordinate system passes through the center of the EMP source region. With this arrangement, the ϕ component of the SREMP field with respect to a burst centered spherical coordinate system transforms directly to the x component of the SREMP field in our enclosure centered system. The SREMP magnetic field ((8.23)-(8.27)) incident at O(0,0,0) on the enclosure can then be written as follows:

$$\begin{aligned} h_x^s(t) &= h_\phi^s(t) = B_\phi(t)/\mu_0 \ , \\ &= h_x^c(t) + h_x^r(t) \ , \end{aligned} \tag{9.61}$$

where

$$\begin{aligned} h_x^c(t) &= h_0^c[\exp(-\alpha_1 t) - \exp(-\alpha_2 t)] \ , \\ h_x^r(t) &= h_0^r[\exp(-\alpha_3 t) - \exp(-\alpha_4 t)] \ , \end{aligned} \tag{9.62}$$

and

$$\begin{aligned} h_0^c &= 2.48\times10^{2} \text{ Amps/m} \ , \\ \alpha_1 &= 1.20\times10^{6} \text{ s}^{-1} \ , \end{aligned} \tag{9.63}$$

Laplace transform of $h_x^s(t)$ and $T1(-d;j\omega)$ is given by (9.43). To determine the transmitted field $h3_x(0,0,-d;t)$ explicitly in this case, it is necessary to evaluate the Laplace transform of $h_x^s(t)$ and the inverse Laplace transform of $H_x^s(j\omega)T1(-d;j\omega)$. This is a task that may be difficult or impossible, depending on the functional form of $h_x^s(t)$. However, when $h_x^s(t)$ has the same form as the antenna current (8.15) used in Section 9.2,

$$h_x^s(t) = h_0[\exp(-\alpha_1 t) - \exp(-\alpha_2 t)] \ , \tag{9.58}$$

then the results of the preceding section can easily be modified to give the appropriate expression for $h3_x(0,0,-d)$ without the need to evaluate any additional Laplace transforms. This can be done by applying the following transformation of parameters to equations (9.53) and (9.55)

$$\begin{aligned} h_o &\longrightarrow A_0 \ , \\ 1 &\longrightarrow (r_1 - r_2\alpha_1 D/C_0)/4\pi \ , \\ 1 &\longrightarrow (r_1 - r_2\alpha_2 D/C_0)/4\pi \ . \end{aligned} \tag{9.59}$$

This transformation effectively replaces the incident magnetic field from the loop with the magnetic field of (9.58). The transmitted field is then given by (9.53) or (9.55) where A, B_1, and B_2 are redefined as follows

$$\begin{aligned} A &= 4h_0 b/\sqrt{\pi} \ , \\ B_1 &= B_2 = 1 \ . \end{aligned} \tag{9.60}$$

In this section, we will use (9.53) and (9.55) together with

It is clear from the figure that the character of the transmitted field in this case is much different than that of the field transmitted by the slotted enclosure even though the same transient source was used in both cases. Notable differences include:

(1) a delay time of 1-2 microseconds with respect to the incident field (compared to 1 ns or less for the slotted enclosure).
(2) a rise time to peak field of 14+ microseconds.
(3) a very slow decay (proportional to $1/\sqrt{t}$).
(4) no high frequency propagating fields.

The figure shows a purely diffusive field whose principal features are determined by the characteristic diffusion time of the enclosure T_c

$$T_c = \tau/4 = \mu 2\sigma 2\ d^2/4\ . \qquad (9.57)$$

For this enclosure, T_c = 7.2 microseconds which is much longer than the duration of the incident field and easily satisfies (9.55). This corresponds to a frequency of $1/T_c = 1.4\times10^5$ Hz which is below the cutoff frequency of the enclosure (72 MHz). After diffusing through the wall the field will continue to diffuse through the interior of the enclosure and then decay.

9.3. A Continuous Rectangular Parallelepiped Exposed to Magnetic Fields from a SREMP

When a transient source is defined directly in terms of a magnetic field $h_x^s(t)$ incident at a point O(0,0,0) on a continuous enclosure rather than as a current on an antenna, the transmitted field at P´(0,0,-d) is given by (8.13) as the inverse Laplace Transform of $H_x^s(j\omega)T1(-d;j\omega)$ where $H_x^s(j\omega)$ is the

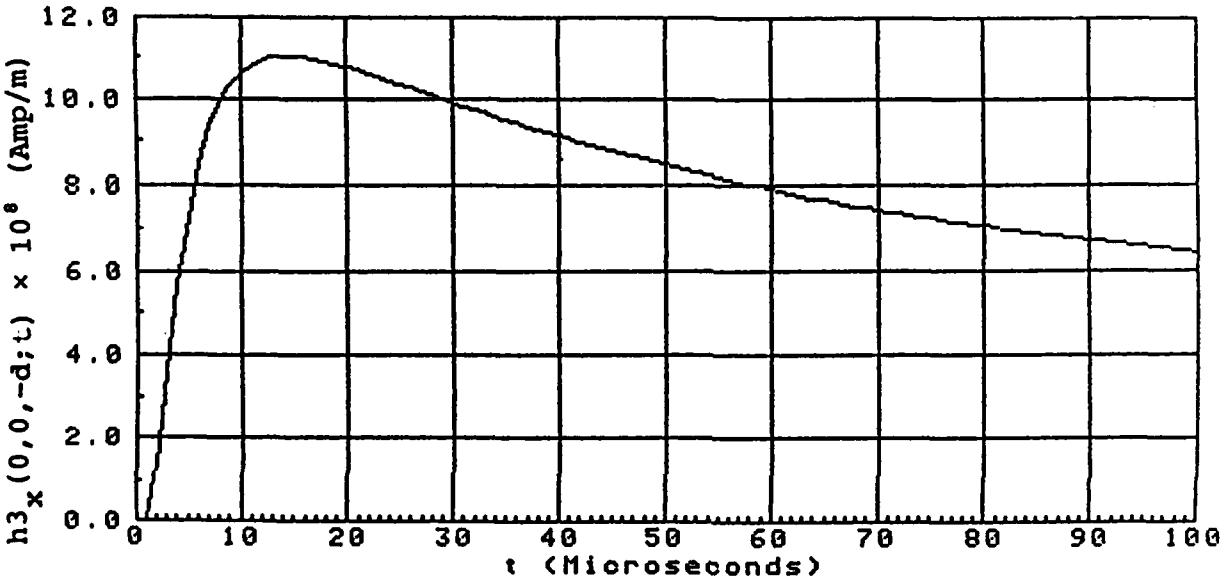

Figure 24. Magnetic field inside a continuous enclosure exposed to transient fields from a square loop antenna.

$$B_1 = (r_1 - r_2\alpha_1 D/C_0)/\sqrt{\pi} \ ,$$

$$B_2 = (r_1 - r_2\alpha_2 D/C_0)/\sqrt{\pi} \ .$$

If the parameters defining the incident field are such that

$$\left.\begin{matrix} 1/\alpha_1 \\ \\ 1/\alpha_2 \end{matrix}\right\} << \ \tau/4 \ , \tag{9.55}$$

then the first term in (9.53) dominates, and the transient field reduces to

$$h3_x(0,0,-d;t) \cong A \left(\frac{B_1}{\alpha_1} - \frac{B_2}{\alpha_2} \right) \frac{\exp(-\tau/4t)}{\sqrt{t}} \ . \tag{9.56}$$

Figure 24 is a plot of $h3_x(0,0,-d;t)$ obtained from (9.56) for the case of a continuous aluminum enclosure exposed to the transient field generated by the loop current shown in figure 16 where

$$A_0 = 1.14 \ A \ , \quad \alpha_1 = 10^7 \ s^{-1} \ , \quad \alpha_2 = 3.72\times10^8 \ s^{-1} \ .$$

The remaining input parameters are

$$a = 10.6" \ , \quad D = 18" \ , \quad h = 3.5' \ ,$$

$$r_1 = .076 \ m^{-1} \ , \quad r_2 = .105 \ m^{-1} \ ,$$

$$d = .032" \ , \quad L = 138" \ , \quad W = 81.5" \ , \quad H = 77" \ ,$$

$$\mu 2 = 12.6\times10^{-7} \text{ henrys/m} \ , \quad \sigma 2 = 35\times10^6 \text{ mhos/m} \ .$$

$$h_1(t) = \frac{AB_1}{\alpha_1}\left[\frac{\exp(-\tau/4t)}{\sqrt{t}} - \int_0^t \frac{\exp(-\tau/4g + \alpha_1(g-t))}{\sqrt{g}}\left(\frac{\tau}{4g^2} - \frac{1}{2g}\right)dg\right] . \qquad (9.52)$$

And, by replacing α_1 and α_2 in (9.52), we obtain an expression for $h_2(t)$. Combining $h_1(t)$ and $h_2(t)$ according to (9.36) gives the transient magnetic field at $P'(0,0,-d)$

$$h3_x(0,0,-d;t) = A\left[\left(\frac{B_1}{\alpha_1} - \frac{B_2}{\alpha_2}\right)\frac{\exp(-\tau/4t)}{\sqrt{t}} - \int_0^t \frac{B_1 \exp(-\tau/4g + \alpha_1(g-t))}{\alpha_1\sqrt{g}}\left(\frac{\tau}{4g^2} - \frac{1}{2g}\right)dg + \int_0^t \frac{B_2 \exp(-\tau/4g + \alpha_2(g-t))}{\alpha_2\sqrt{g}}\left(\frac{\tau}{4g^2} - \frac{1}{2g}\right)dg\right] , \qquad (9.53)$$

where

$$A = A_0 b/\pi = \frac{A_0\omega_c}{\pi Z_0 \tanh(k_c L)}\sqrt{\frac{\mu 2}{\sigma 2}} ,$$

$$\tau = \mu 2\sigma 2 \quad d^2 , \qquad (9.54)$$

the inverse transform of each of the bracketed factors in (9.46) and express $h_1(t)$ as the convolution of these transforms. That is,

$$L^{-1}\left[\frac{r_1 + j\omega r_2 D/C_0}{\alpha_1 + j\omega}\right] = (r_1 - r_2 D\alpha_1/C_0)\exp(-\alpha_1 t') \quad . \qquad (9.48)$$

And from transform 809 of Campbell[37]

$$L^{-1}\left[\frac{\exp(-\sqrt{j\omega\tau})}{b + \sqrt{j\omega}}\right] = \frac{b\,\exp(-\tau/4t')}{\sqrt{\pi t'}} + O(b^2) \quad . \qquad (9.49)$$

The reader can verify that b is small so that terms $O(b^2)$ can be neglected in (9.49). With (9.48) and (9.49), $h_1(t)$ can be written

$$h_1(t) = AB_1\exp(-\alpha_1 t)\int_0^t \frac{\exp(-\tau/4g + \alpha_1 g)}{\sqrt{g}}\, dg \quad , \qquad (9.50)$$

where $t = t' - D/C_0$ is the retarded time and

$$B_1 = (r_1 - r_2\alpha_1 D/C_0)/\sqrt{\pi} \quad . \qquad (9.51)$$

Integrating (9.50) by parts, we obtain a somewhat more convenient expression for $h_1(t)$

---

37 G. A. Campbell and R. M. Foster, Fourier Integrals for Practical Applications, D.Van Nostrand Company Inc. (1948).

Or

$$T1(-d;j\omega) = \frac{4b\ \exp(-\sqrt{j\omega\tau})}{b + \sqrt{j\omega}} \quad , \tag{9.43}$$

where

$$b = \frac{\omega_c}{Z_0 \tanh(k_c L)} \sqrt{\frac{\mu 2}{\sigma 2}} \quad , \tag{9.44}$$

$$\tau = \mu 2 \sigma 2\ d^2 \ . \tag{9.45}$$

Combining (9.3) and (9.11) with (9.43) gives

$$I_1(j\omega)\ G(0,0,0;j\omega)\ T1(-d;j\omega) =$$

$$A\ \exp(j\omega D/C_0)\left[\frac{r_1 + j\omega r_2 D/C_0}{\alpha_1 + j\omega}\right]\left[\frac{\exp(-\sqrt{\omega j\tau}\ )}{b + \sqrt{j\omega}}\right] \quad , \tag{9.46}$$

where

$$A = A_0 b\ /\ \pi \ . \tag{9.47}$$

Now the inverse Laplace transform of (9.46) can be evaluated exactly with the aid of transform 812 in Campbell[37]. However, the exact transform is a complicated expression involving the error function, and we will not make use of it here. Instead, we will carry out an approximate evaluation that leads to a relatively simple expression for $h_1(t)$. To do this, we obtain

37 G. A. Campbell and R. M. Foster, Fourier Integrals for Practical Applications, D. Van Nostrand Company,Inc. (1948).

where Re[ ] is the real part of the argument. Hence

$$F_c = 1/(\pi\mu 2\sigma 2\ d^2) \quad . \tag{9.40}$$

The significance of (9.40) is that one can generally ignore frequencies much larger than F_c in a transient magnetic field incident on a continuous enclosure since these frequencies will be greatly attenuated by the time they reach the interior. Calculations based on (9.40) show that F_c is surprisingly low for most practical enclosures. For example, if we consider an enclosure with aluminum ($\mu 2 = 12.6\times10^{-7}$ henrys/m, $\sigma 2 = 35\times10^{6}$ mhos/m) walls .032" ($d = 8.1\times10^{-4}$m) thick, then $F_c = 1.1\times10^{4}$ Hz. In this case, frequencies greater than say $10F_c = 1.1\times10^{5}$ Hz stand very little chance of reaching $P'(0,0,-d)$ in sufficient strength to significantly affect the field at that point. Furthermore, since the cutoff frequency f_c for most enclosures satisfies the following relation

$$10F_c << f_c \ , \tag{9.41}$$

it is clear that the field reaching $P'(0,0,-d)$ will be composed primarily of frequencies that are well below f_c.

The fact that F_c and f_c satisfy (9.41) for most enclosures of interest greatly simplifies the computation of $h_1(t)$ (and $h_2(t)$) because it means that terms involving $(j\omega/\omega_c)^2$ can be ignored in (9.39). This allows us to rewrite (9.39) as follows:

$$T1(-d;j\omega) = \frac{4\sqrt{2\mu/\sigma 2}\ \exp(-\sqrt{j\omega\mu 2\sigma 2}\ \ d)}{\sqrt{\mu 2/\sigma 2} + \dfrac{\sqrt{j\omega}\ Z_0 \tanh(k_c L)}{\omega_c}} \quad , \tag{9.42}$$

$$T1(-d;j\omega) = \frac{4\sqrt{j\omega\mu 2/\sigma 2}\ \exp(-\sqrt{j\omega\mu 2\sigma 2}\ d)}{\sqrt{j\omega\mu 2/\sigma 2} + \dfrac{j\omega Z_0 \tanh(\gamma 3\ L)}{\omega_c\sqrt{1 + (j\omega/\omega_c)^2}}} \quad , \qquad (9.39)$$

where

$$\gamma 3 = k_c\sqrt{1 + (j\omega/\omega_c)^2} \ .$$

A comparison of (9.15) with (9.39) shows the fundamental difference between the fields transmitted by a slotted enclosure and those transmitted by a continuous enclosure. In (9.15), the exponential term is independent of frequency; whereas,in (9.39), the exponential term is a strong function of frequency through the factor $\sqrt{j\omega}$. This means that the slot itself, as distinct from the enclosure, reduces all frequencies by the same amount and does not affect the waveshape of the transient magnetic field in the slot incident at P´(0,0,-d). On the other hand, the frequency dependent exponential in (9.39) means that in the case of a continuous enclosure some frequencies will be reduced much more than others and the waveshape of the transient magnetic field incident at P´(0,0,-d) is likely to be very different from the waveshape of the magnetic field incident at O. Indeed, it is clear that frequency components above a certain critical frequency F_c will be drastically reduced by the exponential factor in (9.39). F_c can be defined as the frequency at which the magnitude of the field incident at P´(0,0,-d) is reduced by a factor of e^{-1} compared to the field at O. This requires

$$\mathrm{Re}[\sqrt{j2\pi F_c\mu 2\sigma 2}\ d] = 1 \ ,$$

$$H3_x(0,0,-d) = I(j\omega)\ G(0,0,0;j\omega)\ T1(-d;j\omega)\ , \qquad (9.34)$$

(equation (8.5)) where $I(j\omega)$ and $G(0,0,0;j\omega)$ are given by (9.2) and (9.3) respectively. $T1(-d;j\omega)$ is determined from (6.37)

$$T1(-d;j\omega) = 4\eta 2\ \exp(-\dot{\gamma}2\ d)/(\eta 2 + \eta 3)\ , \qquad (9.35)$$

where $\eta 2$ and $\gamma 2$ are given by (6.2) and (6.3) and $\eta 3$ is again given by (9.5).

As in the preceding section, we can split $H3(0,0,-d)$ into two terms corresponding to the two terms comprising $I(j\omega)$ and compute the inverse Laplace transform of each term separately. Thus the transient magnetic field at $P'(0,0,-d)$ can be represented as the difference of two functions

$$h3_x(0,0,-d;t) = h_1(t) - h_2(t)\ , \qquad (9.36)$$

where

$$h_1(t) = L^{-1}[I_1(j\omega)\ G(0,0,0;j\omega)\ T1(-d;j\omega)]\ , \qquad (9.37)$$

$$h_2(t) = L^{-1}[I_2(j\omega)\ G(0,0,0;j\omega)\ T1(-d;j\omega)]\ . \qquad (9.38)$$

As before, we compute $h_1(t)$ and $h_2(t)$ by reducing the bracketed terms in (9.37) and (9.38) to expressions for which the inverse Laplace transform can be obtained by elementary techniques. Since the inverse transforms of $I_1(j\omega)$, $I_2(j\omega)$, and $G(0,0,0;j\omega)$ are known, this means that only $T1(-d;j\omega)$ must be modified. To do this, we first write out $T1(-d;j\omega)$ explicitly as follows using (6.2), (6.3), and (9.5)

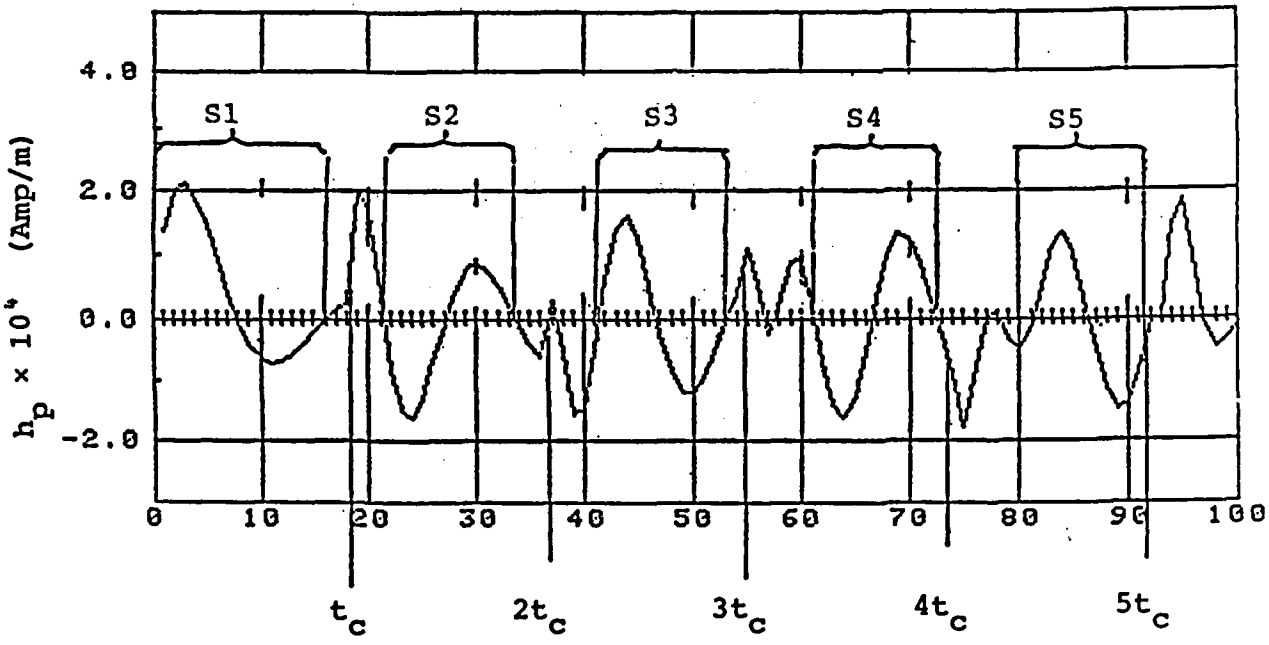

Figure 23. Principal features of the propagating field.

In this case, the rise time of $h_x^r(t)$ is greater than T_c, and (9.55) is not satisfied. Here, the curve is computed with equation (9.53) using numerical integration to evaluate the second and third terms. The effect of these terms is to shift the peak to a much later time (45 microseconds) compared to figure 25.

A comparison of peak incident fields with peak transmitted fields indicates that this enclosure is much more effective in shielding against the Compton field than the return current field. Thus the peak Compton field incident on the enclosure is $3\times10^{-4}T$ = 230 A/m which is about ½ the peak field of the return current. However, the peak Compton field transmitted by the enclosure is only 17×10^{-3} A/m which is smaller than the peak return current field at the same point by a factor of 1/41. Thus the enclosure appears to be more than 20 times more effective against Compton current fields than against return current fields. The reason for this is, of course, the fact that the Compton field is composed of relatively high frequencies, and these frequencies are much more effectively attenuated and reflected by the enclosure than the lower frequencies of the return current field.

10. SHIELDING EFFECTIVENESS OF METALLIC STRUCTURES AGAINST TRANSIENT FIELDS

10.1 Definitions of Shielding Effectiveness in the Time Domain

Time domain definitions of shielding effectiveness can be written in the same form as the frequency domain definitions given in section 7. Thus, if $e1_p^s(0,0,0;t)$ is the p component of the electric field from a transient source s incident on the outside surface of a structure and $e3_p(0,0,-d;t)$ is the corresponding transmitted field on the inside surface of the structure, then the theoretical time domain shielding effectiveness of the structure with respect to this field is

$$se_s^t(e) = 20\log[|e1_p^s(0,0,0;t)/(e3_p(0,0,-d;t)|] \quad . \tag{10.1}$$

And, if $h1_q^s(0,0,0;t)$ is the q component of the magnetic field incident on the structure, then the theoretical time domain shielding effectiveness against the magnetic field is

$$se_s^t(h) = 20\log[|h1_q^s(0,0,0;t)/h3_q(0,0,-d;t)|] \quad , \tag{10.2}$$

where $h3_q(0,0-d;t)$ is the transmitted field. Similarly, the theoretical time domain shielding effectiveness defined in terms of the energy density of the p and q field components is

$$se_s^t(ed) = 20\log[ed1^s(0,0,0;t)/ed3(0,0,-d;t)] \quad , \tag{10.3}$$

where

$$\begin{aligned} ed1^s(0,0,0;t) &= e1_p^s(0,0,0;t)\ h1_q^s(0,0,0;t) \quad , \\ ed3(0,0,-d;t) &= e3_p(0,0,-d;t)\ h3_q(0,0,-d;t) \quad . \end{aligned} \tag{10.4}$$

And corresponding experimental time domain definitions of shielding effectiveness can be written just as easily.

Unfortunately, these definitions have rarely, if ever, been used in practice. This is due to the inherent complexity of most transient fields compared to harmonic fields which makes the definitions difficult to apply. Consequently, there is no standard test method for making time domain shielding effectiveness measurements. The major difficulty in applying these definitions is the fact that the time scale of the transmitted field is usually very much larger than that of the incident field. This will occur when the characteristic diffusion time of a continuous enclosure is much greater than the duration of the incident field (Section 9.2). In this case, the incident field may well have decayed to zero before the transmitted field is detectable, and (10.1), (10.2), and (10.3) are meaningless if the incident and transmitted fields are computed or measured with respect to the same origin (t = 0) and time scale. The same problem could occur with a slotted enclosure (Section 9.1) when most of the energy in the incident field is carried by frequencies greater than the cutoff frequency of the enclosure. In this case, the enclosure could continue to ring with propagating fields of various amplitudes and frequencies long after the incident field has decayed. To avoid these problems, it would be necessary to use different origins and time scales for the incident and transmitted fields. But there is no general method for doing this. Thus, these definitions are likely to be of limited value.

There remains a definite need for a figure of merit that can be applied directly to enclosures exposed to transient fields without the necessity of transforming these fields to the frequency domain ; and to fill this need, modified definitions

of time domain shielding effectiveness can be formulated. Thus, reference 34 defines the shielding effectiveness as the ratio of the peak incident field to the peak of the transmitted field. In terms of the magnetic field, this defintion is written:

$$se_s^t(\max h) = 20\log[\max|h1_q^s(0,0,0;t)|/\max|h3_q(0,0,-d;t)|] \quad . \tag{10.5}$$

And, similar expressions can be written in terms of the electric field and the energy density. Here the problem of disparate time scales is avoided by basing the figure of merit on just one value of the incident field and one value of the transmitted field (or energy density). With (10.5),the shielding effectiveness is expressed very simply as a single number, rather than a function of time as in (10.1)-(10.4). However, the apparent simplicity of (10.5) compared to (10-1)-10-4) is somewhat misleading. To apply (10.5) in practice, it will usually be necessary to evaluate $h3_q(0,0,-d;t)$ over an extensive range of time since there is no other practical way to determine $\max h3_q(0,0,-d;t)$ in the general case. Similarly,it may be necessary to evaluate $h1_q^s(0,0,0;t)$ over an extensive period of time in order to determine $\max h1_q^s(0,0,0;t)$; although this is less likely to be a problem since $h1_q^s(0,0,0;t)$ is usually defined by the investigator. In any case, the effort required to apply (10.5) in the general case will be approximately the same as that required by (10.1)-(10.4). A modified definition that combines features of (10.2) and (10.5) can be written as follows

$$se_s^t(h) = \min se(h(t)) \quad \text{for} \quad 0 < t \leq T \quad , \tag{10.6}$$

---

34 Bell Laboratories, EMP Engineering and Design Principles, Whippany, N.J., (1975).

where $0 < t \leq T$ is the time range of interest and

$$se(h(t)) = 20\log[|h1_q^s(0,0,0;t_m)/h3_q(0,0,-d;t)|] \ , \qquad (10.7)$$

where $t_m \leq T$ is the time at which $h1_q^s(0,0,0;t)$ reaches its peak. To apply (10.6), we determine $h1_q^s(0,0,0;t_m)$ and evaluate $se(h(t))$ using (10.7) at a uniformly spaced set of points over the interval $0 < t \leq T$. The shielding effectiveness is then given according to (10.6) as the minimum value of $se(h(t))$ over this set of points. One advantage of this procedure is that it can be carried out very easily on a computer. This will be shown by an example in the following section. The reader will be able to write corresponding definitions of shielding effectiveness in terms of the electric field and the energy density. In general, it will be found that in the time domain, as in the frequency domain, $se_s^t(h) \neq se_s^t(e) \neq se_s^t(ed)$.

With appropriate modifications, (10.6) can be transforned into an experimental definition of shielding effectiveness analogous to (7.3) and (7.4). Thus,

$$se_s^e(h) = \min se(h(t)) \quad 0 < t \leq T \ , \qquad (10.7)$$

where

$$se(h(t)) = 20\log[|h1_q^s(0,0,-d-D;t_m)/h3_q(0,0,-d-D;t)|] \ . \qquad (10.8)$$

This definition could form the basis of a standardized time domain method of measuring shielding effectiveness analogous to the frequency domain methods described in MIL-STD-285[1]

---

1 Anonymous, MIL-STD-285 "Method of Attenuation Measurements for Enclosures, Electromagnetic Shielding, for Electronic Test Purposed", Dept. of Defense, (25 June 1956).

and IEEE 299.[31] Such a method must be developed in order to carry out experimental shielding studies in the time domain.

10.2 Examples

To illustrate some of the points made in the preceding section, we have computed $se_s^t(h)$ using the results of sections 8 and 9 for a transient source consisting of a small loop antenna driven by a double exponential current pulse. We first computed $se_s^t(h)$ with definition (10.2) where $h1_x^s(0,0,0;t)$ was obtained from equation (8.21) for the case shown in figure 17 and $h3_x(0,0,-d;t)$ was obtained from equation (9.27) for the field transmitted by a slotted enclosure (figure 19). The result is plotted in figure 27. We then computed se(h(t)) with (10.7) using $hi_x^s(0,0,0;t_m) = 6.2\times10^{-3}$ (Amps/m) obtained from figure 17 and $h3_x(0,0,-d;t)$ obtained from equation (9.56) for the field transmitted by a continuous enclosure (figure 24). This result is plotted in figure 28 where

$$se_s^t(h) = \min se(h(t)) \qquad \text{(definition (10.6))}$$
$$= 95 \text{ dB} .$$

is indicated by the arrow at t = 16 microseconds.

Figure 27 shows one of the problems associated with (10.2) as a definition of shielding effectiveness. Here the time scale of $h1_x^s(0,0,0;t)$ is compatible with that of $h3_x(0,0,-d;t)$ since the transmitted field encounters very little time delay in penetrating the slot. Consequently, $se_s^t(h)$ appears well defined for

---

31 Anonymous, Proposed IEEE Recommended Practice for Measurement of Shielding Effectiveness of High Performance Shielding Enlosures, IEEE 299, IEEE Inc., NY,NY, (June 1969).

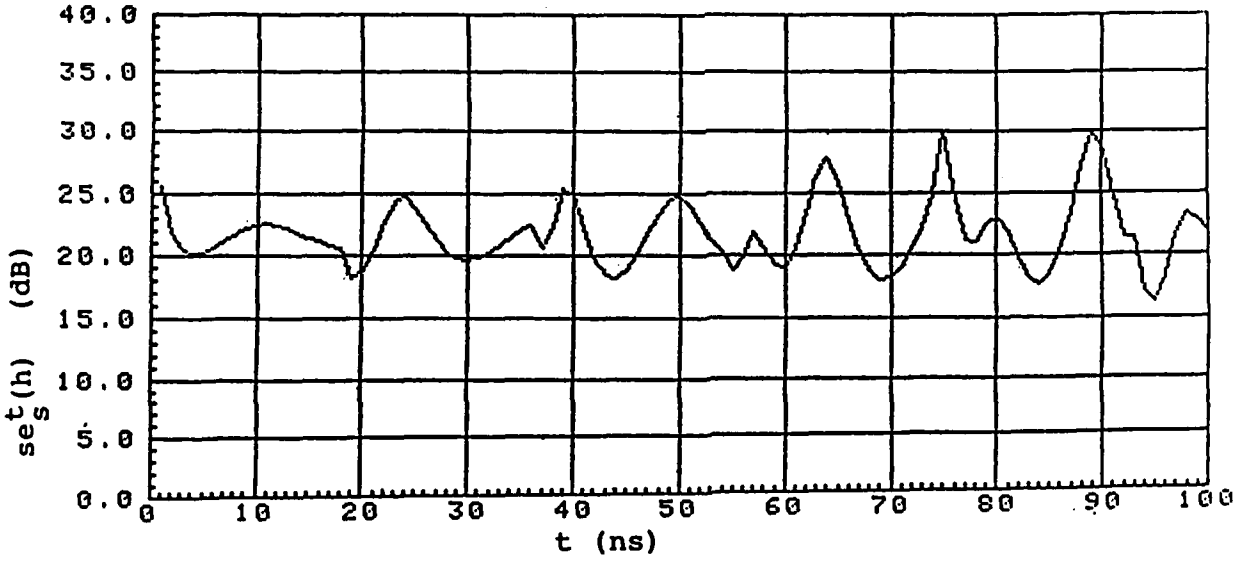

Figure 27. Time domain shielding effectiveness slotted enclosure using definition (10.2).

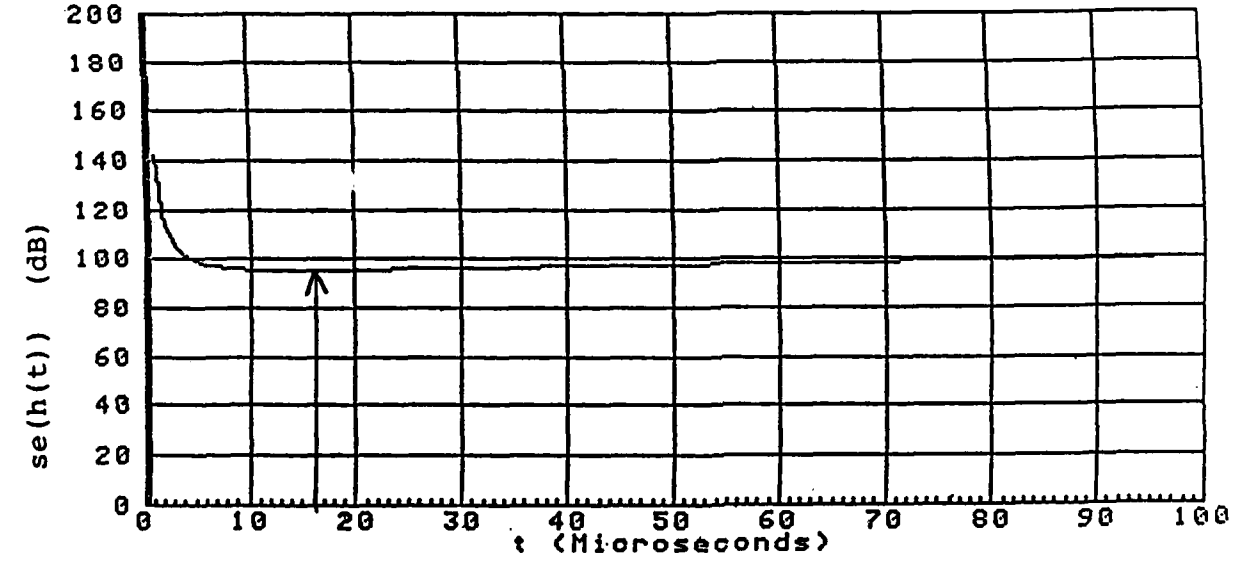

Figure 28. Time domain shielding effectiveness of a continuous enclosure using definition (10.6).

all t. However, instead of remaining within a narrow range of values, $se_s^t(h)$ undergoes larger and larger excursions as time goes on. Thus, it could be difficult to set reasonable limits on $se_s^t(h)$ based on this definition.

When $h1_x^s(0,0,0;t)$ is incident on the continuous enclosure in this example, the time scale of $h3_x(0,0,-d;t)$ is measured in microseconds (compared to nanoseconds for $h1_x^s(0,0,0;t)$, and (10.2) breaks down entirely. In this case, the modified definition (10.6) gives a reasonable estimate of shielding effectiveness as shown in figure 28 even though a direct comparison of $h1_x^s(0,0,0;t)$ and $h3_x(0,0,0-d;t)$ on a point by point basis is meaningless.

11. TEST METHODS FOR MEASURING THE SHIELDING EFFECTIVENESS OF TACTICAL ELECTRONICS SHELTERS AGAINST EMP FIELDS

In the final sections of reference 9, Axford et al review test methods now available or under development for measuring the hardness of small tactical electronics shelters against EMP fields. From this review, they draw the following conclusion: "it is unlikely that any radically new, low-cost methods for performing simple [time domain] EMP tests on shielded structures will be developed without major effort" and, therefore, CW (frequency domain) testing will continue to be "the basic low-cost approach for assuring continuing EMP hardness of small [electronics] shelters." Having concluded that "CW testing will remain as a compromise method of testing EMP hardness", they go on to recommend test methods based on a modified version of IEEE 299[31] which they claim are "generally preferable to those given in MIL-STD-285."

In this section, we wish to point out that, contrary to the statements quoted above, there is a sound basis for believing that new, low-cost methods for performing time domain EMP tests on shielded structures can be developed without a major effort and that CW testing of small electronics shelters may very well be supplanted by these methods in the future. We also wish to point out that, as far as CW testing for EMP hardnesss is

---

9 R. Axford, R. McCormack, and R. Mittra, Evaluation of the Applicability of Standard CW EMI/RFI Shielding Effectiveness Test Techniques to Assessment of EMP Hardness of Tactical Shelters, Construction Engineering Research Laboratories, CERL-TM-M-307, (March 1982).

31 Anonymous, Proposed IEEE Recommended Practice for Measurement of Shielding Effectiveness of High-Performance Shielding Enclosures, IEEE 299, IEEE Inc., NY, NY ,(June 1969).

concerned, there are no convincing reasons for preferring IEEE 299 to MIL-STD-285.[1]

11.1 IEEE 299 VERSUS MIL-STD-285 (AND NSA-65-6)

Considering the latter point first, we note that Axford et al. provide no evidence in reference 9 to support their recommendation. Instead, they repeat the recommendation of an earlier study [38] that compared general EMI test methods (IEEE 299, MIL-STD-285, and NSA-65-6) and made only passing reference to the EMP problem. Thus, it is clear that the decision of Axford et al to recommend IEEE 299 over MIL-STD-285 for EMP testing was not made as a result of comparing these standards in the context of the EMP problem, but was a result of their belief based on Reference 38 that IEEE 299 is "generally preferable" to MIL-STD-285 as an EMI test method. However, a test method that is generally preferable as far as EMI is concerned may not be preferable as an EMP test method, and, therefore, even if one were to accept the recommendation of reference 38, that alone would not establish IEEE 299 as the superior standard for EMP purposes.

In fact,a careful reading of McCormack[38] shows that it does not make a convincing case for the superiority of IEEE 299 to

---

1 Anonymous, MIL-STD-285 "Method of Attenuation Measurements for Enclosures, Electromagnetic Shielding, for Electronic Test Purposes, Dept. of Defense, (25 June 1956).

9 R. Axford, R. McCormack, and R. Mittra, Evaluation of the Applicability of Standard CW EMI/RFI Shielding Effectiveness Test Techniques to Assessment of EMP Hardness of Tactical Shelters, Construction Engineering Research Laboratories, CERL-TM-M-307, (March 1982).

38 R. McCormack, Selection of Recommended Electromagnetic/RFI Test Procedures for Military Tactical Shelters, ESL-TR-80-01, Air Force Engineering and Services Center, (1980).

either MIL-STD-285 or NSA-65-6 as a general EMI test method. According to the author, "the study involved literature research, comparison of existing test specifications, laboratory testing, and summary of past experience. The laboratory testing compared equipment types and testing techniques and examined error possibilities resulting from commonly encountered inaccuracies in equipment set-up." This statement might lead one to expect that the report contains an account of direct experimental comparisons of the three standards and a presentation of experimental data demonstrating the superiority of IEEE 299 over the other two. However, no such experiments are described and no such data are presented in this report. When IEEE 299 is announced as the winner of this competition, the result has the appearance of an arbitrary decision based not on evidence presented in the report but on undocumented references to "previous CERL test experience and engineering judgment."

The report does give data on several interesting and useful experimental comparisons. For example, a comparison between measurements made with electrostatically shielded loops and measurements made with unshielded loops shows that shielded loops are generally preferable to unshielded loops. However, none of the three standards specifies the use of shielded loops so this comparison has no bearing on the choice of a standard.Other data show the errors that result when antennas are misaligned,spaced inaccurately, or subject to interference from nearby structures. But this data also has no bearing on the choice of a standard since all standards assume that antennas are aligned and spaced accurately and are not subject to interference.

Of all the experimental data presented in this report, there is only one set that could reasonably be expected to affect the choice of an EMI standard. This is the data that compares coaxial loop alignment to coplanar loop alignment in small

loop shielding tests. Here, the data show that shielding effectiveness measurements made with transmitting and receiving loops in the coplanar alignment are subject to greater variation due to geometric factors than are measurements made with loops in the coaxial alignment. The reason for this can be seen with the aid of figures 29(a) and 29(b) where 29(a) shows a schematic representation of the electric (-----) and magnetic (———) field lines on the surface of a plane shield (x,y plane) due to a loop antenna lying in a plane perpendicular to that surface (coplanar arrangement) and 29(b) shows the corresponding electric and magnetic field lines due to a loop antenna lying in a plane parallel to the plane of the shield (coaxial arrangement). In figure 29 (a), it is clear that a flaw in the form of a slot or open seam S1 oriented with its length along the x axis will intercept many more electric field lines and therefore will transmit a much larger field through the shield than an identical flaw S2 oriented along the y axis. With this arrangement, the measured effectiveness of the shield with only S1 present would be much less than the measured effectiveness of the shield with only S2 present in spite of the fact that the flaws are identical. In this case, S1 could be easily detected, but S2 might go undetected. To avoid this possibility, it is necessary to rotate the plane of the loop 90 degrees about the z axis (perpendicular to the x,y plane) and carry out a second set of measurements. This rotation of the loop interchanges the positions of the electric and magnetic field lines shown in figure 29(a) and causes S2 to intercept the greater number of electric field lines insuring a maximum response and easier detection. On the other hand, figure 29(b) shows that the circular character of the electric field lines about the center of the loop insures that the same two flaws S1 and S2 will intercept equal numbers of electric field lines and will have an equal chance of detection with just

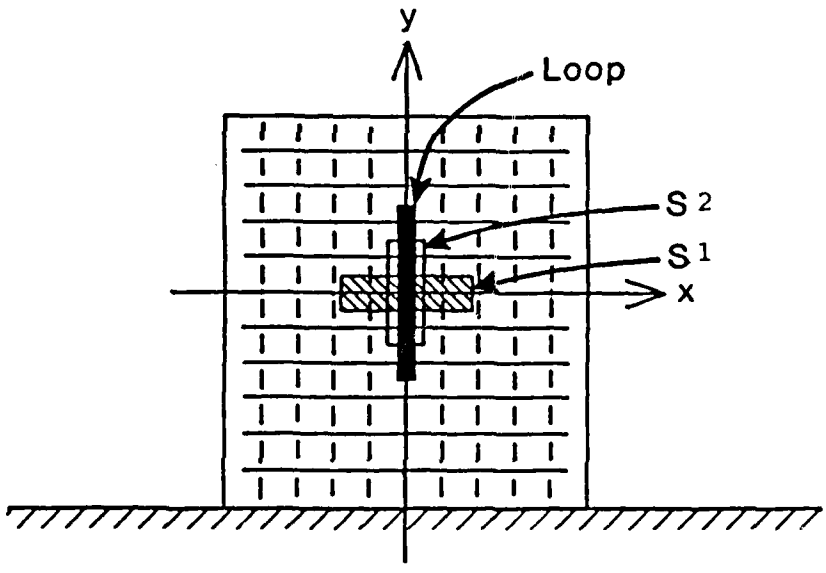

(a) Coplanar Arrangement

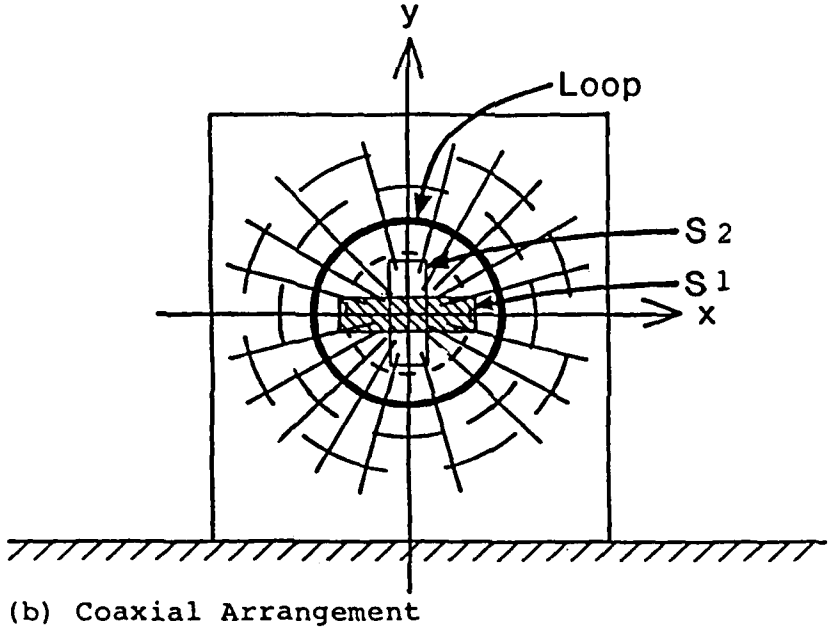

(b) Coaxial Arrangement

Figure29.Electric (----) and magnetic (———) field lines in the x,y plane from coplanar (a) and coaxial (b) loops.

one measurement. Therefore, according to the author: "Use of the coaxial orientation eliminates any need to vary the antenna orientation relative to the geometry of shield defects." He goes on to conclude that "the coaxial method is most desirable for general shelter testing....."

Now in view of this conclusion, one might reasonably have expected the author to be favorably disposed toward NSA-65-6[39] since it alone of the three standards specifies the coaxial arrangement. But this is not the case, and the reader can only guess why NSA-65-6 was not recommended. The author gives no reason why he prefers IEEE 299 to NSA-65-6 when according to his own words he has very good reasons for preferring NSA-65-6 to IEEE 299. He then compounds the confusion by recommending that IEEE 299 be modified by adopting coaxial loops as the preferred arrangement with coplanar relegated to optional use "if conditions warrant and operators are aware of the limitations." He claims that this is a minor modification, but it is very doubtful that the authors of IEEE 299 would agree. Both IEEE 299 and MIL-STD-285 specify the coplanar loop arrangement for the very good reason that it will usually give a lower value of shielding effectiveness than the coaxial arrangement provided two measurements are made with the loop rotated through 90 degrees as we have described. The pay-off for taking the trouble to make two measurements at each location is that it enables one to determine the lowest value of shielding effectiveness for a given structure. It is this value that is of greatest interest in EMI applications since it is a fundamental measure of the quality of the shield. The superiority of the coplanar arrange-

---

39 Anonymous, National Security Agency Specification for R.F. Shielded Enclosure for Communications Equipment: General Specification, NSA 65-6, National Security Agency, (30 October 1964).

First priority must be given to extending and refining our calculations so that a fair experimental test in both the frequency and time domains can be carried out. At present, there is only a single set of measurements available for comparison, and, while there is reasonable agreement between these measurements and the theoretical predictions (figure 15), there are enough potentially significant differences between the theoretical model and the experimental set-up to suggest the possibility that the observed agreement is fortuitous To minimize this possibility in future comparisons between theory and experiment, it is necessary to extend the theory to allow field calculations at points away from the wall of an enclosure and throughout the entire enclosed volume. In its present form, the theory gives only the fields on the inside surface of the wall; whereas,most measurements must be made at points that are a significant distance from the wall. By computing interior fields at points where measurements are made, the inherent discrepancy between the theoretical and experimental definitions of shielding effectiveness (sections 7.1 and 10.1) can be eliminated and a more accurate assessment of the theory can be made. This extension should include the effect of wall losses on internal fields, and it should, if possible, be supported by a more accurate calculation of the internal wave impedance. As previously noted, wall losses play an important role in problems involving transient sources by determining the damping rate of the propagating component of the transmitted field - a factor that should be relatively easy to measure. The internal wave impedance is,of course, crucial to determining the fields at all points inside an enclosure. A more accurate determination of this quantity will improve the accuracy of the field calculations by including contributions from higher order waveguide modes than the single TE_{10} mode we have used here.

Since most practical electromagnetic shields do contain mall openings of the type that approximate the small rectangular slots we have considered in this report, the preceding mplies that these openings will be the primary path by which an xternal field reaches the shielded volume. That is, in practice, he fields that pass through openings in the wall of the field ill dominate the field that diffuses through the continuous ortions of the wall. Therefore, we should expect to see both ow frequency static fields and high frequency propagating ields inside an actual enclosure when it is exposed to an external transient field. However, the ratio of the former to the atter may differ radically from the example of the slotted enclosure considered here due to variations in the frequency ontent of the source field and the cutoff frequency of the nclosure.

To reduce the magnitude of the "slot" fields below that of he diffusion field in a practical enclosure requires very careful construction. A single small opening that may be extremely difficult to detect can transmit a field of sufficient strength o completely dominate the diffusion field. Thus, it is not surprising that high frequency propagating fields can be observed even in high quality shielded enclosures when these are exposed to transient sources such as EMP. In fact, it is doubtful that a purely diffusive field from an EMP source could ever e observed inside an enclosure formed from bolted sections of sheet metal.

The results we have just summarized represent the beginning of a new approach to the study of electromagnetic shielding, but here is still much to be done before the theory can be described as fully developed. In our final paragraphs, we will attempt o point out those areas where further development is most eeded.

of the SREMP source where we showed that the low fequency component of the incident field associated with the return current in the EMP source region is at least 20 times more effective in penetrating the enclosure wall than the high frequency component associated with the radial Compton current.

Several time domain definitions of shielding effectiveness were investigated in an effort to obtain a figure of merit that can be applied directly when an electromagnetic shield is exposed to a transient field without the necessity of transforming the latter to an equivalent harmonic source. Although none of these are entirely satisfactory in all respects, two were used to compute the shielding effectiveness of a continuous and slotted enclosure against the magnetic field from a square loop antenna driven by the transient current described earlier. The two enclosures are virtually identical except for the greater wall thickness of the slotted enclosure (.25" versus .036") and its rectangular .5 m by .0001 m slot in one wall. If the walls are composed of aluminum, the time domain shielding effectiveness of the continuous enclosure against the transient loop source is computed to be 95 dB; the corresponding figure of merit for the slotted enclosure is approximately 20 dB which is close to the frequency domain shielding effectiveness that is computed for the same enclosure when it is exposed to a harmonically driven magnetic dipole. The 75 dB difference in shielding effectiveness shown by these two enclosures demonstrates the severe effect that a small opening can have on the quality of an electromagnetic shield. On the basis of this example, we can expect that the shielding effectiveness of the continuous enclosure will be reduced from 95 dB to 20 dB when a .5 m slot is cut in one wall. And it can be shown that much smaller slots - even those less than 1 cm in length - will reduce the shielding effectiveness of the enclosure by smaller but still significant amounts.

is, of course, a nonphysical result. A more accurate approximation in which the effect of wall losses on fields inside the enclosure are taken into account would show that the propagating fields are damped and do approach zero as $t \longrightarrow \infty$. However, these losses are likely to be small in most enclosures of interest, and therefore are not expected to play an important role until relatively late times.

In the case of the continuous parallelepiped, we find that the transient field inside the enclosure is quite different than the field inside the slotted enclosure even when both are exposed to the same source. The peak field inside the continuous enclosure is many orders of magnitude smaller than the field inside the slotted enclosure, and the rise time of the field is many orders of magnitude slower. Thus, the field is simultaneously reduced in magnitude and stretched in time compared to the field in the slotted enclosure. This is due to the fact that the continuous enclosure eliminates the high frequency components in the source field that account for the large early peak seen in the slotted enclosure. The field that penetrates the wall is purely diffusive field consisting of frequency components that for the most part fall below the cutoff frequency of the enclosure. Consequently, there is no propagating field inside a continuous enclosure.

Since low frequencies penetrate the continuous enclosure more effectively than higher frequencies, the magnitude of the transmitted field depends most importantly on the low frequency content of the incident field. If two transient fields with equal peak values are incident on the same continuous enclosure, the field with more energy at lower frequencies will produce the largest field inside the enclosure. The importance of low frequencies for continuous enclosures was demonstrated in the case

raised in section 1 by showing how and why Schelkunoff's equation can be adapted to practical enclosures. The generalized Schelkunoff equation led to a correction factor that can be used to relate the shielding effectiveness of a structure as seen by one source to the shielding effectiveness of the same structure as seen by another source. This factor is a generalization of the correction factor given in Monroe[2].

The theory was extended from harmonic sources to transient sources for several cases of interest. These consist of a rectangular parallelepiped with a slot in one wall exposed to fields from a square loop antenna driven by a transient current, a continuous rectangular parallelepiped exposed to the same source, and a continuous parallelepiped exposed to SREMP fields. In each case, the time variation of the source is represented as a sum of decaying exponentials, and the field transmitted to the interior of the enclosure is evaluated explicitly using analytic approximations. For the slotted enclosure, the transmitted field is found to consist of the sum of two distinct fields: a nonpropagating , or static, field formed from those frequency components of the source field that fall below the cutoff frequency of the enclosure and a propagating field formed from frequency components above the cutoff frequency of the enclosure. The static field is virtually identical in form to the loop current which decays smoothly to zero as $t \longrightarrow \infty$. In contrast, the propagating field has a rather complicated waveform that can be interpreted in terms of a series of pulses reflected between the front and back walls of the enclosure. In the approximation used here, the propagating field is undamped and, unlike the static field, does not decay with time. This

---

2 R. L. Monroe, EMP Shielding Effectiveness and MIL-STD-285, Harry Diamond Laboratories, HDL-TR-1636, (1973).

electric and magnetic dipoles by using the wave impedance of the dipole field to approximate the wave impedance of the transmitted field. And in a similar way, we obtained the fields transmitted to the interior of a rectangular parallelepiped from a small loop antenna by approximating the wave impedance of the transmitted field with that of the TE_{10} waveguide mode. These calculations were carried out for both continuous shields and for shields with a single narrow slot. We used our results to construct expressions for the shielding effectiveness of these structures. We found that the shielding properties of the infinite plane sheet could be characterized by a single expression identical in form to Schelkunoff's equation. However, we also found that the shielding properties of the rectangular parallelepiped are characterized by two quite distinct expressions: one representing the shielding of the electric field and one representing the shielding of the magnetic field. This result implies that the shielding effectiveness of an enclosure unlike that of a plane sheet cannot be accurately determined using electric or magnetic field measurements alone in the manner prescribed by MIL-STD-285 and IEEE 299. The reason for the difference between the shielding properties of sheets and enclosures was traced to the fact that in the case of the sheet the wave impedance of the incident field is approximately equal to the wave impedance of the transmitted field;whereas,in the case of the enclosure, the wave impedance of the incident field is, in general, quite different than the wave impedance of the transmitted field. This fact can be properly accounted for by defining the shielding effectiveness in terms of the ratio of the power density of the incident field to the power density of the transmitted field. Using this definition, we obtained generalized forms of Schelkunoff's equation that are valid for continuous and slotted sheets and enclosures. These relations answered the second question

12. CONCLUSIONS AND RECOMMENDATIONS

In this report, we have presented a theory of electromagnetic shielding based on a new application of impedance boundary conditions. By applying these conditions to an internal boundary value problem (rather than the customary external reflection and scattering problems), we were able to obtain explicit expressions for the fields transmitted through the wall of a generalized electromagnetic shield from an arbitrary harmonic source. The transmitted fields at a point on the inside surface of the wall are written in terms of the wave impedance of the fields at that point and the tangential components of the magnetic field incident on the outside surface of the wall. Thus, the theory can be applied to a particular combination of source and shield by specifying the source magnetic field incident on the outside of the shield and the wave impedance on the inside of the shield.

As a first step toward applying the theory to practical sources and shields, we obtained expressions for the magnetic fields from elementary electric and magnetic dipoles and from a a small, rectangular loop antenna. These expressions answered one of the questions raised in section 1 by showing that the magnetic field of the magnetic dipole is a good approximation to the corresponding field of the loop antenna at distances from the center of the loop that are not significantly larger than the dimensions of the loop, provided the source frequency is less than 10^7 Hz. They also showed that a square loop antenna 10.6 inches on a side located with its center 36 inches from a plane surface is capable of generating a virtually uniform magnetic field over a 7'x7' area of that surface. With these expressions, we obtained the fields transmitted through an electromagnetic shield in the form of an infinite plane sheet from

posed to the simulated effects of five simultaneous EMP events - surely a worst case.

source. Inevitably, as shown in figure 30(b),there will be a phase difference between the field at O(0,0,0) and the field at another point such as P(0,H/2,0) that would not occur if the incident field were a plane wave. In the time domain,this means that the incident field at P(0,H/2,0) will be delayed with respect to the field at O(0,0,0) by the time it takes the field to travel the distance from Q to P at the speed of light. The distance d(Q,P) is the additional distance the field must travel to reach P from the phase center C compared to the distance D that the field at O must travel from C. In this case, $d(Q,P) = \sqrt{H^2/4 + D^2} - D$ and for the example considered where H = 7' and D = 36", d(Q,P) is .5 meters. Since a field travelling at the speed of light requires 1.6 ns to travel .5 meters this means that the field at P will be delayed by 1.6 ns with respect to the field at O. As far as the fields reaching the interior of the enclosure are concerned this would be a negligible difference in most cases; however, if one wished for any reason to reduce the time delay, this could always be done by moving the antenna farther away from the surface or by using additional antennas.

The versatility of the loop antenna will allow its use as an EMP simulator in ways that would be difficult to duplicate with other simulators. For example, the plane of polarization of the incident field is determined by the plane of the loop which is easy to adjust. Thus, by rotating the loop shown in figure 30(b) 90 degrees about the z axis, a horizontally polarized EMP field can be simulated. And by rotating the loop about an axis perpendicular to the y, z plane through C, various angles of incidence could be reproduced. With an array of small, strategically located loop antennas, many novel EMP simulations could be carried out easily at relatively low cost. One such arrangement would consist of one or two loops mounted on all five exposed surfaces of the enclosure and driven simultaneously by a common source. In this way, an electronics shelter could be ex-

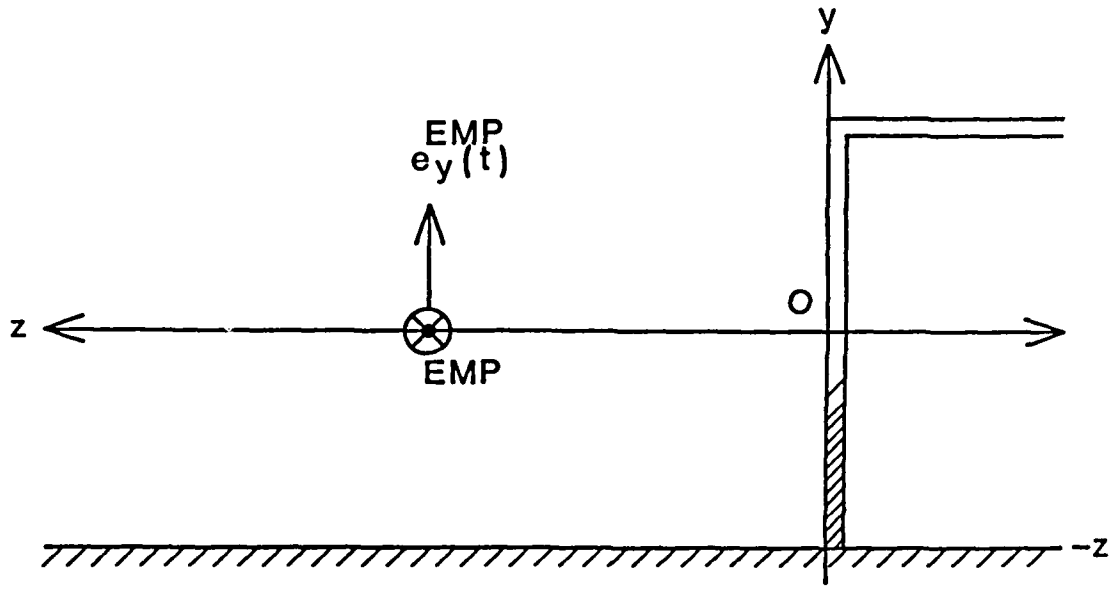

(a) A plane wave EMP field incident normally on the surface of an electronics shelter.

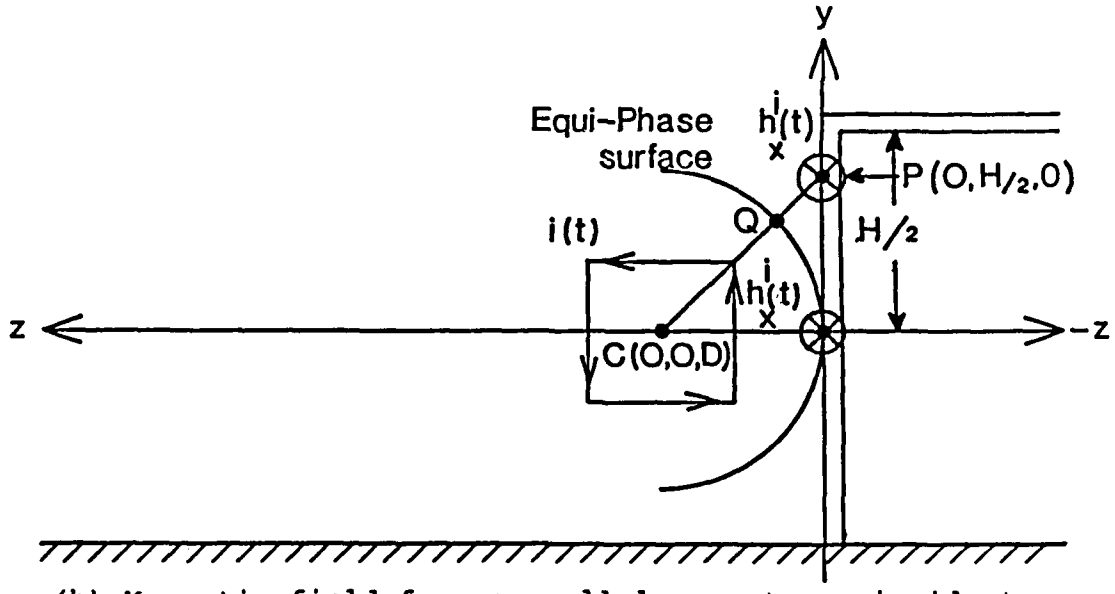

(b) Magnetic field from a small loop antenna incident on the surface of an electronic shelter.

Figure 30. Simulation of an EMP field by a small loop antenna.

tic field on any one surface of the enclosure. For example, an EMP field propagating in the -z direction as shown in figure 30 (a) can be approximated as a vertically polarized plane wave with a single electric field component $e_y^{EMP}(t)$ and a single magnetic field component $h_x^{EMP}(t)$ indicated by the symbol ⊗ .In this case, the tangential component of the incident magnetic field is equal to $h_x^{EMP}(t)$ which is uniform over the exposed surface of the enclosure. To simulate the EMP field it is necessary to reproduce $h_x^{EMP}(t)$ at the surface of the enclosure.

The calculations we have carried out in preceding sections indicate that this should not be a difficult task. In section 5.3, we showed that a small square loop antenna 10.8 inches on a side with its geometric center located at a distance of 36 inches from the geometric center of a square surface 7 feet on a side (approximately the dimensions of one of the smaller surfaces of the HATS shelter) would generate a nearly uniform magnetic field over the entire 49 ft^2 surface and that the dominant component of this magnetic field is the x component for all significant EMP frequencies (0-100MHz) when the loop lies in the y,z plane as represented in figure 30(b). Furthermore, it was shown in section 8.2 that a correctly designed current pulse on the loop can produce an incident magnetic field $h_x^i(t)$ at O that matches the wave form of a high altitude EMP. Clearly then, a square loop antenna used in this way would qualify as an EMP simulator for purposes of determining the time domain shielding effectiveness of an enclosure against a plane wave EMP field incident normally on one surface of an enclosure. One would need to measure $h_x^i(t)$ at O and the transmitted field $h_x^t(t)$ at a designated point or points inside the enclosure and determine the time domain shielding effectiveness of the enclosure using one of the definitions given in section 10.

Of course, it will not be possible to precisely duplicate a plane wave field over the entire surface with a single localized

Not every source and enclosure are such that the fields satisfy an impedance boundary condition on the surface of the enclosure. However, as we have seen, EMP fields will satisfy these conditions on most shielded enclosures (SE>10dB). It follows that an EMP field can be simulated for purposes of shielding effectiveness measurements by any other field that produces the same, or approximately the same, tangential magnetic field on the surface of the enclosure. Thus, the problem of EMP simulation for shielded enclosures reduces to the problem of simulating the tangential magnetic field components of the EMP by another source.

As a practical matter, could such a simulation be carried out? In the case of a general electromagnetic field where two magnetic field components vary both in amplitude and phase at every point on the surface of the enclosure, this would appear to be undertaking only slightly less formidable than a full scale simulation of the entire field. However, in the case of an EMP field incident on an electronics shelter, there are mitigating factors that can simplify this problem. First, the characteristic dimensions of the surfaces of the shelter which can be approximated by flat rectangular planes are likely to be small compared to the scale size of the incident EMP field. When this is the case, the tangential components of the magnetic field will be uniform over any surface of the enclosure.That is, the tangential components will be constant on a given surface of the enclosure except possibly for a phase factor that depends only on the angle between the normal to the surface and a line through the phase center of the source. A second mitigating circumstance is the fact that an EMP field can usually be approximated by a linearly polarized plane wave at the shelter location. Therefore, with an appropriate choice of coordinate systems, we need only deal with a single component of the magne-

believe that IEEE 299 is superior in this regard. The answer is that there is no such reason. Does this mean that MIL-STD-285 is clearly superior to IEEE 299? It does not. In fact, as applied to EMP problems, the two standards in the hands of competent operators would give nearly the same results. The reason for this is that the only part of either standard that is germane to EMP hardness is the small loop test; and, as we have seen in section 7.4, the small loop tests described by these two standards are virtually identical.

11.2 Direct Time Domain Measurements

The information developed in this report suggests that low-cost, time domain methods for measuring the hardness of small tactical electronics shelters to EMP fields could be developed without "major" effort using the small loop test of MIL-STD-285 and IEEE 299 as a model. A theoretical basis for this suggestion is contained in sections 4, 5, 8, 9, and 10. In section 4 it was shown that electric and magnetic fields in the interior of an enclosure generated by an arbitrary electromagnetic source located outside of the enclosure can be written in terms of the tangential components of the magnetic field incident on the outside of the enclosure, provided the electric and magnetic fields satisfy impedance boundary conditions on the outside of the enclosure. In other words, impedance boundary conditions insure that internal electric and magnetic fields are determined solely by tangential components of the incident magnetic field on the surface of the enclosure. This fact has several interesting consequences. It means that two external sources producing the same or nearly the same tangential magnetic fields on the outside of an enclosure will be indistinguishable from inside the enclosure. It also means that the effect of one source on the interior of an enclosure can be simulated by a second source if the latter faithfully reproduces the tangentical magnetic field of the former on the outside of the enclosure.

ment in this respect is borne out by data in table 4 of reference 38. The table lists measured values of shielding effectiveness at several frequencies for two structures: a test panel and a copper screen room. For each frequency, three values of shielding effectiveness are given: one for the antennas in the coaxial position, one for the coplanar position with the plane of the loop oriented vertically, and one for the coplanar position with the loop oriented horizontally. The table shows that one of the coplanar positions gives a smaller shielding effectiveness reading than the coaxial position in every case except one and in that case the two reading are the same. Thus there are well documented reasons for retaining coplanar loops in preference to coaxial loops. In this light, it appears that the reasons given in reference 38 for preferring coaxial arrangement are a matter of convenience rather than substance and that the "limitations" of the coplanar arrangement are greatly exaggerated. If either arrangement has substantial limitations, it is clearly the coaxial not the coplanar arrangement. In view of this, an operator who wishes to take advantage of the convenience afforded by coaxial loops and who is aware of their limitations would be well advized to follow NSA-65-6 rather than IEEE 299 as recommended ir reference 38. Using IEEE 299 in a way that its designers never intended would almost certainly produce even more confusion in an area where confusion already abounds.

Although it is clear from the preceding that McCormack[38] does not make a case for preferring IEEE 299 to MIL-STD-285 as a CW method for measuring the hardness of electronics shelters to EMP fields, one might still ask if there is any reason to

---

38 R. McCormack, Selection of Recommended Electromagnetic/RFI Test Procedures for Military Tactical Shelters, ESI-TR-80-01, Air Force Engineering and Services Center, (1980).

In addition to extending and refining our treatment of these shielding problems, future work should apply the theory to new problems involving different combinations of sources and shields that have well defined applications. An example of such a problem is a large source like the REPS EMP Simulator illuminating a large shielded enclosure. In this problem, the dimensions of the source are not small compared to all wavelengths of the radiated field, and oscillating fields associated with source resonances must be taken into account. As a result, the field incident on the enclosure must be represented as a combination of damped sinusoids rather than as a sum of simple exponentials such as we have considered here. Similarly, in a building sized enclosure slot-like discontinuities may not all be small compared to all wavelengths in the incident field, and slot resonances may have to be considered. Obviously, these factors can be expected to complicate the calculations of the internal fields in this case. More applications of the theory will occur in the development of EMP standards for small shielded enclosures using small EMP simulators as described in section 11.2. These will involve determining the optimum size, location, and orientation of the simulator with respect to the enclosure and synthesizing the correct waveshape of the driving current.

Finally, the theory should be generalized to include a wider range of structures. In its present form, the theory applies to a shield formed from one or more plane sheets that may be penetraded by a number of narrow, rectangular slots. An obvious generalization is a structure composed of one or more sections of curved, metal sheets such as airplane and missile skin or cable shields. Since impedance boundary conditions are valid for curve surfaces under relatively weak restrictions, it is clear that such a generalization would be possible. The difficulty here will be to compute the tangential components of the

incident field on the surface and to determine the wave impedance of the transmitted field.

LITERATURE CITED

(1) Anonymous, MIL-STD-285 "Method of Attenuation Measurements for Enclosures, Electromagnetic Shielding, for Electronic Test Purposes, Dept. of Defense, (25 June 1956).

(2) R. L. Monroe, EMP Shielding Effectiveness and MIL-STD-285, Harry Diamond Laboratories, HDL-TR-1636, (July 1973).

(3) S. A. Schelkunoff, Electromagnetic Waves, Van Nostrand, Princeton, N.J., (1943).

(4) W. Jarva, IEEE Trans. EMC, EMC-12 (1970), 12.

(5) J. R. Moser, IEEE Trans. EMC, EMC-9 (1967), 6.

(6) P. R. Bannister, IEEE Trans. EMC, EMC-10 (1968), 2.

(7) M. B. Kraichman, Handbook of Electromagnetic Propagation in Conduction Media, U.S. Gov't Printing Office,D.C., (1970).

(8) C. R. Davis, E. Villaseca, W. Blackwood, and W. Getson, An Investigation of the Validity of Applying MIL-STD-285 to EMP Shielding Effectiveness, Harris Electronics Systems Division, (15 April 1977).

(9) R. Axford, R. McCormack, and R. Mittra, Evaluation of the Applicability of Standard CW EMI/RFI Shielding Effectiveness Test Techniques to Assessment of EMP Hardness of Tactical Shelters, Construction Engineering Research Laboratories, CERL-TM-M-307, (March 1982).

(10) S. A. Schelkunoff, Bell System Technical Journal, 17 (1938), 17.

(11) C. S. Vasaka, Rept. NADC-EL-N5507, U.S. Naval Air Development Center, (1955).

(12) E. C. Jordan, Electromagnetic Waves and Radiating Systems, Prentice-Hall, Englewood, N.J., (1950).

(13) R. B. Schulz, V. C. Plantz, and D. R. Brush, Shielding Theory and Practice, Proc. 9th Tri-Service Conf. on Electromagnetic Compatibility, Chicago, Ill., (October 1963).

(14) R. B. Cowdell, Electronics, 40 (April 1967), 92.

(15) L. F. Babcock, IEEE Trans. EMC, EMC-9 (Sept. 1967), 45.

(16) R. B. Schulz, IEEE Trans. EMC, EMC-10 (March 1968), 95.

(17) R. B. Cowdell, IEEE Trans. EMC-10 (March 1968), 158.

(18) J. E. Bridges and D. A. Miller, IEEE Trans. EMC, EMC-10 (1968), 175.

(19) R. B. Schulz, IEEE Trans, EMC, EMC-10 (March 1968), 176.

(20) T. B. A. Senior, IEEE Trans. on Antennas Propagt., AP-29 No. 2, (1981), 826.

(21) T. B. A. Senior, Appl. Sci. Res., 8(B) (1960), 418.

(22) M. A. Leontovich, Investigation of Radiowave Propagation, Part II, Moscow: Academy of Sciences, (1948).

(23) S. M. Rytov, J. Exp. Theor. Phys. USSR, 10 (1940), 180.

(24) I. L. Alpert, J. Tech, Phys. USSR, 10 (1940), 1358.

(25) E. L. Feinberg, J. Phys. USSR, 8 (1944), 317.

(26) R. B. Adler, L. J. Chen, and R. M. Fano, Electromagnetic Energy Transmission and Radiation, John Wiley and Sons,Inc. N.Y., p. 432 (1960).

(27) A. Banos, Jr., Dipole Radiation in the Presence of a Conduction Half-Space, Pergamon Press, Oxford,U.K., p.4 (1966).

(28) A. Sommerfeld, Ann. Physik, 28 (1909), 665.

(29) P. R. Bannister, IEEE Trans. Antennas and Propagation, AP-15 (1967), 618

(30) S. Ramo, J. R. Whinnery, T. Van Duzer, Fields and Waves in Communication Electronics, John Wiley and Sons, Inc., New York, (1965).

(31) Anonymous, Proposed IEEE Recommended Practice for Measurement of Shielding Effectiveness of High Performace Shielding Enclosures, IEEE 299, IEEE Inc. NY,NY, (June 1969).

(32) G. Doetsch, Guide to Applications of Laplace Transforms, D. Van Nostrand and Company LTD., London, (1961).

(33) C. L. Longmire, IEEE Trans. Ant. Progt., AP-16, No. 1, 1978.

(34) Bell Laboratories, EMP Engineering and Design Principles, Whippany, N.J., (1975).

(35) T. Wyatt, Harry Diamond Laboratories, Washington, D.C. Private Communication, (June 1984).

(36) E. C. Titchmarsh, The Theory of Functions, 2nd Ed., Oxford University Press, Section 3.2, (1939).

(37) G. A. Campbell and R. M. Foster, Fourier Integrals for Practical Applications, D. Van Nostrand Company Inc., (1948).

(38) R. McCormack, Selection of Recommended Electromagnetic/RFI Test Procedures for Military Tactical Shelters, ESL-TR-80-01, Air Force Engineering and Services Center, (1980).

(39) Anonymous, National Security Agency Specification for R. F. Shielded Enclosures for Communications Equipment: General Specification, NSA 65-6, National Security Agency, (30 October 1964).

DISTRIBUTION

DIRECTOR
DEFENSE COMMUNICATIONS
ENGINEERING CENTER
ATTN CODE R400
ATTN CODE T123, TECH LIB
ATTN CODE R800, COL F. MAYBAUM
ATTN CODE R111 (SICA)
ATTN CODE R112
ATTN CODE R110
ATTN CODE R200
ATTN CODE R430
1860 WIEHLE AVENUE
RESTON, VA 22090

OFFICE OF UNDER SECRETARY OF
DEFENSE RESEARCH &
ENGINEERING
DMSSO
2 SKYLINE PLACE
SUTIE 1403
5203 LEESBURG PIKE
FALLS CHURCH, VA 22041

ASSISTANT CHIEF OF STAFF OF
FOR INFORMATION MANAGEMENT
COMMAND SYSTEMS INTEGRATION
OFFICE
ATTN DAMO-C42, COL D. GRIGGS
THE PENTAGON
WASHINGTON, DC 20301

DIRECTOR
USACC, FT BELVOIR
ATTN CCNB-BLV, ROYE
FT BELVOIR, VA 22060

COMMANDER
US ARMY COMMUNICATIONS COMMAND
ATTN CC-OPS-TT
ATTN CC-ENGR
ATTN CC-OPS-WR, O. P. CONNELL
FT HUACHUCA, AZ 85613

CHIEF
US ARMY COMMUNICATIONS SYS
AGENCY
DEPARTMENT OF THE ARMY
ATTN TECHNICAL DIRECTOR
ATTN CCM-AD-SV
ATTN CCM-RD-T
ATTN CCM-TS-A
FT MONMOUTH, NJ 07703

COMMANDER
PM DCS (ARMY)
ATTN DRCPM-COM-TS-A
FT MONMOUTH, NJ 07703

COMMANDER 7TH SIGNAL COMMAND
ATTN CCN-ENGR, F. HULTSLANDER
FT RITCHIE, MD 21719

COMMANDER
HQ, USA WESTERN COMMAND
ATTN APEN-ISM
FT SHAFTER, HI 96858

COMMANDER
NAVAL ELECTRONICS SYSTEMS
COMMAND
PO BOX 55
ATTN MR. BLAKELY, 210
PORTSMOUTH, VA 23705

NAVFAC ENG COM PAC DIV
ATTN RON CHING
PEARL HARBOR
OAHU, HI 96860

COMMANDER
NAVAL TELECOMMUNICATIONS
COMMAND
ATTN CODE 621A, M. BLANDING
4401 MASSACHUSETTS AVE, NW
WASHINGTON, DC 20390

NEEACTPAC
ATTN CODES 210, 220
PEARL HARBOR, HI 96860

HEADQUARTERS
USAF
ATTN SITI
ATTN XOXXI
ATTN RDSS
WASHINGTON, DC 20330

TELEDYNE BROWN ENGINEERING
CUMMINGS RESEARCH PARK
ATTN D. GUICE
HUNTSVILLE, AL 35807

ADMINISTRATOR
DEFENSE TECHNICAL
INFORMATION CENTER
CAMERON STATION, BUILDING 5
ATTN DTIC-DDA (12 COPIES)
ALEXANDRIA, VA 22314

NATIONAL COMMUNICATIONS
SYSTEM
DEPARTMENT OF DEFENSE
OFFICE OF THE MANAGER
ATTN NCS-TS, D. BODSON
WASHINGTON, DC 202305

ASSISTANT TO THE SECRETARY
OF DEFENSE
ATOMIC ENERGY
ATTN EXECUTIVE ASSISTANT
WASHINGTON, DC 20301

DIRECTOR
DEFENSE COMMUNICATIONS AGENCY
ATTN CODE B410, PARKER
ATTN CODE B430
ATTN CODE J300, KNAPP
WASHINGTON, DC 20305

DIRECTOR
COMMAND CONTROL ENGINEERING
CENTER
ATTN C-661, DR. T. TRINKLE
ATTN G-630, R. LIPP
WASHINGTON, DC 20305

DIRECTOR
DEFENSE COMMUNICATIONS
ENGINEERING CENTER
ATTN CODE R400
ATTN CODE R123, TECH LIB
ATTN CODE R111, SICA
1860 WIEHLE AVENUE
RESTON, VA 22090

DIRECTOR
DEFENSE INTELLIGENCE AGENCY
ATTN DB-4C2, D. SPOHN
WASHINGTON, DC 20301

CHAIRMAN
JOINT CHIEFS OF STAFF
ATTN J-3
ATTN C3S
WASHINGTON, DC 20301

DIRECTOR DEFENSE NUCLEAR AGENCY
ATTN NATA
ATTN RAEV
ATTN DDST
ATTN RAEE
ATTN TITL
WASHINGTON, DC 20305

UNDER SECY OF DEF FOR RSCH & ENGRG
DEPARTMENT OF DEFENSE
ATTN STRATEGIC & SPACE SYS 90S0 RM 3E129
ATTN STR`T & THEATER NUC FORCES
WASHINGTON, DC 20301

DEPUTY DIRECTOR FOR THEATER/TACTICAL C3 SYS
JOINT STAFF
WASHINGTON, DC 20301

COMMANDER-IN-CHIEF
US FORCES, EUROPE
ATTN ECC3S
APO, NY 09128

ASSISTANT CHIEF OF STAFF FOR AUTOMATION & COMMUNICATIONS
ATTN DAMO-C4T
ATTN DAMO-C4S
DEPARTMENT OF THE ARMY
WASHINGTON, DC 20360

US ARMY BALLISTIC RESEARCH LABORATORY
ATTN DRDAR-TSB-S (STINFO)
ABERDEEN PROVING GROUND, MD 21005

COMMANDER
US ARMY COMM-ELEC INSTAL AGENCY
ATTN CCC-CE-TS
FT HUACHUCA, AZ 85613

COMMANDER
5TH SIGNAL COMMAND HEADQUARTERS
ATTN DCS OPS, K. MILLER
APO, NY 09056

US ARMY ELECTRONCIS TECHNOLOGY & DEVICES LABORATORY
ATTN DELET-DD
FT MONMOUTH, NJ 07703

US ARMY ENGINEER DIV HUNTSVILLE
DIVISION ENGINEER
ATTN HNDED FD, T. BOLT
PO BOX 1600
HUNTSVILLE, AL 35807

COMMANDER
US ARMY MATERIEL COMMAND
ATTN DRCRE
ATTN DRCDE
5001 EISENHOWER AVE
ALEXANDRIA, VA 22333-0001

DIRECTOR
US ARMY MATERIEL SYSTEMS ANALYSIS ACTIVITY
ABERDEEN PROVING GROUND, MD 21005

COMMANDER
US ARMY MISSILE & MUNITIONS CENTER & SCHOOL
ATTN ATSK-CTD-F
REDSTONE ARSENAL, AL 35809

COMMANDER
US ARMY NUCLEAR & CHEMICAL SOCIETY
ATTN MONA-WE
7500 BACKLICK RD
SPRINGFIELD, VA 22150

DEP CH OF STAFF FOR RSCH DEV & ACQ
DEPARTMENT OF THE ARMY
ATTN DAMA-DCC-N
WASHINGTON, DC 20310

COMMANDER
US ARMY RSCH & STD GP (EUR)
ATTN CHIEF, PHYSICS & MATH BRANCH
FPO NEW YORK 09510

CHIEF
US ARMY SATELLITE COMMUNICATIONS AGENCY
ATTN DRCPM-SC
FT MONMOUTH, NJ 07703

DIRECTOR
TRI-TAC
ATTN TT-E-SS, CHARNICK
FT MONMOUTH, NJ 07703

COMMANDER-IN-CHIEF
ATLANTIC
ATTN J6
NORFOLK, VA 23511

COMMANDER
NAVAL ELECTRONIC SYSTEMS COMMAND
ATTN PME 110-241D,D.O'BRYHIM, A.LARSON
WASHINGTON, DC 20360

CHIEF OF NAVAL MATERIEL
THEATER NUCLEAR WARFARE PROJECT OFFICE
ATTN PM-23, TN-31, TATE
WASHINGTON, DC 20360

COMMANDER
NAVAL OCEAN SYSTEMS CENTER
ATTN CODE 7309,R. GREENWELL
ATTN CODE 8123,S. LICHTMAN
ATTN CODE 83, J. STAWISKI
SAN DIEGO, CA 92152

COMMANDING OFFICER
NAVAL ORDINANCE STATION
ATTN STANDARDIZATION DIVISION
INDIAN HEAD, MD 20640

COMMANDER-IN-CHIEF
PACIFIC
ATTN C3S-RP-1
CAMP H. M. SMITH, HI 96861

COMMANDING OFFICER
NAVAL RESEARCH LABORATORY
ATTN CODE 4720, J. DAVIS
WASHINGTON, DC 20375

COMMANDER
NAVAL SURFACE WEAPONS CENTER
ATTN CODE F-56
DAHLGREN, VA 22448

COMMANDER
NAVAL SURFACE WEAPONS CENTER
ATTN CODE F32, E. RATHBURN
ATTN CODE F30
WHITE OAK LABORATORY
SILVER SPRING, MD 20910

DEPARTMENT OF THE NAVY
DIRECTOR, NAVAL TELECOMM. DIVISION
OFFICE OF THE CHIEF OF NAVAL OPERATIONS
ATTN OP941, HAILSMAIER
ATTN OP943
WASHINGTON, DC 20350

HQ, USAF/SAMI
WASHINGTON, DC 20330

AIR FORCE COMMUNICATIONS COMMAND
ATTN EPPD
SCOTT AFB, IL 62225

COMMANDER
US AIR FORCE SPACE COMMAND
ATTN KKO
ATTN KRQ
ATTN XPOW
PETERSON AFB, CO 80912

1842 EEG
ATTN EEISG
SCOTT, AFB, IL 62225

HEADQUARTERS
ELECTRONIC SYSTEMS DIVISION/ YS
ATTN YSEA
HANSCOM AFB, MA 01730

HEADQUARTERS
USAFE
ATTN DCKI
RAMSTEIN AFB, GERMANY

SYSTEM INTEGRATION OFFICE
ATTN SYE
PETERSON,AFB, CO 80912

AIR FORCE WEAPONS LABORATORY/ DYC
ATTN NTC4, TESD, IESM
KIRKTLAND AFB, NM 87117

CENTRAL INTELLIGENCE AGENCY
ATTN OWSR/NED
ATTN OWSR/STD/MTB, A. PADGETT
WASHINGTON, DC 20505

DIRECTOR
FEDERAL EMERGENCY MANAGEMENT AGENCY
OFFICE OF RESEARCH/NPP
ATTN STATE & LOCAL PROG SUPPORT
500 C STREET, SW
WASHINGTON, DC 20472

FEDERAL PREPAREDNESS AGENCY
GENERAL SERVICES ADMINISTRATION
ATTN ESTE-M MURTHA
18th & F STREETS, SW
WASHINGTON, DC 20405

LAWRENCE LIVERMORE NATIONAL LAB
ATTN TECHNICAL INFO DEPT LIBRARY
ATTN L-156, H. CABAYAN, L. MARTIN
PO BOX 808
LIVERMORE, CA 94550

DIRECTOR
NATIONAL SECURITY AGENCY
ATTN R15
9800 SAVAGE ROAD
FT MEADE, MD 20755

AMERICAN TELEPHONE &
TELEGRAPH CO
ATTN SEC OFC FOR W. EDWARDS
1120 20th STREET, NW
WASHINGTON, DC 20036

AT&T BELL LABORATORIES
ATTN R. STEVENSON
ATTN J. MAY
1600 OSGOOD ST
N. ANDOVER, MA 01845

AT&T BELL LABORATORIES
ATTN J. SCHOLL
ATTN J. SERRI
CRAWFORDS CORNER ROAD
HOLMDEL, NH 07733

BDM CORP
ATTN CORPORATE LIBRARY
7915 JONES BRANCH DRIVE
MCLEAN, VA 22102

BOEING CO
ATTN R. SHEPPE
PO BOX 3707
SEATTLE, WA 98124

COMPUTER SCIENCES CORP
SYSTEMS DIVISION
ATTN A. SCHIFF
1400 SAN MATEO BLVD, SE
ALBUQUERQUE, NM 87108

ELECTROMAGNETIC APPLICATIONS,INC
ATTN R. PERALA
PO BOX 26263
1978 SOUTH GARRISON ST
DENVER ,CO 80226

ENGINEERING SOCIETIES LIBRARY
ATTN ACQUISITIONS DEPT
345 EAST 47TH STREET
NEW YORK, NY 10017

GEORGIA INSTITUTE OF
TECHNOLOGY
OFFICE OF CONTRACT
ADMINISTRATION
ATTN RES & SEC COORD FOR
H. DENNY
ATLANTA, GA 30332

IIT RESEARCH INSTITUTE
ATTN J. BRIDGES
ATTN I. MINDEL
10 W. 35TH STREET
CHICAGO, ILL 60616

INTERNATIONAL TEL & TELEGRAPH
CORP
ATTN A. RICHARDSON
ATTN TECHNICAL LIBRARY
500 WASHINGTON AVENUE
NUTLEY , NJ 07110

MISSION RESEARCH CORP
PO BOX 7816
ATTN W. STARK
COLORADO SPRINGS, CO 80933

MISSION RESARCH CORP
EM SYSTEM APPLICATIONS DIV
ATTN A. CHODOROW
1720 RANDOLF ROAD, SE
ALBUQUERQUE, NM 87106

RI, INC
TTN W. HAAS
121 LINCOLNIA RD
LEXANDRIA, VA 22312

ICHARD L. MONROE ASSOCIATES
911 R STREET,NW
UITE 203
'ASHINGTON, DC 20009

:&D ASSOCIATES
'O BOX 9695
\TTN W. GRAHAM
IARINA DEL REY, CA 90291

R&D ASSOCIATES
\TTN DIRECTOR,DR.J.THOMPSON
.401 WILSON BLVD
SUITE 500
\RLINGTON, VA 22209

ROCKWELL INTERNATIONAL CORP
PO BOX 3105
\TTN D/243-068, 031-CA31
\TTN G.E. MORGAN
\NAHEIM, CA 92803

SCIENCE APPLICATIONS, INC
PO BOX 1303
\TTN W. CHADSEY
MCLEAN, VA 22102

SCIENCE ENGINEERING ASSOC
\TTN P. FLEMMING
\TTN V. JONES
MARINER SQUARE
SUITE 127
1900 N. NORTHLAICE WAY
PO BOX 31819
SEATTLE, WA 98103

SRI INTERNATIONAL
ATTN A. WHITSON
ATTN E. VANCE
333 RAVENSWOOD AVENUE
MENLO PARK, CA 94025

TRW DEFENSE & SPACE SYSTEMS GROUP
ATTN J. PENAR
ATTN W. GARGARO
ONE SPACE PARK
REDONDO BEACH, CA 92078

TRW DEFENSE & SPACE SYSTEMS GROUP
ATTN E. P. CHIVINGTON
2240 ALAMO, SE
SUITE 200
ALBUQUERQUE, NM 87106

TRW, INC
COMMAND & CONTROL & COMMUNINCATIONS SYS DIVISION
ATTN N. STAMMER
5203 LEESBURG PIKE
SUITE 310
FALLS CHURCH, VA 22041

US ARMY ELECTRONICS RESEARCH & DEVELOPMENT COMMAND
ATTN COMMANDER, DRDEL-CG
ATTN PUBLIC AFFAIRS OFFICE, DRDEL-IN

COMMANDER
HARRY DIAMOND LABORATORIES
ATTN D/TSO/DIVISION DIRECTORS
ATTN RECORD COPY, 81200
ATTN HDL LIBRARY, 81100(3 COPIES)
ATTN HDL LIBRARY (WOODBRIDGE)
ATTN TECHNICAL REPORTS BRANCH, 81300

RY DIAMOND LABORATORIES(Cont'd)
TN LEGAL OFFICE, 97000
TN CHIEF, 21000
TN CHIEF, 21100
TN CHIEF, 21200
TN CHIEF, 21300
TN CHIEF, 21400
TN CHIEF, 21500
TN CHIEF, 22000
TN CHIEF, 22100
TN CHIEF, 22300
TN CHIEF, 22800
TN CHIEF, 22900
TN CHIEF, 20240
TN A. SAMBUCO, DRDEL-PO-SA
TN R. CHASE, 21300(50 copies)
TN A. CUNEO, 21100
TN W. SCOTT, 21500
TN H. ROBERTS, 21400